Brain stimulation reveals neural mechanisms of stereopsis

Lukas Fabian Schaeffner

Fitzwilliam College

University of Cambridge

A thesis submitted for the degree of

Doctor of Philosophy

September 2018

Acknowledgements

Firstly, I would like to thank the Department of Psychology and Fitzwilliam College for providing an outstanding environment in which to work, learn and live. I have had the opportunity to interact with so many wonderful people on a daily basis and have learnt more from this than any thesis could ever describe.

I want to thank everyone in the Adaptive Brain Lab, Polytimi Frangou, Vasilis Karlaftis, Nuno Reis Goncalves, Reuben Rideaux, Joseph Giorgio, Monica Gates, Elisa Zamboni, Seb Wride, Liam Doherty, Kathy Purdy, Avraam Papadopoulos and Ke Jia for their support, good advice and friendship over the last four years.

I want to say thank you to everyone in the PRISM network, Zarko Milojevic, Sabrina Hansmann-Roth, Jan Jaap van Assen, Carlos Jorge Zubiaga Peña, Dicle Dövencioğlu, Tatiana Kartashova, Fan Zhang, Thomas Maier and Irene Caprara, for their support and friendship. I also want to thank the senior scientists of the network, Roland Fleming, Karl Gegenfurtner, Peter Janssen, Pascal Mamassian and Sylvia Pont, for providing a wonderful environment in which we could all learn and grow during our PhDs.

I also want to thank Tristan Bekinschtein for advising me during my PhD and Valdas Noreika for teaching me on the matter of brain stimulation research.

A special thank you goes to Elizabeth Michael without whom the third chapter of my thesis would not have been possible. I am very grateful for your invaluable help with neuroimaging and patience with my questions.

I want to thank Julie Harris and Jon Simons for agreeing to read and discuss this lengthy manuscript with me.

I would like to thank the European Commission (FP7, PRISM) and the Wellcome Trust for funding my doctorate degree.

Finally, I want to thank Katrin Fischer for her support, inspiration and reassurance. Thank you for being part of this journey.

Preface

My time as a graduate student at the University of Cambridge was full of intellectual stimulation. In the Adaptive Brain Lab, a had the opportunity to research the workings of human vision with a variety of different neuroscience research techniques such as magnetic resonance imaging, electroencephalography and transcranial magnetic stimulation. I had the privilege to work on fascinating topics of stereopsis. Specifically, I investigated how the brain uses signals from the left and right eye to estimate visual depth. This is the central point of this thesis.

The contents of the thesis result from my own work, guided by my supervisor Dr. Andrew Welchman. I have not submitted any parts of the thesis for any other degree in the University of Cambridge or any other institution. The thesis does not exceed the word limit established by the Degree Committee for the Faculty of Biology.

Abstract

Stereopsis is critical for interaction with our environment. However, binocular disparity in natural images is often ambiguous and this makes it difficult to establish a binocular correspondence solution. In my thesis, I focus on both the challenges of this problem and solutions that the brain applies. To study brain function, I use Transcranial Magnetic Stimulation (TMS) which allows me to causally relate induced changes in neural activity with changes in depth perception. This way I can map out neural mechanisms of stereopsis within the visual cortex.

As a first step, I conducted a proof of concept study to confirm where in the visual cortex TMS can be used to study perception. I systematically mapped out where in the visual cortex TMS triggers self-propagating, perceptually noticeable neural activation. I related this to the retinotopic organisation and the location of object- and motion-selective areas, identified by functional Magnetic Resonance Imaging. My work confirms that TMS can trigger perceptually significant neural activation in early and dorsal visual areas.

In my second chapter, I investigated how incoherent binocular disparity challenges stereopsis. As disparity coherence is reduced it becomes increasingly challenging to establish global correspondence and consequently observers struggle to perceive depth. Interestingly, this problem is less severe when images contain a mixture of bright and dark features (mixed contrast polarity). By locating where in the brain disparity processing benefits from mixed contrast polarity, I can infer where incoherent disparity might challenge mechanisms of stereopsis. I applied TMS during discrimination of incoherent disparity in images with mixed or single contrast polarity. I found that stimulation over V1 differentially affects perception of mixed and single polarity stimuli. My findings show that mechanisms of stereopsis in early visual cortex process mixed and single polarity differently and suggest these mechanisms are challenged by incoherent disparity.

In my final chapter, I investigated the role of parietal cortex in the processing of incoherent disparity information. Findings in both macaque monkeys and human observers suggest that the dorsal visual cortex is particularly involved in the processing of incoherent disparity signals. Here, I tested the role of the posterior parietal cortex in human observers. I used brain stimulation to suppress synaptic transmission in parietal cortex and recorded electroencephalography during incoherent disparity processing. Disrupting parietal cortex caused changes in early, disparity responses in visual cortex. This suggests that parietal cortex provides top-down influence to the visual cortex relevant to incoherent disparity processing.

Contents

List of Figures &Tables

1. Introduction

1.1 Binocular vision

Advantages of front-facing eyes

Visual perception allows animals to form a sensory representation of their environment using a given spectrum of light which is reflected by the natural world. Reflected light is captured by an eye's pupil and directed on the retina at the back of the eye. Photoreceptors in the retina react to the impacting photons of light and convert impact frequency to electrical signals which are interpreted by the nervous system to construct perception.

Most prey animals have laterally positioned eyes with minimal overlap between the view of the eyes (Allman, 2000). This way the retinae capture the maximum amount of the environment while sampling the minimum amount of redundant information. Such an arrangement of the eyes allows an animal to detect changes in its environment at up to 360° radius (McFarlane, 1976; J. H. Prince, 1970). This ability is useful to spot approaching predators.

In contrast, most predators have front-facing eyes. There is substantial overlap between the fields of view of the two eyes at a cost of panoramic vision. This arrangement has proven successful because front-facing eyes capture redundant visual information allowing the animal to use binocular disparity (differences in the two retinal images) to estimate distances between elements in its environment. This ability is useful for a wide range of skills such as identifying and capturing prey (Cartmill, 2005), grasping fine branches (Martin, 1990; Watt & Bradshaw, 2002), arboreal acrobatics (Le Gros Clark, 1934), breaking camouflage (Bredfeldt & Cumming, 2006; Julesz, 1971), overcoming visual occlusions (Changizi & Shimojo, 2008) or estimating surface reflectance (Blake & Bülthoff, 1990).

Geometry of binocular vision

Front-facing eyes are horizontally separated and therefore view the world from slightly different vantage points. When an observer attends to a point in their environment their eyes converge on this point so that the point projects on the fovea, where vision is most acute (Whittaker & Cummings, 1990). This is shown as fixation F in **Fig. 1.1**. The projections of

any other point P falling onto the left and right retinae will be displaced relative to the fovea in a way that depends on the distance between P and the observer.

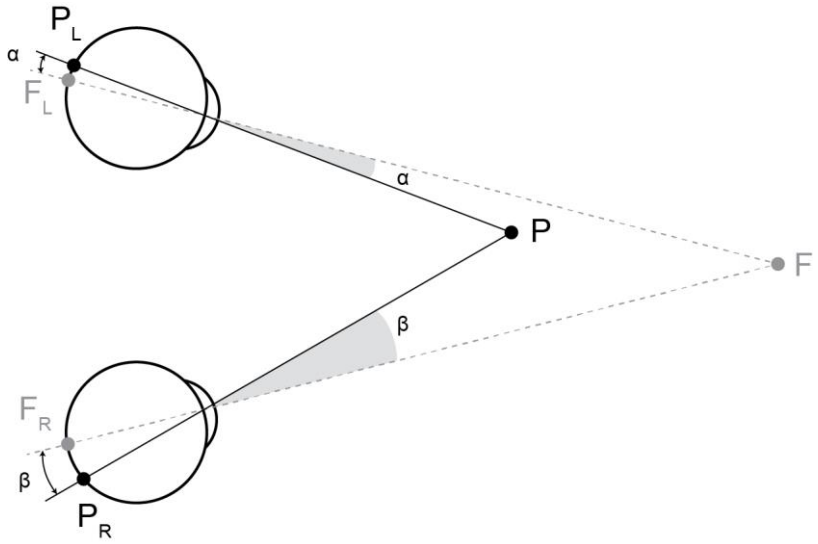

Figure 1.1: The geometry of stereopsis. A point (P) in the environment often projects onto non-corresponding locations on the two retinae. The difference of the resulting angles (α – β) between the point projections and fixation (F) is called binocular disparity.

The difference in angular displacement between the projections of P and F is defined as absolute binocular disparity. Here, I refer to the angles between the projections of P and F onto the left and right retinae as α and β. Absolute disparity is then given by δ = α – β. Although absolute disparity depends on the position of P, it also changes as a function of F. This information can, therefore, only be used to extrapolate the distance between P and F. To find the distance between P and the observer, one needs to know the distance between the observer and the point at which fixation is maintained. Convergent eye movements and pupil accommodation could be used for this purpose.

Points that project to corresponding locations in the left and right retinae form a surface called the horopter. All points in the horopter have zero disparity because α = β. The Vieth-Müller circle depicts an approximation of the horopter (see **Fig. 1.2**). Non-zero disparities can be grouped into crossed or uncrossed. Crossed disparities have projection lines that cross in front of the point of fixation and greater overall temporal displacements on the retina. Points with crossed disparity are therefore closer to the observer in relation to the fixation point. Uncrossed disparities' projection lines, on the other hand, do not cross in front

of fixation and have greater overall nasal displacements. Points with uncrossed disparity are thus further away than the fixation point. The relative disparity between point C with crossed disparity and point U with uncrossed disparity is defined as the difference between their absolute disparities $\delta_{CU} = \delta_C - \delta_U$. This can inform an observer about the distance between U and C.

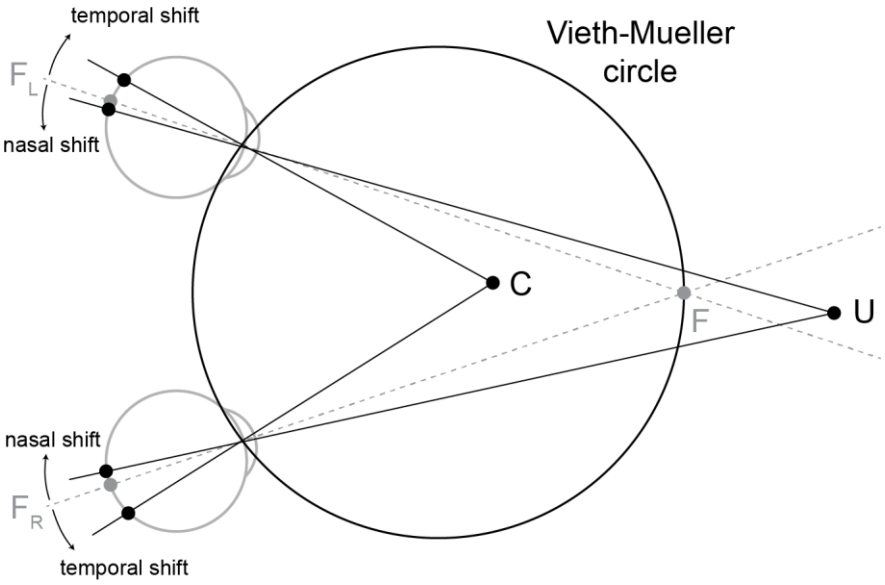

Figure 1.2: Crossed and uncrossed disparity. Example points with crossed (C) and uncrossed (U) disparity. Points with crossed disparity predominantly project on temporal retinal locations, relative to fixation (F), and are perceived as near. Points with uncrossed disparity predominantly project on nasal retinal locations, relative to F, and are perceived as far. Points on the horopter, which is approximated by the Vieth-Mueller circle, fall on corresponding locations in the left and right retina and therefore have zero disparity. Adapted from Howard and Rogers (2002).

Stereopsis

In the previous section, I have described how two eyes with overlapping visual fields give rise to binocular disparity. This disparity could, in theory, be used by the observer to resolve the visual depth of the environment. However, do observers actually use this information for depth perception?

The first experiment which addressed this question was conducted by Charles Wheatstone (Wheatstone, 1838). He invented the first stereoscope to present drawings of a scene from

two horizontally separated perspectives to the left and right eye. Observers were able to perceive the depth structure of the objects depicted in the scene drawing. Heinrich Dove showed that this stereopsis could not be driven by the vergence of eye movements or by pupil accommodation because stereopsis could occur quicker than voluntary eye movements (Dove, 1841, 1860). Further, Bela Julesz was able to show that binocular disparity alone is sufficient to produce perception of depth (Julesz, 1964). He created a new type of stimulus called a random dot stereogram (RDS) in which binocular disparity can be introduced while keeping all other visual information constant (see **Fig. 1.3**). Observers can perceive depth structures in such stimuli based purely on binocular information. This confirms that binocular disparity is used by observers to construct depth perception.

Figure 1.3: The first random-dot stereogram. Invented by Bela Julesz. Adapted from Julesz (1964).

Observers are much more sensitive to relative disparities compared to absolute disparity, which only allows for coarse depth judgements (Blakemore, 1970; Westheimer, 1979). At short viewing distances, observers can discriminate disparity differences of up to 5 arcsec at the fovea, which corresponds to 25 µm of depth difference (about the width of a human hair) (Ponce & Born, 2008). This smallest distinguishable depth difference is ultimately defined by the smallest disparity that can be resolved on the retina. The binocular disparity produced by a given depth difference varies as the inverse square of the viewing distance, which means that stereopsis becomes less acute with longer viewing distances.

Stereopsis when disparity signals are noisy

When first discussing the RDS, Julesz commented on the striking process of filling-in through which observers perceive smooth surfaces in RDSs, which actually consist of uneven clouds of dots (Julesz, 1964). However, he also noted that observers maintain a high sensitivity for sharp disparity differences, which breaks the perception of smooth, coherent surfaces (Julesz, 1971). This makes sense because in a natural environment objects tend to have much more complex, variable depth profiles (e.g. the branches of a tree spreading in all directions). For this reason, psychophysicists normally measure the depth acuity of human observers with tasks which require observers to discriminate disparity differences in the form of a disparity-based step edge in a RDS (see **Fig. 1.4A**). When depth information is coherent (see **Fig. 1.4B**), all dots in the stereogram can be considered a part of a reliable depth signal. In principle, the observer can solve this task by sampling only the disparity of one point on either side of the step edge.

To make the task more challenging for the observer, the experimenter can reduce the coherence of the disparity signal. In **Fig. 1.4C** the position of all dots in the step edge is shifted by a disparity sampled from a normal distribution. All dot positions averaged together (dashed line) accurately describe the position of the step edge. However, individual dots no longer carry reliable information of the step edge position. The strategy of an ideal observer would be to integrate the disparity of all dots to make a decision. In **Fig. 1.4D** a given proportion of dots are randomly repositioned. These dots no longer carry reliable depth information of the step edge (crossed out), while dots which remain in their position still signal the step edge. An ideal observer should try to identify the position of the step edge by locating the depth where most dots are located, while ignoring all other dots. Such a task manipulation is called a signal-in-noise task because noise, a random shift in dot position, has been added to a signal, the step edge position, which needs to be detected by the observer for successful depth discrimination. For the remainder of this thesis, I will refer to these random dot position shifts as ‘disparity noise’ and to a disparity signal with added noise as a ‘noisy disparity signal’.

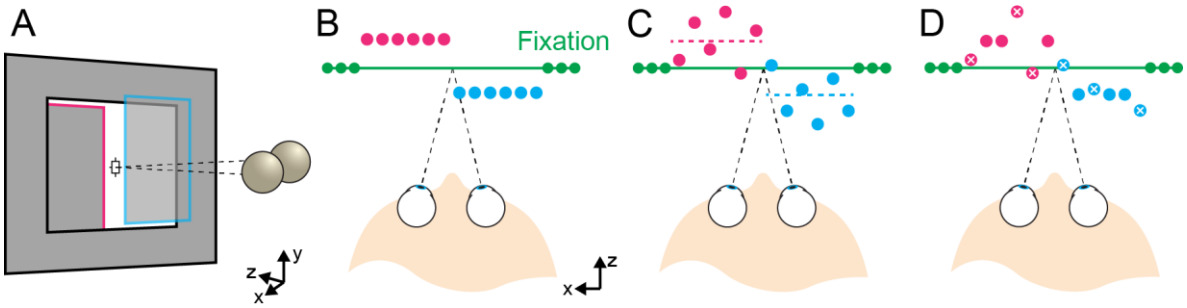

Figure 1.4: Coherent and incoherent disparity discrimination. A) Task which requires an observer to discriminate a disparity based step edge in a RDS. In this example an observer is asked to discriminate which surface is closer. **B)** Example where disparity information is coherent. All dots reliably signal the step edge position. **C)** and **D)** illustrate examples with noisy disparity information. In **C)** the position all dots in the step edge is shifted by a disparity sampled from a normal distribution. In **D)** a given proportion of dots are randomly repositioned (crossed out).

An interesting question is whether stereopsis works equally well for scenes with a noisy disparity signal. As it turns out, stereopsis becomes increasingly inefficient when disparity information gets noisy and the ability of an observer to distinguish fine depth differences suffers greatly. For a noisy disparity signal, as shown in **Fig. 1.4C** (with 150 dots, a 23-120 arcsec step edge, and disparity noise sampled from a 2-4 arcmin SD normal distribution), human stereo acuity equals the performance of an ideal observer who uses only 2% of the dots in the RDS (J. M. Harris & Parker, 1992). This reveals a striking limitation of stereopsis which is surprising given that the visual system has evolved in an environment of noisy depth scenes which it needs to navigate.

There are challenges of processing disparity information. A noisy disparity signal might increase these challenges which could explain this inefficiency of stereopsis. In order to compute binocular disparity, an observer first needs to establish correspondence between visual features present in the left and right retinal image. This is known as the stereo-correspondence problem. For smooth depth structures it is fairly trivial to find a global solution while for noisy disparity structures this task becomes much harder due to the increasing probability of false matches. In **Chapter 1.2**, I will introduce mechanisms with which the visual brain potentially establishes stereo correspondence and how this process could be challenged by noisy disparity information.

Alternatively, the visual system might struggle to combine the noisy disparity signal into an unambiguous depth percept. At a later stage of disparity processing, the observer needs to

'read out' the different, correctly detected disparities and produce an unambiguous depth map of the viewed scene. As described earlier, observers can adopt different strategies, such as averaging noisy disparities or ignoring some visual features identified to contain noisy disparity, to deal with different types of disparity noise. In **Chapter 1.3**, I will discuss the crucial role of higher visual brain areas in stereopsis, where such strategies may be applied.

The mixed polarity benefit

When Harris and Parker (1995) investigated human depth acuity for noisy disparity signals they made a surprising observation: observers' depth perception is better for noisy binocular disparity when stimuli contain a mixture of bright and dark visual features compared to stimuli containing only one feature colour. This phenomenon has been called the mixed polarity benefit. Interestingly, this benefit only arises for stimuli that contain a noisy disparity signal (see Fig **1.4C**), but not in tasks that use a coherent disparity signal (see **Fig 1.4B**). Therefore, answering how this perceptual benefit arises might give us a better understanding of how noisy disparity challenges the visual system. Read, Vaz, and Serrano-Pedraza (2011) were able to replicate the polarity benefit by de-correlating smooth disparity surfaces in a RDS. This stimulus manipulation involves randomly replacing a dot in one stereo image which leaves a pair of unmatchable dots in the left and right stereo image. Stimulus de-correlation should predominantly challenge early mechanisms of stereopsis which establish stereo correspondence. This is because this task manipulation only reduces binocular image correlation but does not introduce fusible disparity noise. Additionally, established computational models of disparity processing in early visual cortex, such as the binocular energy model (Read & Cumming, 2018) or the binocular neural network (Goncalves & Welchman, 2017), can produce such a mixed polarity benefit. These findings suggest that the mixed polarity benefit arises in the early visual cortex and is tied to brain mechanisms which establish stereo-correspondence. However, thus far, there has not been any conclusive evidence to suggest where in the brain disparity processing benefits from mixed contrast polarity. In **Chapter 2**, I will investigate where in the visual cortex sensory processing benefits from the availability of mixed contrast polarity. I use non-invasive brain stimulation to change neural activity in different areas of the visual cortex during noisy disparity processing. A change in this perceptual phenomenon following stimulation will suggest that the mixed polarity benefit arises in the stimulated brain area.

1.2 Disparity processing in primary visual cortex

In the previous section, I described how researchers study stereopsis. I discussed that stimuli that contain only binocular disparity information give rise to the perception of depth, which shows that observers do in fact use disparity for stereopsis. Further, I reported that noise in the disparity signal challenges stereopsis, and I described strategies that the observer might use to overcome these challenges. To understand how the visual nervous system within an observer processes binocular disparity, we need to investigate how neurons in the brain behave when incoming depth information is being processed. In the following section, I will discuss how neurons in the primary visual cortex respond to binocular disparity, and how they could extract visual depth information from incoming disparity information. Additionally, I will discuss how these neurons could be challenged with the task of processing noisy disparity.

Neural encoding of binocular disparity

In order to process binocular disparity, a neuron must have access to visual information from both eyes. Binocular neurons are cells that respond to incoming light in both eyes (Hubel & Wiesel, 1959, 1962). Incoming visual information is largely separated by eye until it reaches the primary visual cortex (V1). V1 is the first area in the visual system with binocular neurons; it is therefore assumed that stereopsis starts in V1. We distinguish two types of binocular neurons in primary visual cortex which are relevant for stereopsis (Hubel & Wiesel, 1962, 1968): simple cells have clearly defined excitatory and inhibitory subregions for dark and light in their receptive fields. Complex cells, on the other hand, do not seem to be modulated by the precise position of the stimuli within their receptive field. The receptive fields for these binocular neurons are horizontally offset and therefore respond optimally to disparity between the two retinal images (Barlow, Blakemore, & Pettigrew, 1967; Nikara, Bishop, & Pettigrew, 1968; Pettigrew, Nikara, & Bishop, 1968; Poggio & Fischer, 1977; Poggio & Talbot, 1981). Such cells have the potential to encode binocular disparity and support stereopsis.

Simple cells are the first binocular neurons along the stream of the visual system (Anzai, Ohzawa, & Freeman, 1999b; Cumming, 1997; Ohzawa, DeAngelis, & Freeman, 1990). These neurons only respond to a given portion of the field of view called their receptive field (Anzai, Ohzawa, & Freeman, 1997, 1999a; Ohzawa et al., 1990). They encode disparity via two different mechanisms: some simple cells encode binocular disparity via a horizontal

position shift of their receptive fields (Ferster, 1981; von der Heydt, Adorjani, Hänny, & Baumgartner, 1978) (see **Fig. 1.5A**). These cells respond optimally to offset regions in the visual fields of the two eyes. Other simple cells encode disparity through a phase shift in their response profiles (Anzai et al., 1997, 1999a, 1999b; DeAngelis, Ohzawa, & Freeman, 1991; S. J. D. Prince, Cumming, & Parker, 2002; Tsao, Conway, & Livingstone, 2003) (see **Fig. 1.5B**). These cells respond optimally to offset regions of the same receptive field in both eyes. But because simple cells only respond to a given portion of the visual field they are not sufficient to support global stereopsis.

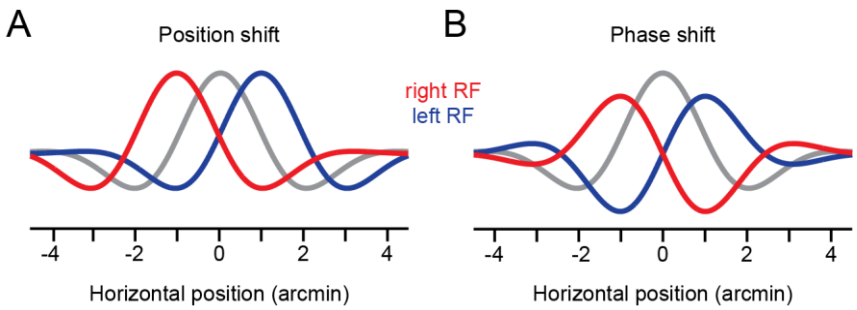

Figure 1.5: Binocular receptive fields with position and phase shifts. A) Positional disparity: Identical receptive fields in the left and right eye are horizontally shifted. **B)** Phase disparity: Receptive fields in the left and right eye are situation in the same location of the visual field, but have different response functions, which can be related through a shift in the phase parameter of a Gabor model.

Complex cells, on the other hand, are invariant to the stimulus position within their receptive field and the stimulus contrast polarity (black or white) (Ohzawa et al., 1990). They are therefore better equipped to be disparity detectors. They receive excitatory input of simple cells for a preferred disparity (Anzai, Ohzawa, & Freeman, 1999c; Ohzawa et al., 1990; Ohzawa, DeAngelis, & Freeman, 1997; Ohzawa & Freeman, 1986). Complex cells have very diverse tuning properties: some are tuned to specific disparities while others are tuned to a range of crossed or uncrossed disparity (Poggio & Fischer, 1977; Poggio, Gonzalez, & Krause, 1988; S. J. D. Prince et al., 2002). They cover a wide range of binocular disparities and a system that pools their responses could theoretically achieve human-like stereo acuity (Lehky, Pouget, & Sejnowski, 1990; Lehky & Sejnowski, 1990). Additionally, it has been shown that complex cells signal binocular disparity in RDSs (Poggio et al., 1988; Poggio & Poggio, 1984), suggesting that complex cells in V1 play a critical role in stereopsis. However, human depth perception does not always match the responses of complex cells.

Stereo images can be manipulated in such a way that every white feature in the left eye has a black matching feature in the right eye. This is called an anti-correlated stereogram. Such stereograms do not elicit a perception of depth for human observers, yet complex cells will still exhibit selectivity for anti-correlated disparity (tuning curves are inverted and attenuated) (Cumming & Parker, 1997, 2000). From this follows that complex cells in V1 do not constitute stereopsis alone, which indicates that subsequent processing in extra-striate cortex must be involved.

The stereo-correspondence problem

As a first crucial step in the process of extracting binocular disparity the visual system needs to establish correspondence between features in the left and right retinal images. This challenge is known as the stereo-correspondence problem. It is a difficult task because the visual environment may contain many similarly looking features and a feature in the left eye could be matched with many features in the right eye. **Fig. 1.6** illustrates this problem: different real world dot positions could produce similar projections onto the retinae and therefore give rise to the same percept. The visual system must resolve this ambiguity and generate a globally consistent solution.

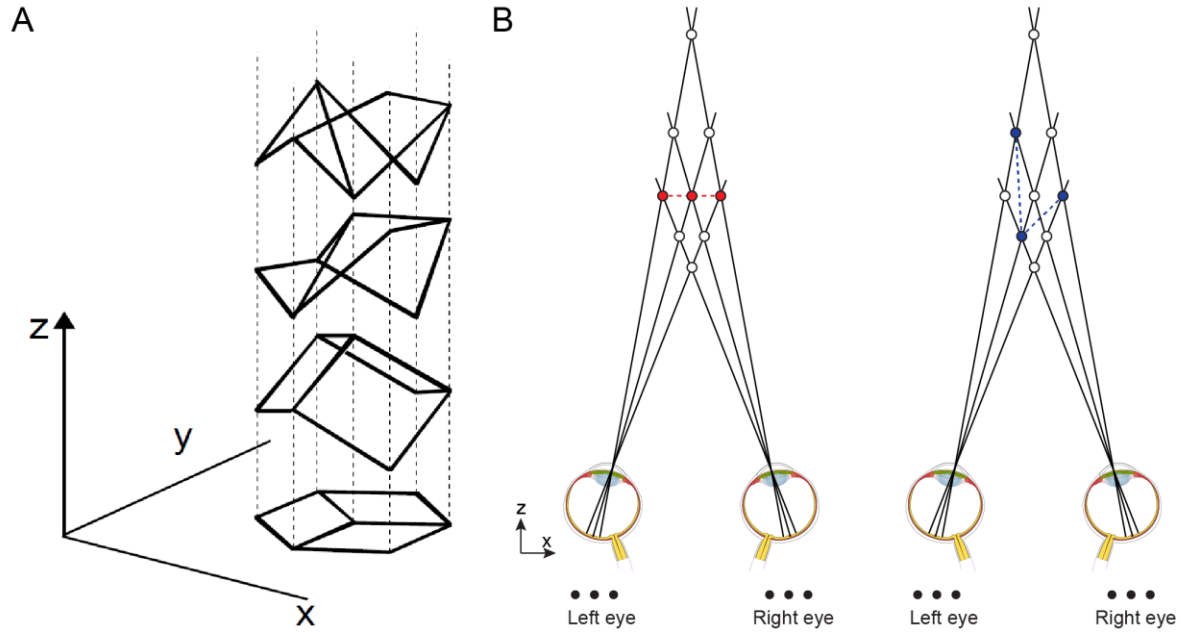

Figure 1.6: The stereo correspondence problem. A) Illustration of the inverse problem of visual perception: Multiple different physical geometries can give rise to the same 2D projection on the retina. The visual system is challenged with identifying the correct shape. Adapted from Sinha and Adelson (1993). **B)** In stereopsis, this inverse problem makes it challenging to retrieve the correct distance of points in the environment from binocular retinal input. Three black dots projected into the eyes could be located in many potential 3D locations (empty circles). Coloured circles show two potentially correct arrangements of dot positions. This problem is called the stereo correspondence problem.

There are different possible explanations of how observers could establish stereo correspondence. The visual system might match low-level features such as the brightness of small dot elements (Marr & Poggio, 1976; Mayhew & Frisby, 1981), or areas of zero crossing where contrast polarity shifts from positive to negative or vice-versa (Grimson, 1981; Marr & Poggio, 1979). Alternatively, the visual system might match more complex features such as average brightness or contours (Kaufman, 1964; Kaufman & Pitblado, 1965; Ramachandran, Madhusudhan Rao, & Vidyasagar, 1973; Ramachandran & Nelson, 1976).

A good strategy for solving local correspondence problems in the visual scene is to establish global correspondence: there are always many possible local feature matches between the left and right eye, and the visual system can verify or falsify them by taking into account global information of the scene. For example, an observer could constrain the number of potential matches based on their physiological plausibility: disparity in surfaces normally

varies smoothly and an observer could reject large, local variations in disparity (Dev, 1975; Marr & Poggio, 1976; Nelson, 1975; Sperling, 1970). Such a constraint could explain why the visual system struggles to compute binocular disparity when incoming disparity information is noisy, because such disparity profiles contain large local variety in binocular disparity. This rejection of implausibly large disparity variations could help an observer solve the stereo correspondence problem. However, such a strategy assumes that observers match image features, but it is currently unclear whether the visual system does in fact match visual information from left and right eye to support stereopsis. To answer this question one needs to investigate how neurons respond to binocular disparity information to infer how they compute visual depth.

Computational models of stereopsis

As summarized above, a large body of research has provided us with insight into how binocular neurons respond to binocular disparity. A powerful approach to understand how stereopsis is supported by the brain is to build a computational model. Such a model consists of processing elements which mimic the behaviour of simple and complex cells when exposed to binocular disparity. The success of such a model can be judged by how well its output can be used to detect binocular disparity.

Ohzawa et al. (1990) developed the most influential model of binocular V1 neuron responses to disparity: the binocular energy model. According to this model, simple cells perform a spatial summation over their receptive fields in the left and right eye followed by a rectification to ensure non-negative firing rates (Movshon, Thompson, & Tolhurst, 1978). These responses are disparity selective due to interocular differences in receptive field position or response profile shape in the left and right eyes (see **Fig. 1.5**). Disparity selective complex cells pool the output of four simple cells in quadrature phase (see **Fig. 1.7**). The output of these complex cells in the binocular energy model supports disparity detection. It is noteworthy that this model does not, strictly speaking, match visual features to solve the stereo-correspondence problem. Instead, it computes energy as a measure of information, which is defined as the interocular cross-correlation between the left and the right retinal image. In this way, the binocular energy model differs from theoretical feature-matching based approaches described above.

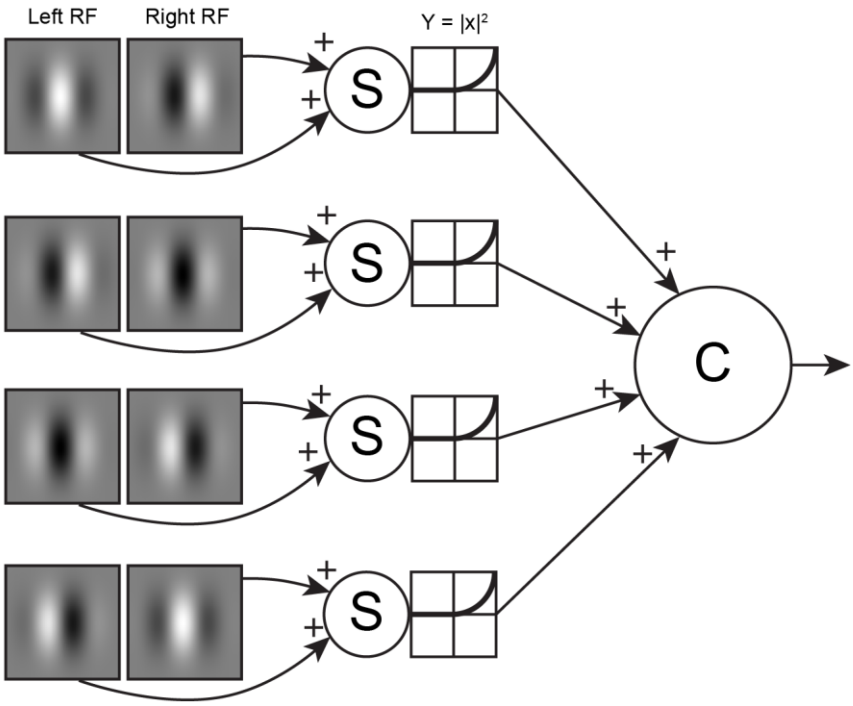

Figure 1.7: The binocular energy model. Simple cell units (S) have receptive fields (Gabor filter) in both the left and right eye image. The output of these filters is summed (binocular summation) and rectified. The output of the simple cell units is then combined into a complex cell unit (C) which signals binocular disparity.

Does the binocular energy model explain why observers struggle with noisy disparity? In this model, the final choice of disparity is based on a maximum energy criterion, which means that the preferred disparity of the most activated complex cell unit is taken as the predicted disparity (Qian, 1994; Qian & Zhu, 1997; Read, Parker, & Cumming, 2002). Read and Cumming (2018) described how with decreasing consistency of disparity signals, the binocular image interocular cross-correlation decreases. Therefore, the energy peak of the originally consistent disparity step edge shrinks as the disparity signal becomes noisier, which results in a less reliable prediction of depth. As a result, an observer would struggle to discriminate depth differences with noisy disparity based on less reliable predictions of disparity. It is therefore possible that the visual system applies binocular disparity processing mechanisms which are similar to the binocular energy model, which struggles with noisy disparity.

Another relevant question is whether the binocular energy model can explain the mixed polarity benefit. Indeed, Read and Cumming (2018) describe how the binocular energy model can produce such a phenomenon. When interocular cross-correlation decreases as

disparity becomes less consistent, interocular cross-correlation decreases more strongly for images with single contrast polarity compared to images with mixed contrast polarity. As a result, the energy peak for the original, consistent disparity signal decreases more strongly for single compared to mixed polarity stimuli, and the reliability of disparity predictions is affected more strongly. As a result, an observer would be better at discriminating noisy depth structures when visual information contains mixed contrast polarity information, compared to when only one contrast polarity is available.

This suggests that the mixed polarity benefit could be a by-product of the same disparity processing mechanism in the primary visual cortex as described by the binocular energy model. However, the binocular energy model is most likely a simplified version of the true computations taking place in primary visual cortex. This can be assumed because there are still phenomena of early disparity processing which are not explained by the standard binocular energy model such as attenuated responses to anti-correlated visual input (Cumming & Parker, 1997, 2000). More advanced computational models of disparity processing may ultimately explain this perceptual benefit in an entirely different way. Additionally, Harris and Parker (1995) proposed that separate ON and OFF channel processing in primary visual cortex could also explain the mixed polarity benefit. In **Chapter 3**, I will discuss how different computational models of disparity processing could explain the mixed polarity benefit.

1.3 Disparity processing in parietal cortex

In the previous section, I discussed how neurons in primary visual cortex can already function as disparity detectors and support stereopsis. I also examined how noisy disparity could challenge disparity processing in primary visual cortex which could explain inefficiencies of stereopsis. However, binocular disparity is also processed in many extra-striate areas in the brain (Parker, 2007). In this section, I will describe the potential roles of extra-striate sensory processing in stereopsis.

As discussed in **Chapter 1.1**, binocular disparity has been found to support many other functions aside from comparing the depth of different objects, such as breaking camouflage or control grasping movements. As a consequence, there is no isolated area in the brain where binocular disparity is processed. Disparity selective neurons can be found in many extra-striate areas involved in vision (Parker, 2007) such as V2 (Hubel & Wiesel, 1970; Poggio & Fischer, 1977), V3/V3a (Hubel & Wiesel, 1959; Zeki, 1978), middle temporal lobe

(MT) (DeAngelis, Cumming, & Newsome, 1998; DeAngelis & Newsome, 1999), medial superior temporal lobe (MST) (Eifuku & Wurtz, 1999), V4 (Shiozaki, Tanabe, Doi, & Fujita, 2012; Tanabe, Doi, Umeda, & Fujita, 2005; Umeda, Tanabe, & Fujita, 2007; Watanabe, Tanaka, Uka, & Fujita, 2002) and IT (P. Janssen, Vogels, Liu, & Orban, 2003; P. Janssen, Vogels, & Orban, 1999, 2000; Uka, Tanaka, Yoshiyama, Kato, & Fujita, 2000). Further, disparity selective neurons have been found in anterior- (Srivastava, Orban, De Maziere, & Janssen, 2009; Verhoef, Vogels, & Janssen, 2010, 2015), lateral- (Genovesio, 2004) and ventral (Colby, Duhamel, & Goldberg, 1993) parietal cortex, as well as the frontal eye fields (Ferraina, Paré, & Wurtz, 2000).

Disparity processing in the dorsal and ventral pathway

Given that disparity processing seems to be dispersed over such large portions of the brain, it is difficult to assign potential mechanisms of extra-striate disparity processing to isolated brain areas. However, there are general concepts which organize the visual brain into different processing structures, and would allow us to better map disparity processing in the brain. In vision research, two anatomically and functionally distinct processing pathways have been proposed in the brain (Goodale & Milner, 1992; Mishkin, Ungerleider, & Macko, 1983). The ventral pathway projects from the primary visual cortex to infero-temporal cortex, and has been suggested to be predominantly involved in object processing. The dorsal pathway progresses from primary visual cortex to the PPC and is primarily involved in action-oriented, visuo-spatial processing. This dichotomy has proven conceptually useful and successfully accounts for a wide range of experimental findings. However, this framework is a simplification of a highly complex system and we can almost certainly rule out the idea that the ventral and dorsal streams should be functionally independent processing pathways (de Haan & Cowey, 2011; Schenk & McIntosh, 2010).

One prominent hypothesis is that the dorsal and ventral pathways specialise in absolute and relative disparity, respectively. This idea is based on the finding that neural populations in dorsal areas signal different disparity magnitudes while ventral areas process signal relative depth positions categorically (Goncalves et al., 2015; Preston, Li, Kourtzi, & Welchman, 2008; Srivastava et al., 2009). Based on these observations it has been suggested that the dorsal pathway predominantly processes absolute disparity while the ventral pathway processes relative disparity (Neri, Bridge, & Heeger, 2004; Uka & DeAngelis, 2006; Umeda et al., 2007). However, this proposed dichotomy is controversial. Several studies have shown that relative disparity is in fact processed in both pathways (Cottereau, McKee, Ales, & Norcia, 2011, 2012; Patten & Welchman, 2015).

Another proposed dichotomy incorporates fast but coarse disparity processing in the dorsal pathway, and slow but finer disparity processing in the ventral stream. This idea is based on the fact that neurons in dorsal areas monkey MT (Uka & DeAngelis, 2003, 2006) and AIP (Srivastava et al., 2009) process disparity faster than ventral neurons. However, the disparity differences processed in these sites are coarse. It has been suggested that this precision versus speed trade-off could be useful for adjusting hand movements during grasping (P. Janssen, Verhoef, & Premereur, 2018). In contrast to these findings, disparity processing in monkey ventral areas V4 (Shiozaki et al., 2012; Umeda et al., 2007; Watanabe et al., 2002) and inferior temporal cortex (IT) (P. Janssen et al., 2003, 2000; Verhoef, Vogels, & Janssen, 2012) has been found to be slow, yet finer disparity differences are still distinguished. In line with the general role of the ventral stream in vision, this mechanism could support more detailed 3D shape perception for successful object recognition (P. Janssen et al., 2018).

Finally, it has been proposed that the dorsal and ventral pathways specialise in different types of depth structures. Dorsal areas MT and caudal intraparietal sulcus (CIP) in monkeys have been found to respond to disparity which informs about surface slant (Thomas, Cumming, & Parker, 2002; Umeda et al., 2007). Ventral areas V2 and V4 in monkeys, on the other hand, are activated by disparity in centre surround constellations (Nguyenkim & DeAngelis, 2003; Rosenberg, Cowan, & Angelaki, 2013).

Which areas are involved in processing noisy disparity?

As discussed in this section, neurons along the dorsal and ventral pathway process increasingly complex aspects of stereopsis. An interesting question is where in the extrastriate cortex neurons specifically respond to noisy depth profiles. When testing observers, researchers have widely used noisy depth structures and asked observers to distinguish the depth profile of a centre-surround configuration. Based on the traditional dichotomy of dorsal and ventral pathways in disparity processing, we would anticipate that observers would disproportionately rely on the ventral processing pathway to process fine relative disparity differences in such centre-surround configurations.

However, contrary to this expectation, studies have found that dorsal area MT in monkeys preferentially responds to noisy disparity stimuli (DeAngelis et al., 1998; Uka & DeAngelis, 2003). Importantly, disruption of this area affects observers' depth perception for noisy depth structures which suggests that this area plays a crucial role in constructing a depth percept from noisy binocular disparity. In humans very similar results have been found in the posterior parietal cortex where the response to noisy depth structures is strongest

throughout the brain (Patten & Welchman, 2015), and where disruption of normal brain activity causes deficits in depth judgements for noisy depth structures (Chang, Mevorach, Kourtzi, & Welchman, 2014).

There are different potential explanations for this. Typical characteristics of dorsal disparity processing (as discussed above) could be beneficial for discriminating depth differences in noisy depth structures (e.g. using sufficiently large absolute disparities to make a quick but coarse near-far judgement). Alternatively, it is possible that these higher dorsal regions serve a purpose that is different from the previously proposed roles of the dorsal pathway in stereopsis. In the human brain, PPC has been shown to be involved in higher control mechanisms of perception such as evidence accumulation (Kelly & O'Connell, 2013; O'Connell, Dockree, & Kelly, 2012) and attentional control for optimal feature processing (Pessoa, Kastner, & Ungerleider, 2003).

To make matters more complicated, in both monkeys (Chowdhury & DeAngelis, 2008) and humans (Chang et al., 2014), the contribution of late dorsal regions is abolished by training observers on discrimination of fine depth differences with smooth depth structures. Additionally, after this training, ventral areas become critical for the judgement of noisy depth. This suggests that the role of higher dorsal areas in the processing of noisy disparity is only temporarily useful and becomes redundant through optimized processing of noisy disparity in ventral areas.

In **Chapter 4**, I investigate the contribution of the parietal cortex in the processing of noisy disparity. I use neuroimaging with a sufficiently high time resolution to identify whether PPC is engaged in early, feedforward disparity processing or late, top-down feedback to control perception and decision making. Further, I investigate the causal involvement of PPC in disparity processing, using brain stimulation intervention methods.

1.4 Brain stimulation

Now that I have established the perceptual problems that I investigate in this thesis, I will introduce the main research technique that was used to probe brain function. I applied brain stimulation to change brain activity and thereby reveal causal links between the function of brain areas and mechanisms of stereopsis. Here, I will describe how brain stimulation works and why it is a powerful tool to study stereopsis. Importantly, I will establish that brain stimulation can be successfully used in human observers to study visual perception.

Artificial stimulation of neurons

In 1781, Luigi Galvani discovered ‘animal electricity’ (electrophysiology). He found that connections of nervous tissue conduct electricity, and that this electricity controls contraction in connected muscle tissue (Bresadola, 1998). Hodgkin and Huxley (1952) were the first to reveal the role of this electricity for signal transmission in nervous tissue. They discovered that signals travel along nerve fibres as positive membrane voltages. Further, they pioneered the concept of artificial stimulation of neurons. The induction of positive stimulating currents inside a neuron increases the cell’s membrane voltage. If it reaches the neuron’s internal threshold, membrane sodium channels open and further increase the voltage to an action potential. This process can also be triggered by a stimulating current situated outside the neuron (Histed, Bonin, & Reid, 2009; Rattay, 1999). Indeed, external stimulation can trigger membrane potentials at the axon of the neuron, typically at areas where axon geometry becomes irregular.

Artificial stimulation of nerve cells has become a powerful tool for the research of the nervous system. Specifically, it allows the researcher to causally map functions inside the nervous system by relating induced changes in neural activity with observed changes in the behaviour of an organism. Fritsch and Hitzig (1870) pioneered this approach in living, behaving dogs to study the role of the motor system for voluntary body movement.

Electric stimulation has the potential to both drive or suppress neural activity in the brain (Rattay, 1999). While it is possible for an electric current to hyperpolarize neurons, this only happens under very specific conditions (Rattay, 1999), and it is therefore assumed that neuron suppression following stimulation results from the activation of inhibitory connections (Berman, Douglas, Martin, & Whitteridge, 1991; Chung & Ferster, 1998; Creutzfeldt, Watanabe, & Lux, 1966; Kara, Pezaris, Yurgenson, & Reid, 2002). Electrical stimulation of neural tissue triggers initial short excitation (Adrian & Moruzzi, 1939; Patton & Amassian, 1954) followed by two waves of GABA-ergic inhibition (Connors, Malenka, & Silva, 1988).

Transcranial Magnetic Stimulation

If we want to use brain stimulation to study brain function in humans, we have to do so non-invasively from outside of the head. Direct electric stimulation of the cortex from outside the head is challenging due to the high resistivity of the skull. Electrical currents administered on the scalp can affect the likelihood of neural activity in underlying brain areas with manageable side effects (Nitsche & Paulus, 2001). However, high voltages have to be used

to actively change neural activity and this creates very unpleasant side effects such as headaches, nausea, muscle pain, disorientation and memory loss (Datto, 2000; Devanand, Fitzsimons, Prudic, & Sackeim, 1995). An alternative approach is to use a magnetic field to induce an electric current into the brain. A strong electric pulse is discharged through a coil which is placed on the scalp. This creates a rapid, time-varying magnetic field which safely passes through the skull and creates electric current within the underlying brain area (see **Fig. 1.8**). This technique is called transcranial magnetic stimulation (TMS) and was first pioneered by Barker, Jalinous and Freeston (1985). When placed over the motor cortex, the coil reliably triggers motor potentials which result in observable muscle twitches.

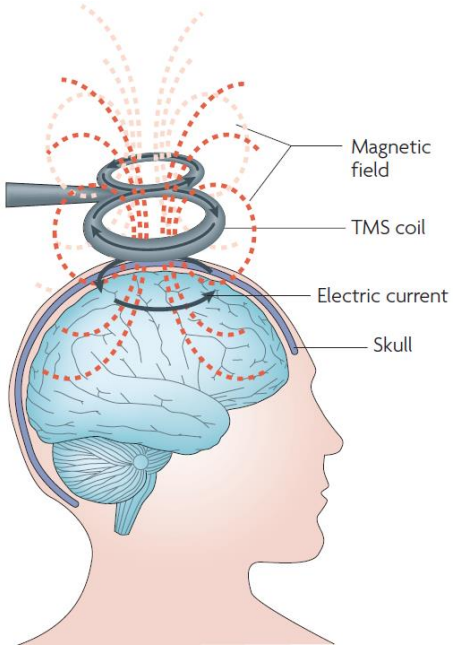

Figure 1.8: Illustration of TMS. An electric current is passed through a coil and creates a magnetic field which passes through the scalp (see magnetic field lines in red). In the brain the magnetic field induces a secondary electric current which in turn changes neuron activity. Adapted from Ridding and Rothwell (2007).

TMS has been shown to cause similar effects in nervous tissue as direct, intra-cranial stimulation. The characteristic effects of initial excitation (Boroojerdi, Battaglia, Muellbacher, & Cohen, 2001; Devanne, Lavoie, & Capaday, 1997; C. W. Hess, Mills, & Murray, 1987; Ziemann, Lönnecker, Steinhoff, & Paulus, 1996) and subsequent GABA-ergic inhibition (Kujirai et al., 1993; Murphy, Palmer, Nyffeler, Müri, & Larkum, 2016; Premoli et al., 2014) of neurons has been observed with TMS in the human motor cortex. This technique should, in

principle, work similarly for any part of grey matter tissue in the brain (Histed et al., 2009). In cat primary visual cortex, TMS predominantly triggers suppression of simple and complex cells (**see Fig. 1.9**) (Moliadze, Giannikopoulos, Eysel, & Funke, 2005; Moliadze, Zhao, Eysel, & Funke, 2003).

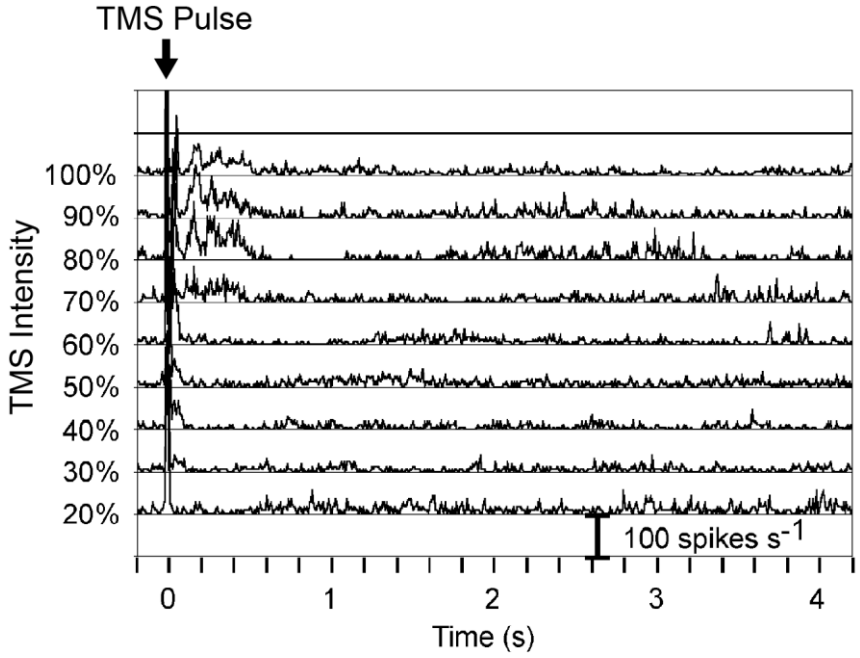

Figure 1.9: Effect of TMS on V1 neuron activity. Firing rate of a cat complex cell in V1 following TMS during spontaneous activity. TMS changes neuron activity and these changes become more pronounced as the stimulation intensity is increased. Adapted from Moliadze et al. (2003).

Depending on the structure of a neural circuit, TMS will trigger a different ratio between activation and inhibition. Further, depending on the role of these networks in perception, activation and inhibition of certain neuron sub-populations will have different effects on sensory perception. Additionally, it has been shown that changes in neural activity, caused by TMS, do not simply wipe out sensory activation. Rather, both activity patterns interact (Miniussi, Harris, & Ruzzoli, 2013). TMS has been shown to impair sensory discrimination for visual cues such as motion direction (Pascual-Leone, Bartres-Faz, & Keenan, 1999), motion speed (McKeefry, Burton, Vakrou, Barrett, & Morland, 2008), object shape (Silson et al., 2013) and Gabor orientation (Rahnev, Maniscalco, Luber, Lau, & Lisanby, 2012). It has been argued that brain stimulation results in random neural noise, which compromises cell populations that encode relevant visual features (J. A. Harris, Clifford, & Miniussi, 2008).

However, TMS induced activation has also been shown to sum with sensory activation in a meaningful way to improve detection accuracy (Abrahamyan, Clifford, Arabzadeh, & Harris, 2015, 2011; Schwarzkopf, Silvanto, & Rees, 2011). It has been suggested that TMS induced activation can push sensory activation over an internal threshold for signal detection (Miniussi et al., 2013).

However, these explanations are often formulated post hoc to intuitively describe an effect of TMS on perception. In most studies, brain activity is not recorded during stimulation and thus we cannot know how TMS affects brain activity. Many parameters such as the distance between coil and cortex (Stokes et al., 2013), stimulation frequency (Brasil-Neto, McShane, Fuhr, Hallett, & Cohen, 1992; Robertson, Théoret, & Pascual-Leone, 2003), electric current flow direction relative to the brain tissue (Brasil-Neto, Cohen, et al., 1992; A. M. Janssen, Oostendorp, & Stegeman, 2015; Kammer, Beck, Erb, & Grodd, 2001) and the state of neurons prior to stimulation (Kiers, Cros, Chiappa, & Fang, 1993; Thompson et al., 1991) have been found to affect the outcome of stimulation. Importantly, the geometry of the neuron within the electric current will ultimately define whether its activity is changed by TMS (Rattay, 1999). Consequently, it is challenging to assess the efficacy of human brain stimulation and interpret null results in TMS research. Did brain stimulation not change neural activation? Does the architecture of excitatory and inhibitory connections in a brain area not allow net-effects of stimulation to become relevant on a behavioural level? Or is there no sufficient bottle neck of sensory processing, meaning that we are affecting neural activity locally but a different area of the brain with normal neuron activity can compensate?

So how can we assess whether a certain part of the human brain is amenable to brain stimulation? In specific systems of the brain, stimulation can trigger propagating activation which becomes externally observable. With the motor system at rest, TMS over the motor strip can reliably trigger cortico-spinal activation which results in muscle twitches in the contra-lateral hand (Barker et al., 1985). When applied to the visual cortex, TMS can trigger brain activation which results in a conscious percept. These sensations are described as flashes of light and the term ‘phosphenes’ was coined to describe them (Marg & Rudiak, 1994). Concurrent functional Magnetic Resonance Imaging (fMRI) and TMS shows that TMS triggers local activation which in turn causes a cascade of activation spreading throughout the brain when phosphenes are reported (Caparelli et al., 2010). Animal models of phosphenes suggest that activation spreading back to V1 underlies the conscious percept (Tehovnik & Slocum, 2013). These phosphenes are therefore a useful marker to identify whether a particular portion of cortex is amenable to stimulation with TMS. However, so far there has not been a systematic attempt to map out where in the visual cortex TMS can trigger phosphenes. In **Chapter 1** of this thesis, I investigate where in the visual cortex

stimulation can produce phosphenes. This tells us whether stimulation of a given area in the brain by TMS drives propagating neural activation.

Thus far, I have discussed how brain stimulation can change neuron activity during its application. However, brain stimulation has been shown to have lasting effects on neuron activity beyond the window of stimulation. Repetitive electrical stimulation can manipulate the efficacy of synaptic transmission leading to long-term potentiation and depression of synaptic connections of individual neurons (Froc, Chapman, Trepel, & Racine, 2000; G. Hess & Donoghue, 1996; Larson & Lynch, 1986; Trepel, 1998). Repetitive theta-burst TMS for 40 seconds has been shown to introduce long term depression of synaptic transmission in human motor cortex (Huang, Edwards, Rounis, Bhatia, & Rothwell, 2005). Theta burst stimulation affects NMDA receptors which modulate synaptic connections (Huang, Chen, Rothwell, & Wen, 2007) and thereby reduces the probability of synaptic transmission in underlying brain tissue. This intervention is powerful because it allows researchers to record brain activity while TMS affects neural activity. In this way we can relate changes of perception after stimulation to recorded changes in brain activity and identify the contribution of brain areas to perception. However, the effect of theta-burst TMS has, thus far, only been replicated in the motor cortex (Huang et al., 2007) and the outcome of stimulation can be variable among individuals (Hamada, Murase, Hasan, Balaratnam, & Rothwell, 2013; Hasan et al., 2012; Hordacre et al., 2016). It is unclear whether theta-burst stimulation can affect synaptic connections in sensory cortex. Specifically, it is unknown whether the effect of theta-burst relies on the unique neural network architecture of the cortico-spinal projections in the motor cortex (Hamada et al., 2013). In **Chapter 3** of this thesis, I investigate how theta burst stimulation can affect synaptic transmission in parietal cortex and how this affects stereopsis.

1.5 Thesis overview

In the following chapters, I will describe three research projects in which I have used brain stimulation to study perception.

In **Chapter 2**, I describe where in the human brain TMS triggers phosphenes. I relate this to the retinotopic organisation and the location of object- and motion-selective areas. The goal is to substantiate where in the visual cortex TMS can be used to change neural activity.

In **Chapter 3**, I characterize a mechanism of stereopsis which is challenged by noisy binocular disparity and produces a mixed contrast polarity benefit for stereopsis. Particularly, it is unclear where in the brain this mechanism of stereopsis is located. I use TMS to change normal neural activity in several key areas of binocular disparity processing to identify where the benefit arises and thereby located the mechanism that is challenged by noisy depth information.

In **Chapter 4**, I examine what role the PPC plays for stereopsis with noisy depth information. I apply TMS to disrupt synaptic transmission in the parietal cortex and subsequently record electroencephalography (EEG) from the visual cortex. The goal is to establish whether PPC is engaged in early, feedforward disparity processing or late, top-down feedback to control perception and decision making.

2. Mapping the visual brain areas susceptible to phosphene induction through brain stimulation

This chapter reproduces the work associated with the following published manuscript: Schaeffner, L. F., & Welchman, A. E. (2017). Mapping the visual brain areas susceptible to phosphene induction through brain stimulation. Experimental Brain Research, 235(1), 205–217.

While the content of the chapter is identical to the manuscript, some modifications have been made to ensure that the chapter is well integrated with the rest of the thesis. For consistency, the references to figures have been updated to reflect the structure of the thesis.

2.1 Introduction

TMS is a non-invasive technique that can be used to temporarily disrupt normal neural activity (Robertson et al., 2003; Sandrini, Umilta, & Rusconi, 2011; Walsh, Pascual-Leone, & Kosslyn, 2003). This makes it possible to investigate the causal relationship between particular cognitive functions and the network of brain activity that supports those functions (De Graaf & Sack, 2014; Pascual-Leone, Walsh, & Rothwell, 2000).

However the efficacy of TMS related effects relies on a great number of parameters: for instance, the timing, intensity, duration or current flow direction of stimulation (De Graaf & Sack, 2011; Robertson et al., 2003; Sandrini et al., 2011). This poses an interpretative challenge to experimenters: when we apply TMS we need some reassurance that the method can effectively change neural activity at a particular target site in the brain (De Graaf & Sack, 2011).

In most regions of the brain it is difficult to directly observe the effects of TMS since there is no immediate, overt perceptual or behavioural response. However, in limited areas of the brain TMS triggers a response making it possible to probe the efficacy of TMS at the target location. In particular, in the visual cortex TMS can result in an visual phosphene (Marg & Rudiak, 1994), that provides a measure of whether a given stimulation protocol evokes

sufficient neural excitation to reach conscious awareness (De Graaf & Sack, 2011; Silvanto, 2013; Walsh et al., 2003). Thus, this marker is useful in identifying that a particular portion of the cortex is amenable to testing using TMS.

Nevertheless, there is some uncertainty about exactly which parts of the visual cortex will yield a phosphene through stimulation. Previous work reported that phosphenes are induced most reliably over early visual cortex near the cortical midline (Kammer, Puls, Erb, & Grodd, 2005; Marg & Rudiak, 1994), although this work did not investigate the stimulation outcome for all identified retinotopic visual areas.

Other work has suggested stimulation locations relative to anatomical landmarks such as the inion (Elkin-Frankston, Fried, Pascual-Leone, Rushmore, & Valero-Cabre, 2010; Gerwig, Kastrup, Meyer, & Niehaus, 2003). However these suggestions vary between studies and there is evidence that functional brain architecture is not well described by scalp landmarks (Sack et al., 2009).

Salminen-Vaparanta et al. (2014) used detailed retinotopic maps and current modelling to show that separate stimulation of both V1 and V2d is equally capable of inducing phosphenes. Their approach underlines that we need to have knowledge of the individual functional structure of the visual cortex if we want to understand where in the brain phosphenes can be induced.

Here, I therefore sought to assess the efficacy of TMS for phosphene induction where I had an understanding of which portions of visually responsive cortex were being targeted by TMS. In particular, I systematically map out the locations at which participants report phosphenes and relate these to the retinotopic organisation and the location of object- and motion-selective areas of the visual cortex as revealed by fMRI measurements. To anticipate, my results demonstrate that phosphenes are induced reliably over early visual areas (V1, V2d, V2v) and dorsal areas (V3d, V3a), and confirm previous observations that phosphenes are more likely to be induced close to the cortical midline (Kammer et al., 2005; Marg & Rudiak, 1994).

2.2 Methods

Participants

I tested 30 healthy participants (18 female; age range from 20 to 38, *M* = 26.43, *SD* = 4.32, including the author L.F.S.) to determine whether they perceived phosphenes under TMS

stimulation. Before the experiment, participants provided written informed consent and were screened for contraindications to fMRI and TMS (Rossi, Hallett, Rossini, & Pascual-Leone, 2009; Wassermann, 1998). Procedures were approved by the University of Cambridge ethics committee and were performed in accordance with the ethical standards laid down in the Declaration of Helsinki. Twenty-one participants (70%) reported a percept after stimulation; the remaining nine did not report experiencing a phosphene under my TMS protocol. Eight participants reported a percept after control stimulation and were therefore excluded from the experiment. One participant aborted the screening procedure complaining of the side effects of TMS. Twelve participants reported phosphenes reliably. Of these, seven participants (two female; age range from 23 to 32, *M* = 26.29, *SD* = 3.4, including the author L.F.S.) agreed to continue to the main experiment.

Experimental setup and Stimulation

The experiment was conducted in a dimly lit room using a black screen with low luminous intensity (0.15 cd/m^2). I instructed participants to maintain fixation at a bright dot in the centre of the screen. I allowed five minutes for adaptation to the illumination before the start of the experiment.

I applied single TMS pulses with a biphasic MagStim Rapid^2 stimulator (MagStim, Whitland, UK) via a figure-of-eight coil (outer winding diameter = 70 mm). Throughout the experiment a minimum stimulation onset asynchrony of 3 seconds was used to avoid TMS related long term effects and muscle fatigue (Kammer, Beck, Erb, et al., 2001; Kammer et al., 2005). The induced current direction (during the initial, rising phase of the biphasic waveform) was lateral to medial in the targeted hemisphere (Kammer, Vorwerg, & Herrnberger, 2007; Taylor, Walsh, & Eimer, 2010) and the coil handle pointed away from the head laterally. Stimulation was applied over the left hemisphere.

Phosphene Screening

Phosphenes were described to participants as flashes of light or distortions of the visual field. I provided verbal and graphic illustrations of phosphenes described by previous literature (Marg & Rudiak, 1994). Participants were asked to give a conservative yes-no response, only reporting a percept when they were absolutely sure. At the start of the experiment participants performed a control task to test if phosphenes could be induced and to validate the percept:

(i) Feedback about the percept had to match previous descriptions from Marg and Rudiak (1994).

(ii) Phosphenes had to appear in the visual hemifield contralateral to the stimulated hemisphere or both hemifields, due to the organization of the early visual cortex (Kammer et al., 2005).

(iii) Perception of phosphenes had to be possible with eyes open and closed (Fried, Elkin-Frankston, Rushmore, Hilgetag, & Valero-Cabre, 2011; Kammer & Baumann, 2010).

(iv) Stimulation of brain tissue distant from the visual cortex, over the vertex (Cz), should not produce a percept (Fried et al., 2011).

Participants were tested for phosphenes with a hunting procedure in a 4x4cm window over the visual cortex. The centre of the window was located 4cm caudal and 2cm lateral relative to the inion (Elkin-Frankston et al., 2010; Gerwig et al., 2003). For two participants a MRI anatomical scan was available prior to the experiment. For these participants hunting stimulations were applied at 16 equally spaced stimulation targets. For the remaining participants stimulations were applied randomly within the defined window on the scalp. I applied stimulation at 80% stimulator output, approximately 130% of the average phosphene threshold reported in previous studies using the same stimulator and coil model (Abrahamyan, Clifford, Ruzzoli, et al., 2011; Stokes et al., 2013).

I applied 48 hunting stimulations. The coil was moved to a new location after each hunting stimulation. If participants reported a phosphene, ten stimulations with eyes open and ten stimulations with eyes closed were applied at the same location to assess how frequently phosphenes could be induced. The screening was successfully finished after participants described phosphenes at five different stimulation locations. If participants did not describe a percept in 48 hunting stimulations the screening was aborted. At three different times during the screening ten control stimulations were applied over the vertex (Cz). The number of stimulations I applied during screening depended on the performance of the participant and could range from 48 stimulations (no phosphenes perceived) to 178 stimulations. Participants that reported more than one phosphene after vertex stimulation (n = 8) or could not perceive more than three phosphenes out of ten TMS pulses at any stimulation location (n = 9) were excluded from the experiment.

Functional Magnetic Resonance Imaging

Data were acquired with a three-tesla scanner. For all participants a high resolution anatomical scan (1 mm^3) was acquired. For all scans blood oxygen level-dependent signals were measured with an echo-planar imaging sequence. Retinotopic areas V1, V2, V3d, V3a, V7, V3v, and V4 were defined with standard retinotopic mapping procedures using rotating wedge stimuli. The borders between functional areas were defined by the resulting angular maps (Wandell, Dumoulin, & Brewer, 2007). I identified the hMT+/V5 complex as a group of voxels that responded significantly more ($p < 0.01$) to a coherently moving array of dots than to a static array of dots (Zeki et al., 1991). The lateral occipital complex (LO) was mapped as the set of voxels that responded significantly ($p < 0.01$) stronger to intact than scrambled images of objects (Kourtzi, Betts, Sarkheil, & Welchman, 2005). I analysed fMRI data with BrainVoyager QX (BrainInnovation B.V.).

Neuronavigation

I created a curvilinear reconstruction of the cortex from anatomical MRI data. I used a fully automated algorithm provided by Brainsight 2.2.12 (Rogue Research, Montreal, Canada) which is based on the Brain Extraction Tool (Smith, 2002). I "peeled" the reconstruction 4 mm deep to guarantee that stimulation targets were located within the cortex. The curvilinear reconstruction was co-registered to the participant through anatomical landmarks on the head (the tip of the nose, the bridge of the nose and the notch above the tragus for the left and right ear). During the experiment, I monitored the position of the TMS coil and the participant's head with an infrared camera and Brainsight 2.2.12 neuro navigation software. A normal vector originating in the centre of the figure-of-eight TMS coil helped to guide the coil to a defined location over the curvilinear reconstruction.

I generated a 6x8 stimulation target grid (10 mm inter-target-distance). I placed this over the curvilinear cortical reconstruction with a 5 mm offset from the interhemispheric cleft and the cerebellum (See **Fig. 2.1A**). For each target an ideal trajectory was defined approximately normal to the curvilinear surface. A targeting error was defined as the distance from a target in the brain to the vector projecting from the coil into the human head. Angular error was defined as the angle of the coil vector with respect to the target trajectory (See **Fig. 2.1B**). During stimulation both values were monitored, targeting error was kept <1 mm, angular error was kept <15° as suggested by the Brainsight 2.2.12 manual.

The coil positions for respective targets in the brain covered a large window on the scalp at the back of the head. The location of this window is described relative to the inion for easy replication without stereotactic neuronavigation (See **Fig. 2.1C**).

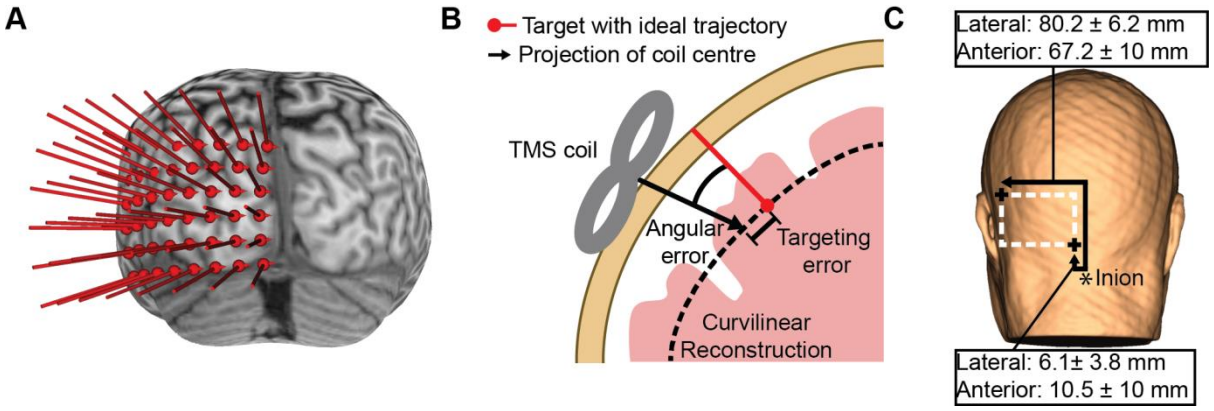

Figure 2.1: Illustration of systematic TMS over the visual cortex. A) Posterior view of the curvilinear reconstruction of the cortex (peel depth 4 mm) for one participant. Stimulation targets were placed equidistant over the visual cortex with a 5 mm offset to the interhemispheric cleft and the cerebellum. **B)** Illustration of online coil monitoring during the experiment with stereotactic neuronavigation. One stimulation target and the ideal trajectory are shown in red on the curvilinear reconstruction (dashed line). The trajectory marks the ideal coil position on the scalp. A vector projecting from the centre of the TMS coil defines the current position relative to brain and stimulation target. For the displayed coil position, the targeting error (distance on the curvilinear surface) and the angular error (angle of the coil vector with respect to the target trajectory) are shown. **C)** Window of coil locations on the scalp (dashed line) for stimulation targets in **A**. The outer borders of an average stimulation window for all participants is described as the offset (Mean ± SEM in mm Euclidean distance) of two corner points (plus sign) to the inion (asterisk) along the scalp.

Cortical excitability

For each participant, I defined an excitation threshold, using the REPT adaptive staircase method (Abrahamyan, Clifford, Ruzzoli, et al., 2011). REPT estimates excitation thresholds from 30 stimulations. Thresholds mark the stimulation intensity (% stimulator output) at which a phosphene can be elicited in 50% of the stimulations.

I defined the phosphene threshold at the grid target closest to the centre of area V3d (This target tended to lie in the centre of the window that was used in the initial phosphene

screening test). Stimulations were applied in a range of 45 to 90% stimulator output. For the remaining 47 stimulation targets, I used an adjusted phosphene threshold calculated by correcting stimulation intensity for the distance to the underlying cortical surface (Stokes et al., 2013). I obtained the surface of the cortex with the segmentation routine (Kriegeskorte & Goebel, 2001) from Brainvoyager QX 2.8 (Brain Innovation, Maastricht, The Netherlands). I then calculated the average distance from the TMS coil on the scalp to the closest 100 vertices of the cortical surface segmentation (Cai et al., 2012). For all targets this method gave a slightly closer distance estimation than the estimate used by Stokes et al. (2013) (Mean difference:–2.17 mm, SD: 0.52 mm).

Mapping phosphenes

In the main experiment, stimulation at each grid target was set at 110% of the estimated phosphene threshold (Salminen-Vaparanta et al., 2014). For some targets stimulation intensity suggested by the adjustment algorithm exceeded 90% stimulator output which I used as an upper limit on stimulation intensity. In these cases, stimulation was delivered at 90% of the stimulator's output. For one participant with a high phosphene threshold all targets reached this correction limit, hence no correction was performed. Stimulation results for this participant are marked in **Fig. 2.2A**. In another four participants between 1 and 4 targets were corrected. Overall for 59 out of 336 targets the stimulation intensity was corrected to an upper limit.

An important question is whether this correction limit systematically affected the stimulation outcome. Targets where stimulation intensity was corrected to an upper limit were located in almost all functional areas (V1(x1), V2v(x1), V2d(x6), V3d(x4), V3a(x5), hMT+/V5(x2), LO (x8)). Of the corrected stimulations (n = 590) 23% induced a phosphene. For comparison: considering all stimulations applied in this study, 30% induced a phosphene. It is therefore possible that the outcome of stimulations, where intensity was capped at an upper limit, underestimates the susceptibility of the targeted areas for phosphene induction. However, this correction limit was applied mostly in both areas with a high (V3, V3a) and a low (hMT+/V5, LO) phosphene incidence which shows that this did not uniquely affect specific areas.

The intensities used in this experiment ranged from 48 to 90% stimulator output. For each grid location 10 stimulations were given, totalling 480 stimulations per participant. The order of the stimulations for all targets was randomized. Participants were tested on separate days in three sessions that lasted approximately two hours (160 stimulations per session).

Location of TMS effects in the brain

I located the centre of gravity (CoG) of TMS which estimates the point on the cortical surface where the maximum electric field is induced. For this, I used a balloon inflation projection method (Okamoto & Dan, 2005). The algorithm uses the centre position of the coil on the scalp and a segmentation of the grey matter surface (~140,000 vertices for one hemisphere). I identified the 200 surface points closest to the coil centre. A vector was drawn from the coil centre through the mean coordinates of the 200 surface points. I defined a rod with a 5mm radius around the vector, given that stimulation targets in the brain were placed in 10mm equidistant steps. The surface point within the radius closest to the vector was defined as the CoG for TMS stimulation for the given coil position. This CoG was used to assign stimulation effects to underlying functional areas in the visual cortex.

This algorithm takes into account the local curvature of the cortex and gives a more realistic estimate of the location of strongest current induction than a perpendicular vector projection from coil to cortical surface (Diekhoff et al., 2011; Weiss et al., 2013). Specifically this projection method is not affected by coil tilt, whereas perpendicular projections have been found to overestimate the effect of coil tilt for a range of up to 15 degrees used in this study (Opitz et al., 2013).

To validate the CoG locations from my projection method, I created a realistic current model for stimulation at 17 coil positions that targeted functional areas in one participant. I used simNIBS 2.0 (www.simnibs.org; Windhoff, Opitz, & Thielscher (2013)) to model current distributions with a finite element method. This model respects the effects of coil tilt as well as the effects of different tissue conductivity and individual cortical architecture on the induced current. I constructed a finite element method model consisting of 1.1 million tetrahedra based on a structural MRI. I assigned electrical conductivities to different tissue types as described by Windhoff et al. (2013). Isotropic conductivity was assumed. A magnetic dipole model for a MagStim 70mm figure-8 coil was provided by simNIBS. I simulated stimulation for all targeted areas with coil position coordinates as used in the experiment. Stimulator output for a given stimulation intensity was defined relative to the peak current at 100% stimulator output as provided by MagStim. Since the output is a sinusoidal waveform, stimulator output was calculated as the root mean square of the peak current for a pulse duration of 300ms.

To validate that functional areas received stimulation as predicted by my projection method, I defined an area of stimulation for each coil position based on the current model: This area was defined as all surface points where the electric field intensity was between 80 and 100% of the maximum current (Wagner, Rushmore, Eden, & Valero-Cabre, 2009). By comparing

which of these surface points fell into which functional areas, I defined the functional area that received the maximum amount of stimulation as the target for a given coil position.

Effects of current direction on phosphene induction

I retested three participants in a control study to test whether current direction of TMS systematically affected the stimulation outcome. Participants received twenty training stimulations with the stimulation parameters of the main experiment to confirm that TMS still created a percept. Additionally all participants received ten control stimulations over Cz to reconfirm that percepts were not induced through stimulation side effects.

I applied stimulations with the original lateral to medial current direction as well as three alternative current directions: Posterior to anterior (coil rotated 90 degrees counter clockwise), medial to lateral (coil rotated 180 degrees counter clockwise) and anterior to posterior (coil rotated 270 degrees counter clockwise). A range of 360 degrees was tested because (Kammer et al., 2007) found different stimulation outcomes for opposing current directions with a biphasic stimulator.

For each participant, I applied stimulations for all current directions at nine coil locations: three locations that yielded no phosphenes during phosphene mapping, three locations that yielded a small number of phosphenes (1-5 out of 10 stimulations) and three locations where a high number of phosphenes were induced (6-10 out of 10 stimulations). This allowed me to assess whether current orientation systematically affected the differences in susceptibility to phosphene induction that I observed during phosphene mapping.

Reliability of phosphenes as a signature of stimulation

In this study, 18 out of 30 participants did not perceive phosphenes reliably through TMS. It is possible my single pulse protocol induced insufficient neural activation in these participants. I retested six participants that reported no percept through single pulse stimulation with a more powerful repetitive TMS (rTMS) protocol that was reported to induce a percept in every participant (Boroojerdi et al., 2002; Ray, Meador, Epstein, Loring, & Day, 1998). 32 pulse trains (10Hz, 5 pulses, 0.5sec) were applied with 70% stimulator output at original screening locations until a percept was reported. rTMS was followed by another screening with single pulse stimulation.

Data analysis

I conducted statistical analysis using SPSS (IBM, Inc). I fitted a binary logistic regression model to a pooled data set of all stimulations to test whether distance of stimulation site to the interhemispheric cleft could predict the outcome of stimulation. Stimulation intensity and the distance between coil and cortical surface were included as potential covariates. Stimulations were grouped in four groups of stimulation intensity (48-60%, 61-70%, 71-80% and 81-90% stimulator output) and four cortical distance groups (8-11 mm, 12-14 mm, 15-17 mm and 18-22 mm distance to the cortical surface). Since I adjusted stimulation intensity for the underlying cortical distance the two potential covariates were correlated (r = .33, p < .01) and were therefore added in separate models. I performed polynomial contrasts to test if there was an increase in the number of phosphenes for higher stimulation intensity or decrease for higher cortical distance. For all significant predictors a partial correlation was derived from the respective Wald statistic.

I assessed whether the probability of inducing a phosphene changed during a two hour testing session. In particular, I compared the number of phosphenes reported over intervals of 20 stimulations (~15 minutes of testing) using a Repeated Measures ANOVA. I also calculated Cronbach's α as a measure of test-retest reliability for the number of phosphenes reported over session intervals. Additionally, I examined whether the probability of inducing a phosphene changed between different testing sessions. I calculated Cronbach's α for the number of phosphenes reported at different testing days.

2.3 Results

Participants were initially screened to determine whether TMS of the visual cortex would yield the perception of phosphenes. Of the thirty people tested, I found that twelve reliably reported phosphenes. From this group, seven participants were willing to take part in the phosphene mapping experiment. I systematically applied TMS over a grid of locations covering the visual cortex (see **Fig. 2.1A**) and recorded the probability of inducing a phosphene at each location.

Phosphene Frequency at stimulation targets

Across all the TMS stimulation locations tested, I found that phosphenes were induced with a probability of 30% (SD: 6%). **Fig. 2.2A** shows a map for each participant with the number

of phosphenes that were induced with ten stimulations at targets over the visual cortex. For most participants, stimulations in the dorsal visual cortex close to the interhemispheric cleft were most likely to induce a phosphene percept. **Fig. 2.2B** shows this trend in a group map.

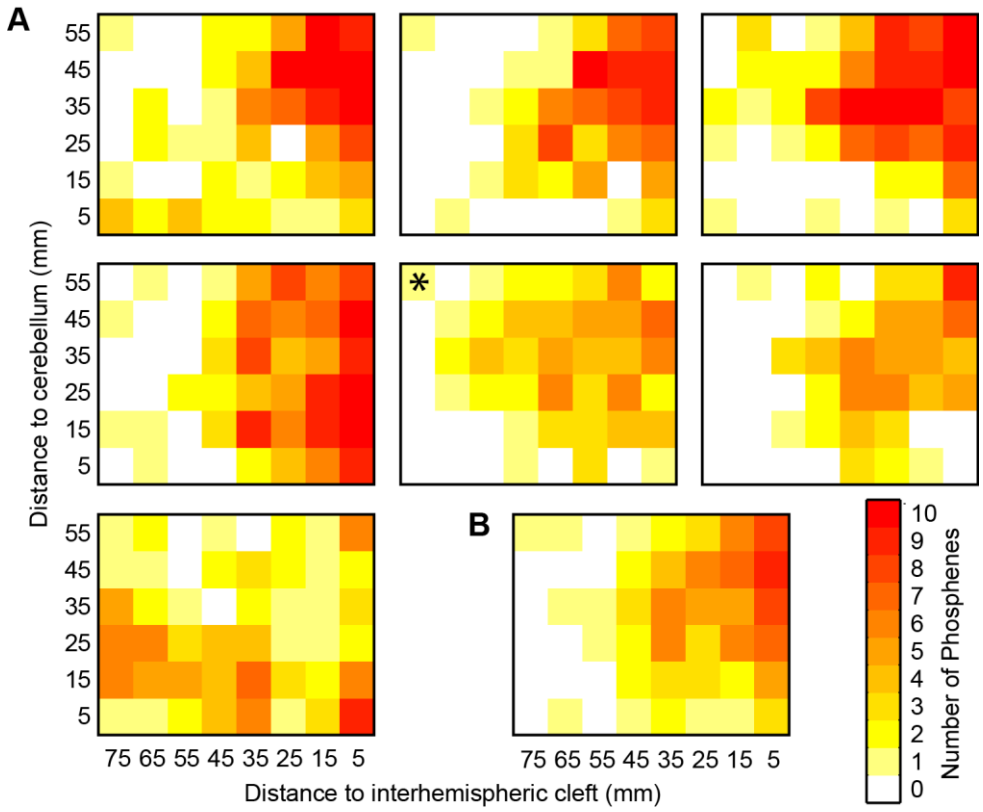

Figure 2.2: Probability of phosphene induction over the visual cortex. Individual (**A**) and median (**B**) stimulation results for all participants (n=7). The colour of the heat map indicates the number of phosphenes that were perceived in ten stimulations at the defined targets shown in **Fig. 2.1A**. An asterisk marks the stimulation results for one participant for whom stimulation was always applied at the maximum stimulator output used in this experiment.

I used a logistic regression analysis to identify stimulation parameters that predict the outcome of stimulation. I found that moving the stimulation site away from the interhemispheric cleft in 10 mm steps reduced the probability of inducing a phosphene through stimulation (B=–0.046, SE=0.002, p<.001, R=–.35), model fit: $\chi^2(1)=624.21$, p<.001. (**Fig. 2.3**). There was no significant increase in the number of perceived phosphenes with

increasing stimulation intensity (*B*=–0.18, *SE*= -0.2, *p* = .370) or decrease in the number of phosphenes with larger distances to the cortical surface (*B* = -0.08, *SE* = 0.2, *p* = .68).

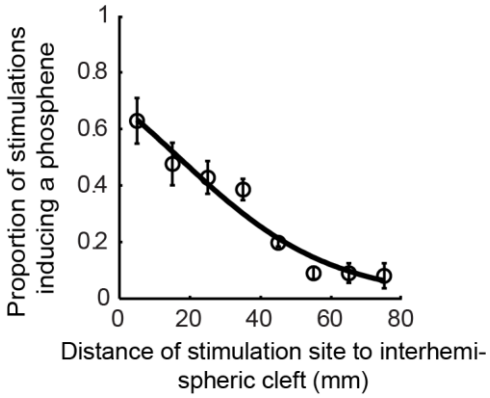

Figure 2.3: Probability of phosphene induction at the interhemispheric cleft. Mean proportion of TMS stimulations that induced a phosphene (circles), displayed as a function of the distance from stimulation site to the interhemispheric cleft. Error bars show the variability (SEM) of results for individual participants. A solid line shows the outcome of stimulation predicted for different stimulation locations by a binary logistic regression model that was fitted to the observed data

Phosphene induction in different functional areas of the visual cortex

For each coil position, I defined a point of the maximum stimulation effect on the cortical surface. **Fig. 2.4** shows a flatmap of the visual cortex (pial surface) for two participants, the defined centre points of stimulation and outlines of functional areas are superimposed. Since the effect of TMS decays as a function of distance from the coil to the cortical surface, maximum stimulation effects were often located on gyral crowns in the superior parts of the visual cortex (see **Fig. 2.4**). From this, it follows that some functional areas were targeted more often than others.

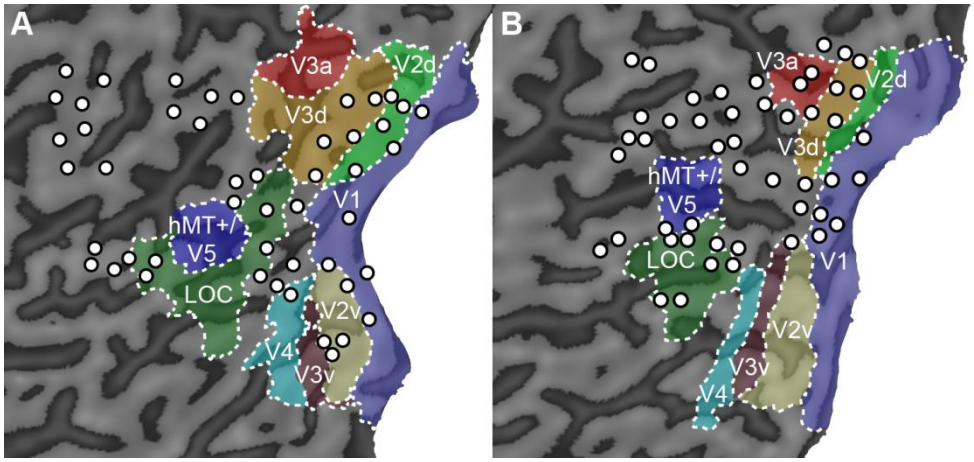

Figure 2.4: Retinotopic maps and projected TMS effect locations. Flatmaps for two participants showing retinotopic areas, hMT+/V5 and LO projected on the pial surface with Brainvoyager 'VOI to POI plugin'. Sulci are shown in dark grey, gyri in light grey. For each stimulation target I defined a centre of TMS related effects (circles). Due to the decay of TMS related effects over distance they are mostly located on gyral crowns. Depending on individual brain anatomy, I was not able to target areas with TMS that are located on the bottom of a sulcus (**A** V3a and hMT+/V5) or buried between cerebrum and cerebellum (**B** V2v, V3v and V4)**.**

Table 2.1 shows the mean probability of inducing phosphenes for all stimulations that fell in respective functional areas. Stimulations of early visual cortex produced phosphenes reliably (V1: 40.8%, V2d: 45.4%, V2v: 41.7% of stimulations). Stimulation of areas along the dorsal pathway had the highest chance of inducing a phosphene (V3d: 60%, V3a: 56.4% of stimulations). At higher visual areas stimulation seldom produced a percept (hMT+/V5: 13.8%, LO: 12.8% of stimulations).

There was a significant difference in how often TMS produced phosphenes between primary visual cortex (V1) and dorsal visual areas (V2d, V3d, V3a) ($F_{3,9}$=3.8, p=.05). The probabilities in **Table 2.1** suggest that TMS induces phosphenes more frequently over dorsal areas than over the primary visual cortex. However, pairwise comparisons did not reveal significantly higher phosphene probabilities over dorsal areas compared to the primary visual cortex (V1 vs. V2d: t_5=-0.84, p=.44; V1 vs. V3d: t_5=-2, p=.11; V1 vs. V3a: t_3=-2.12, p=.12). This could be due to the very small number of people tested in this study and so these pairwise comparisons unfortunately cannot reveal in which dorsal area TMS induces phosphenes significantly more often than in the primary visual cortex.

There were only very few stimulations that targeted ventral visual areas V3v and V4 (less than fifty stimulations pooled over all participants). These functional areas are hidden between the bottom part of the Cerebrum and the Cerebellum and are therefore hard to reach with TMS in most people (see **Fig. 2.4**). Due to the anatomical constraints, increasing the number of participants would not necessarily have resulted in a dramatic increase in the number of stimulations to these areas. I therefore present the data, but deliberately do not include these areas in the discussion of the study.

Table 2.1: Probability of phosphene induction in different visual areas. Probability (percentage) of producing a phosphene through stimulation of functional areas. Results are averaged across participants.

Functional area	Mean (±SEM) phosphene probability in % of stimulations	Number of stimulations	Number of participants
V1	40.8 (9.5)	260	6
V2d	45.4 (7.3)	280	7
V3d	60 (9.3)	200	7
V3a	56.4 (12.8)	120	5
V2v	41.7 (22.4)	60	3
V3v	40 (20)	20	2
V4	40 (0)	10	1
hMT+/V5	13.8 (8.9)	80	4
LO	12.8 (5.6)	290	7

Cortical excitability

TMS related effects might build up over time during repeated stimulation, changing cortical excitability over the duration of a TMS experiment (Walsh et al., 2003). In this experiment the average number of phosphene perceptions did not differ significantly over eight subintervals (8x20 stimulations) of a test session ($F_{7,140}<1$, $p=.75$), and showed good test-retest reliability for all participants (Chronbach's $\alpha=.76$). This suggests that cortical excitability did not change as a function of time or number of applied stimulations during the experiment. Given

that I applied single pulse stimulation and kept a minimum stimulus onset asynchrony of 3 seconds I did not expect any long lasting effects induced by TMS.

Another concern was that cortical excitability might fluctuate for different days and therefore affect my findings at different testing sessions (Walsh et al., 2003). I found that the average numbers of phosphenes perceived in different testing session did not differ significantly ($F_{1.12,6.72}$=2.96, p=.13) and were reliable (Cronbach's α=.69) for all participants. This suggests that any changes in cortical excitability across testing days are unlikely to have had a strong influence on my findings.

Location of TMS effects in the brain

To validate localization of stimulation effects with a projection method I compared the outcome to a realistic current model for 17 coil positions. I found a good correspondence between the target areas predicted by the projection and the target areas indicated by the current model: For 14/17 coil positions there was an exact match between the outcome of the projection method and the outcome of the current model, while for 2/17 positions the projections fell on a neighbouring area that received the second strongest stimulation. For one position the projection method predicted stimulation of a functional area where no electric field was induced.

Reliability of phosphenes as a signature of stimulation

Six participants that did not perceive phosphenes through single pulse stimulation were retested with a more powerful rTMS protocol. Three out of six participants reported phosphenes through rTMS. Subsequently they were able to perceive a stable percept through a single pulse phosphene screening. Two participants very sporadically reported a percept through rTMS. They did not report any percept through subsequent single pulse stimulation. One participant never reported a phosphene after rTMS or single pulse stimulation.

2.4 Discussion

In this study, I systematically map out where in the visual cortex TMS can induce phosphenes (**Fig. 2.2**). Stimulation of the early visual cortex (V1, V2d and V2v) and

structures along the dorsal pathway (V3d, V3a) induce phosphenes reliably (see **Table 2.1**). This suggests that in these areas of the visual cortex TMS stimulation reliably induces neural activation that will propagate to a degree at which it creates a conscious percept. These findings suggest that we can use TMS in the early and dorsal visual cortex to make causal inferences regarding the functional role of underlying areas in the human cortex.

Probability of inducing phosphenes in the visual cortex

The probability of producing a phosphene with TMS is variable for different parts of the visual cortex. Moving the stimulation site closer to the interhemispheric cleft increases the probability of inducing a phosphene (**Fig. 2.3**). Similar findings were reported previously (Kammer et al., 2005; Marg & Rudiak, 1994).

One possible explanation for this could be that the part of the cortex next to the cortical midline lies close to the scalp (Stokes et al., 2005) and should therefore receive stronger TMS related effects (Kammer et al., 2005; Stokes et al., 2013; Wagner et al., 2009). In this study, I corrected stimulation intensity for the underlying distance between the coil and the cortical surface. I found that, after correction, stimulation intensity or distance from the coil to the underlying cortical surface did not significantly predict whether TMS would yield a percept. This suggests that I successfully controlled for these predictors of TMS efficacy.

It is also possible that only TMS related activation of a specific neural structure or network close to the cortical midline will produce phosphenes. Different parts of the visual cortex are suggested as potential generator structures for phosphenes: the striate cortex (V1), extrastriate areas (V2/V3), cortico-cortical tracts projecting from V2/V3 back to V1 or the optic radiations as a subcortical structure (Kammer et al., 2005). Pascual-Leone & Walsh (2001) showed that phosphene perception induced through extra-striate stimulation can be disrupted through subsequent stimulation of V1. Studies of brain-lesioned patients showed that an intact V1 is necessary for phosphene perception (Cowey & Walsh, 2000; Gothe et al., 2002). These findings suggest that the spread of TMS related neural activation at the target site through a network connected to early visual structures might underlie phosphene perception. Structural connectivity between V1 and V3d has been demonstrated in non-human primates (Arcaro & Kastner, 2015; Felleman & Van Essen, 1991; Markov et al., 2014). In humans strong functional connectivity between V1 and V3d during resting state fMRI proposes a similar anatomy (Genç, Schölvinck, Bergmann, Singer, & Kohler, 2016; Heinzle, Kahnt, & Haynes, 2011). The higher susceptibility to phosphene induction that I

found for dorsal areas V3d and V3a might therefore be explained by the connectivity between these areas and the early visual cortex.

Finally, intracranial parameters that we cannot control (e.g. local orientation of neurons relative to the induced current orientation) might play a key role for stimulation in the visual cortex (Wagner et al., 2009). Structures close to the midline such as the tracts projecting from V2/V3 back to V1 and the optic radiations are more prone to TMS due to their bending structure (Kammer et al., 2005). Also, with induced currents running lateral to medial, a higher number of phosphenes close to the interhemispheric cleft could be due to current orientation running perpendicular to the stimulated gyrus which marks the onset of the interhemispheric cleft (Kammer et al., 2007). However, in this study I only found slight changes in the stimulation outcome for different current directions (see Effects of current direction on phosphene induction) which makes it unlikely that the observed results are driven by an interaction between current orientation and intracranial parameters such as the orientation of local neurons to the induced current.

It is worth noting that the phosphene probabilities provided in **Table 2.1** are specific to the left hemisphere. Previous work indicated that phosphenes can be induced in both hemispheres, and suggests that cortical excitability does not differ between hemispheres (Kammer, 1999; Kammer et al., 2005; Marg & Rudiak, 1994) in occipital areas V2 and V3 (Kammer, Beck, Erb, et al., 2001). This gives me no reason to expect any interhemispheric differences.

Phosphene induction in different functional areas

My results suggest that phosphenes are induced through TMS related neural activation in visual areas close to the midline. In this study, I predicted a location of the maximum induced current to describe TMS related effects relative to functional areas (Okamoto & Dan, 2005). I found that stimulation of early visual areas produces phosphenes reliably (V1: 40.8%, V2d: 45.4%, V2v: 41.7% of stimulations) as previously reported (Abrahamyan, Clifford, Ruzzoli, et al., 2011; Salminen-Vaparanta et al., 2014). However, my results suggest that TMS induces a percept most frequently when aimed at dorsal visual areas (V3d: 60%, V3a: 56.4% of stimulations).

It is conceivable that intrinsic parameters of the targeted areas might explain these results: Stimulation of neurons with larger receptive fields in V3a might produce larger phosphenes compared to neurons in V1. This could cause participants to spot phosphenes more easily

after dorsal stimulation and potentially explain different susceptibility to phosphene perception at different functional areas. However in a previous study participants reported slightly smaller phosphenes for stimulation of the dorsal visual cortex (V3d and V3a) compared to primary visual cortex V1 (Kammer et al., 2005). In general, previous phosphene studies have reported that the overall appearance of phosphenes does not change significantly when different areas of the brain are stimulated (Kammer et al., 2005; Salminen-Vaparanta et al., 2014). This makes it unlikely that phosphene appearance systematically affected the stimulation outcome of this experiment.

The area with the highest average phosphene incidence (V3d) was the same area where individual cortical excitability was defined. One concern is that the experiment was therefore in some way biased towards ideal stimulation parameters for V3d and neighbouring areas. While I cannot rule out this possibility, I think it is unlikely to have played a major role. This is because for all different areas in the visual cortex, I controlled all stimulation parameters that I can influence extracranially (stimulation intensity, current direction and stimulation accuracy) to induce comparable stimulation effects.

For areas in the ventral visual cortex (V3v, V4) I was only able to apply a relatively low number of stimulations in two participants (see **Table 2.1**). Due to their hidden location at the inferior ventral side of the brain these areas are hard to reach with TMS in most participants (see **Fig. 2.4**). I therefore cannot draw any firm conclusions regarding the excitability of these areas.

In higher visual areas, TMS stimulation had a low chance of producing a phosphene (hMT+/V5: 13.8%, LO: 12.8% of stimulations). For area hMT+/V5 these findings are unexpected as previous studies were able to induce moving phosphenes through stimulation at this area (Antal, Nitsche, Kincses, Lampe, & Paulus, 2004; Najib, Horvath, Silvanto, & Pascual-Leone, 2010). One possible explanation could be state dependency of phosphene behaviour: the absence of any motion priming might have made it harder to spot moving phosphenes (Guzman-Lopez et al., 2011).

It is important to note here that the absence of phosphenes in some parts of the visual cortex cannot be used as an indicator that TMS did not induce neural activation. First, there is no reason to believe that one part of the brain is excitable and another not (Walsh et al., 2003). Second, the underlying process that is triggered by TMS and leads to phosphene perception is not understood (Kammer et al., 2005). Finally, TMS related activation of neurons might have been below a critical threshold to induce a phosphene, however a population of neurons was still activated (Silvanto, 2013; Wagner et al., 2009). In particular, Ramos-Estebanez et al. (2007) showed that subthreshold stimulation causes substantial neural

activation while no percept occurs. With the paradigm used in this experiment, I am not able to draw any conclusion from stimulations that did not yield a percept, however it is unlikely that no neural excitation was triggered through TMS.

Locating the effects of TMS

A key limitation of TMS studies is the unknown location and spatial specificity of TMS related neural activation. In this study TMS effects where assigned to a single point on the cerebral surface where the induced current is estimated to be maximal. This is based on the assumption that the impact of TMS on neural tissue is maximally initiated where currents are maximal under the centre of the coil (Wagner et al., 2009). This approach has two limitations:

First, depending on the stimulator output the induced electric field is reported to spread approximately 100-200 mm^2 on the cerebral surface (Wagner et al., 2009). Due to this coarse focality and individual differences in functional brain architecture it is often not possible to constrain the induced electric field to a single functional area (Salminen-Vaparanta, Noreika, Revonsuo, Koivisto, & Vanni, 2012). It is possible that stimulations in this study might have activated neurons in multiple neighbouring areas.

One possibility is to define the neural activation based on a model of the theoretical current spread of TMS in the brain (Salminen-Vaparanta et al., 2014). However this approach has its' own limitations: It is currently unclear in what way the interactions between the electric current and brain tissue trigger neural firing and whether there is a linear relationship between current intensity and neural activation (Bestmann, de Berker, & Bonaiuto, 2015).

The second limitation of this approach is that neural activation due to TMS is predicted to be maximal where the induced current was maximal. However this is not necessarily true: Recent studies have proposed that a subcomponent of the electric field that is induced by TMS can best predict stimulation outcomes in the motor cortex (A. M. Janssen et al., 2015; Laakso, Hirata, & Ugawa, 2014). This subcomponent is perpendicular to and directed into the cortical surface and, for TMS, maximally affects neurons situated in the sulcal wall. Most importantly this component is not necessarily located at the electric field maximum (Laakso et al., 2014).

In this study, I used a realistic electric field model to validate the assignment of stimulation effects to functional areas based on a projection method. I found a good correspondence between the target areas predicted by the projection and the target areas indicated by the

current model. This suggests that the projection method used in this study successfully identified functional areas in the visual cortex targeted by stimulation, notwithstanding the complications of localizing the effects of TMS pulses in the brain.

Reliability of phosphenes as a signature of stimulation

A challenge in understanding the efficacy of TMS through phosphenes is to draw general conclusions based on a limited subsample. For this experiment, I recruited 30 participants but found that only 12 participants (40%) perceived phosphenes reliably. In particular, nine participants (30%) did not report phosphenes after any TMS stimulation. While I sought to provide the optimal conditions for phosphene perception (see Methods), there are two main reasons why this might have occurred. First, it is possible they were overly conservative in their responses and were not sufficiently confident in their perception of very briefly induced phosphenes. Second, it is possible that the single pulse stimulation induced only subthreshold neural activation that was insufficient to induce a conscious percept (Silvanto, 2013; Wagner et al., 2009).

To test these two possible explanations, I retested six participants that reported no percept with a more powerful rTMS protocol that was reported to induce a percept in every participant (Boroojerdi et al., 2002; Ray et al., 1998). Additionally, this protocol creates a more vivid, easy-to-spot percept (Kammer et al., 2005; Marg & Rudiak, 1994).

Three participants reported phosphenes through rTMS. Notably they also were able to perceive a stable percept through subsequent single pulse stimulation. This suggests that they had not previously spotted the percept through single pulse TMS. Two participants very sporadically reported a percept through rTMS. They did not report any percept through single pulse stimulation. One participant never reported a phosphene after rTMS or single pulse stimulation. It is possible that TMS only induced subthreshold neural activation in these participants.

In this project, I only applied single pulse stimulation while some participants were not able to gain a percept from this protocol. I did so because rTMS has certain drawbacks: the area of the induced current will be larger making it hard to locate TMS related effects (Robertson et al., 2003). Also, repeated stimulation protocols are more prone to not only trigger action potentials during the pulse but also alter the level of neural excitability of targeted tissue over time (Wagner et al., 2009).

Finally, there is some evidence suggesting that there might be functional differences in visual neural networks between participants that report phosphenes through TMS and participants that do not. Specifically, fMRI activation has been found to differ during visual checkerboard stimulation (Meister et al., 2003) as well as TMS (Caparelli et al., 2010) for participants that do not report phosphenes. However, Caparelli et al. (2010) observed TMS-related blood oxygenation level dependent signal changes in both types of participants. These findings suggest that, while the behavioural outcome varies between participants, TMS does affect neural activity in both types of participants.

Effects of current direction on phosphene induction

Recent studies which used current modelling have shown that the direction of the induced current relative to local brain anatomy has an impact on the strength of the induced electric field (A. M. Janssen et al., 2015; Laakso et al., 2014; Opitz et al., 2013). These findings are in line with a direct relationship between a change in current direction and the amount of triggered neural activation in the motor cortex (Brasil-Neto, McShane, et al., 1992; Kammer, Beck, Thielscher, Laubis-Herrmann, & Topka, 2001; Mills, Boniface, & Schubert, 1992).

In the visual cortex this relationship is less clear cut. Kammer et al. (2007) reported that individual brain regions have an ideal current direction for phosphene induction (perpendicular to the underlying gyral crown) however these effects were marginal. I therefore chose to standardize the current direction for all coil locations. However a standardized current direction is unlikely to stimulate a maximum number of neurons at any given location in the visual cortex. This might compromise my interpretation that a difference in susceptibility to phosphene induction was due to the intrinsic properties of different areas in the visual cortex.

I therefore conducted a control study with three participants (these were the only ones from the original participants who were available) to test whether the current direction would affect the systematic differences in susceptibility to phosphene induction that I observed. I found very slight differences for phosphene induction with different current directions as previously reported by Kammer et al. (2007). Importantly, the pattern of high-, medium-, or low phosphene susceptibility for different coil locations was preserved irrespective of the coil orientation. This suggests that it is unlikely that my results are specific to the lateral-to-medial current direction used during phosphene mapping.

Effects of stimulation intensity corrections

In this study, I corrected stimulator output to induce comparable stimulation effects at different sites in the brain. However for one participant with a high excitation threshold all stimulations were delivered at the maximum stimulator output used in this study, hence stimulator output was not controlled as a potential predictor of the stimulation outcome. One concern was that this might have systematically affected the overall results. However, **Fig. 2.2A** shows that stimulation results for this participant were similar to the results of most of the other participants. This shows that the overall results of this study were not systematically affected by a partial lack of stimulator output correction.

2.5 Conclusion

My results show that single pulse TMS can reliably induce phosphenes in early (V1, V2d, V2v) and dorsal (V3d and V3a) areas of the visual cortex close to the interhemispheric cleft. I propose that TMS-related maximum induced currents located at functional areas V1, V2d, V2v, V3d, and V3a can trigger a critical amount of neural activation that will propagate and create a conscious percept. Stimulation in dorsal visual areas (V3d, V3a) was most likely to induce a phosphene. This could indicate that TMS induced extra-striate neural activation that propagates back to primary visual cortex will create the phosphenes. More investigations will be necessary to identify the neural activation pattern that drives this artificial conscious percept.

3. The mixed polarity benefit of stereopsis arises in early visual cortex

This chapter reproduces the work associated with the following published manuscript: Schaeffner, L. F., & Welchman, A. E. (2018). The mixed polarity benefit of stereopsis arises in early visual cortex. Manuscript submitted for publication.

While the content of the chapter is identical to the manuscript, some modifications have been made to ensure that the chapter is well integrated with the rest of the thesis. For consistency, the references to figures have been updated to reflect the structure of the thesis.

3.1 Introduction

Depth perception is better when observers view stimuli which contain a mixture of bright and dark visual features. Harris and Parker (1995) showed that a RDS, with a noisy disparity profile, allows for better depth judgements when it contains black and white dots (mixed polarity) compared to when it only contains one dot colour (single polarity) (see **Fig. 3.1**).

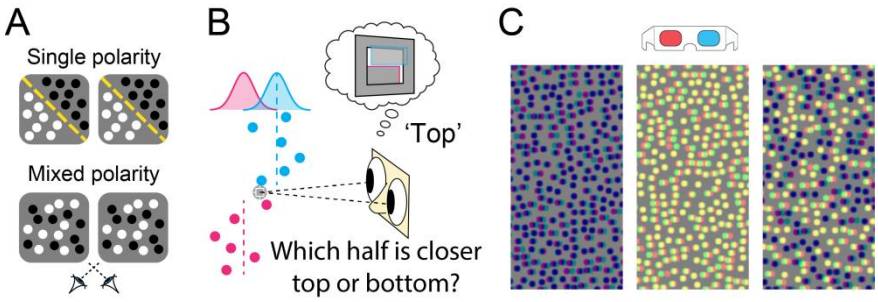

Figure 3.1: The mixed polarity benefit. A) Mixed- versus single-polarity stereograms. Single-polarity stereograms were either all dark or all bright. **B)** The task was to discriminate the step arrangement of the stereogram. Stimulus disparity was comprised of a disparity step to which crossed and uncrossed disparity noise was added (sampled from Gaussian distribution centred at stimulus location). **C)** Example anaglyphs which illustrate the mixed polarity benefit (designed for red filter over left eye).

An unanswered question is where in the visual cortex disparity processing benefits from the availability of different contrast polarity. The stimulus in **Fig. 3.1** might challenge both early mechanisms which establish stereo correspondence and/or subsequent mechanisms of disparity discrimination. Read et al. (2011) were able to replicate the mixed polarity benefit using a de-correlated RDS: Instead of binocular dot pairs having different horizontal offsets, in a de-correlated RDS some dots do not have a match in the other eye. This stimulus should challenge mechanisms of stereo correspondence more strongly, and indeed they observed a stronger mixed polarity benefit for de-correlated RDSs. This indicates that early mechanisms of disparity processing might benefit from mixed contrast polarity. However, it remains unclear where in the brain these mechanisms are located.

Here, I sought to answer the question where in the brain the mixed polarity benefit arises. I applied TMS to early (V1) and higher (V3a & LO) visual brain areas, which have been shown to be involved in disparity processing (Goncalves et al., 2015; Patten & Welchman, 2015; Preston, Li, Kourtzi, & Welchman, 2008). I assume that the benefit is produced by a neural mechanism which extracts a more reliable disparity signal from mixed polarity compared to single polarity RDSs. By changing normal neural activity in this system through brain stimulation, I expect to differentially disrupt stereopsis for mixed and single polarity stimuli. This allows me to locate where in the visual cortex disparity processing benefits from the additional information carried by mixed contrast polarity.

I found that stimulation over V1 but not V3a or LO affected depth perception for mixed- but not single polarity stimuli. This confirms that mechanisms of stereopsis in primary visual cortex, which are concerned with stereo correspondence, give rise to the mixed polarity benefit. Contrary to my expectation TMS over V1 does not disrupt stereopsis. Instead, brain stimulation amplifies the mixed polarity benefit by improving depth perception for mixed polarity stimuli. I suggest two potential explanations for this surprising result: TMS might amplify disparity signals for mixed polarity stimuli due to non-linear processing in visual cortex. Alternatively, TMS might drive suppression of binocular contrast mismatches for mixed polarity stimuli, which could improve the reliability of disparity signals.

3.2 Methods

Participants

For this study, I screened 83 naïve participants. All had normal or corrected-to-normal vision with good visual acuity (between -0.1 and 0.1 LogMAR). I screened participants with the

demanding depth discrimination task used in this experiment (see Experiment Procedure). 22 participants successfully passed the screening and were tested for this study. Before the experiment, participants provided written informed consent and were checked for contraindications to fMRI and TMS (Rossi et al., 2009; Wassermann, 1998). Procedures were approved by the University of Cambridge ethics committee and were performed in accordance with the ethical standards laid down in the 1964 Declaration of Helsinki. For this study, I initially tested seven participants where all brain regions of interest received TMS. Another eight participants were tested in a shorter version of the experiment to confirm that the main finding holds for a larger sample size. Additionally, seven participants were tested in a replication without the acquisition of fMRI data. For this replication, I targeted the primary visual cortex and a control site with TMS which should be feasible without fMRI based neuro-navigation.

Stimuli

Participants performed the experiment task with a haploscope in which the two eyes viewed separate 22 inch Samsung (2233) LCD displays through front-silvered mirrors. Both screens were gamma corrected to linear luminance output. Viewing distance was 50cm. Stimuli were displayed on 1680 x 1050 pixel screen at a vertical refresh rate of 60 Hz. Participants were instructed to maintain fixation on a square fixation cross at the centre of the screen with horizontal and vertical nonius lines.

Stimuli were RDSs (Dot radius: 0.068 deg, number of dots: 492, stimulus size: 4 x 4 deg) depicting a noisy disparity based step function on a medium grey background (see **Fig. 3.1**). Participants performed a 2AFC task and were asked to judge whether the top or bottom half of the stimulus appeared closer to them. Stimuli were surrounded by a correlated pink noise background to promote stable vergence.

Task difficulty was manipulated changing the magnitude of the step function relative to the fixation point (i.e., I simultaneously varied the crossed and uncrossed disparities in tandem). Additionally, each dot in the RDS was randomly assigned crossed or uncrossed Gaussian disparity noise (see **Fig. 3.1B**). Given individual differences in stereoscopic capabilities of naïve participants, and the fact that discrimination performance with this type of task can improve substantially through training (Chang, Kourtzi, & Welchman, 2013), I varied both the step size and variance of the disparity noise during the training portion of the experiment. I thereby tailored the stimuli to the participant's discrimination capabilities. During the main experiment, only the step size was changed to manipulate task difficulty. Disparity at the left

and right edges of the RDS was tapered to zero to avoid monocular cues of the relative position in depth.

Stimuli were displaced to the left or right of the fixation point to maximize the amount of information processed in one hemisphere, and thereby increase the potential to reveal the effects of brain stimulation. Specifically, the stimulus was displaced 2 deg horizontally, so that one edge of the stereogram became aligned with the centre of the screen. Stimuli were presented to the left of fixation on two-thirds of trials (corresponding to the stimulated right hemisphere) and to the right of fixation on one-third of trials (corresponding to the unstimulated hemisphere). This imbalance represented the intersection between the need to acquire sufficient data in an individual condition and the limit of how many TMS can be safely applied per day (Rossi et al., 2009; Wassermann, 1998). All testing conditions in this experiment had this same imbalance; I recorded eye movements to ensure that there was no significant left-side bias of version eye movements.

Stimuli were rendered for two different RDS conditions: In the single polarity condition all dots of the RDS were either white or black. In the mixed polarity condition 50% of the dots were white, 50% black. For a given experiment block I always presented 50% mixed polarity and 50% single polarity stimuli. I also balanced the number of black and white single polarity RDSs to ensure equal overall light exposure between the mixed and single polarity condition.

Experiment Procedure

Stimuli were presented for 300ms and observers had unlimited time to give a response. If no TMS was applied during the experiment I kept an inter-stimulus interval (ISI) between response and stimulus onset of 800ms. For trials that were accompanied by TMS the ISI was a jittered period between 5 and 6 seconds. A longer average ISI was chosen to contain TMS effects within the trial duration (Kammer et al., 2005), and the timing was jittered to avoid stimulation effects that might build up through rhythmically applied TMS.

At the beginning of the experiment participants performed a one hour training session to familiarize themselves with the task: Participants viewed single and mixed polarity RDSs with a range of step sizes of 0.2 – 20 arcmins. They received feedback on their judgments. During training the Gaussian disparity noise was increased stepwise, from $\sigma = 1$ to $\sigma = 3$ arcmins, to define an optimal noise level at which a range of RDS step sizes would yield performance from near chance to near perfect performance. Participants trained for between

576 and 1152 trials until a stable performance was reached. During the main experiment RDSs always contained the disparity noise magnitude tailored to each participant based on the training results.

Next, I defined a psychometric function for each stimulus polarity condition using the method of constant stimuli (MOCS). For each polarity condition, I presented stimuli at seven disparity step sizes (between 0.2 and 20 arcmin) with 108 trials per stimulus intensity level (total number of trials 2268). Trials of different difficulty and polarity were randomized. For each stimulus condition a psychometric function was fitted to the data using psignifit [4.0] (Fründ, Haenel, & Wichmann, 2011). I also presented 360 catch trials for lapses (step size 10/20 arcmin, σ = 0 arcmin) to fix the lapse rate of the psychometric functions. Seven participants were unable to fuse the largest disparity step size of the MOCS procedure (which was also used as lapse stimuli). For these participants psychometric functions were fitted to only six difficulty steps and no lapse data was used.

From the psychometric function for mixed polarity I estimated a threshold of 80% correct performance. Based on previous results, performance differences between single and mixed polarity should be largest at this performance range (Read et al., 2011). For the subsequent main experiment, stimuli were presented at the task difficulty that was estimated to yield 80% correct discrimination for mixed polarity stimuli.

The experiment consisted of five different TMS conditions: In one condition no TMS was applied; in the remaining conditions TMS was applied over V1, V3a, LO or Cz during stimulus presentation (see **Fig. 3.2**). Each condition included a total of 456 trials.

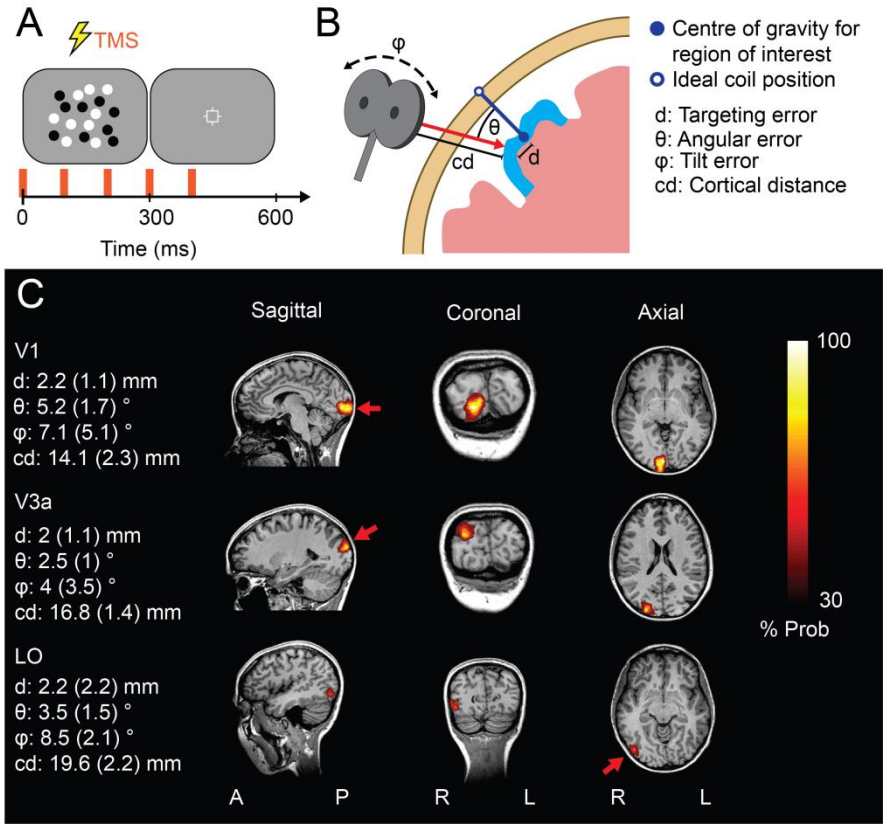

Figure 3.2: Illustration of TMS application. A) Brain stimulation was applied at 10Hz with stimulus onset and covered the full stimulus presentation time. **B)** I used neuro navigation for brain stimulation. Stimulation targets were defined as the centre of gravity of areas V1, V3a and LO. The closest point on the scalp results as an ideal coil location for stimulation. I report three parameters that describe how precise I could target this ideal location: Targeting error d describes the distance between a coil centre projection and an ideal trajectory to the stimulation target at the brain surface level. Angular error θ describes the angle between the coil projection and the ideal trajectory. Tilt error φ describes the angle between the coil tilt and an ideal current direction defined for each stimulation target. The distance between coil centre and stimulation target in the brain is described as cortical distance (cd). **C)** Probability maps of V1, V3a and LO location in talairach space. A red arrow describes the average coil position for all participants. For each stimulation location, I report the mean (+/-SEM) targeting error, angular error, tilt error and cortical distance.

Participants were tested on eight separate days so that I did not exceed the maximum number of stimulations that can be safely applied per day (Rossi et al., 2009; Wassermann, 1998). Each stimulation site was targeted on two different days. I only targeted one brain site per day to avoid confounding effects of TMS to different networks in the brain. The no-TMS

condition was tested on the same days as TMS conditions, prior to the application of brain stimulation to avoid carry-over effects. The order of stimulation sites between testing days was randomized to average out potential training effects of disparity discrimination that might build up throughout the experiment.

To test whether task difficulty affects the stimulation outcome, I retested nine participants. Task difficulty for the mixed and single polarity conditions were adjusted so that participants had matched performance for both conditions prior to brain stimulation. Participants were retested for V1 stimulation and a no stimulation condition.

TMS

I applied stimulation with a MagStim Rapid^2 stimulator (MagStim, Whitland, UK), using a figure-of-eight coil (70mm outer diameter). The TMS coil was placed tangentially on the head, aiming at the defined region of interest in the brain (see **Fig. 3.2B**). A coil holder (Magic Arm; Manfrotto, Bassano del Grappa, Italy) retained the coil at its position on the head. Stimulation was applied to the right hemisphere. The right hemisphere was chosen based on previous success of right LO stimulation with a similar depth judgement task (Chang, Mevorach, Kourtzi, & Welchman, 2014). For stimulation targets V1 and V3a, I had no reason to expect any hemispheric differences.

Stimulation was applied at 10 Hz (5 pulses, 0.4sec) synchronous with stimulus onset at a fixed intensity of 60% of maximum stimulator output (see **Fig. 3.2A**). For all stimulation targets, coil orientation was defined based on previous reports of successful TMS stimulation. Specifically, for V1 the coil handle was facing to the left (current direction medial to lateral) (Mulckhuyse, Kelley, Theeuwes, Walsh, & Lavie, 2011). For V3a (McKeefry et al., 2008) and LO (Chang et al., 2014), the coil handle was facing upwards (current direction superior to inferior). For control stimulations at Cz, the coil handle was facing from the front to the back of the head (current direction anterior to posterior) (Chang et al., 2014) . For participants with available MRI data, the orientation of the coil was subsequently adjusted based on the underlying anatomical structure of the brain. This was done to ensure that the induced electric current ran perpendicular to the underlying sulcus, and thereby maximize the likelihood of neural activation through stimulation (A. M. Janssen et al., 2015; Laakso et al., 2014; Thielscher, Opitz, & Windhoff, 2011).

fMRI

fMRI data were collected on a 3T Siemens Prisma MRI scanner with a 32 channel head coil. Blood oxygen level-dependent signals were measured with an echo-planar imaging sequence (TE 29 ms; TR 2000 ms; 1.5 × 1.5 × 2 mm, 30 slices covering the visual cortex). For each participant, I acquired a high resolution anatomical scan ($1mm^3$). fMRI data was analysed with BrainVoyager QX [2.8] (Brain Innovation, Maastricht, The Netherlands) (Goebel, Esposito, & Formisano, 2006). Functional data were pre-processed using three dimensional motion correction, slice time correction, linear trend removal and high-pass filtering. Retinotopic areas V1 and V3a were defined with standard retinotopic mapping procedures using rotating wedge stimuli and expanding ring stimuli. The borders of functional areas were defined by the resulting angular and eccentricity maps (Wandell et al., 2007). LO was mapped as the set of voxels that responded significantly ($p < 0.01$) stronger to intact than scrambled images of objects (Kourtzi et al., 2005). **Fig. 3.2C** shows probability maps of V1, V3 and LO position for all participants in talairach space.

Neuronavigation

During the experiment an anatomical scan was co-registered to the participant's head using anatomical landmarks. For all participants with MRI data, their individual structural scan was used, for all remaining participants an average MNI 152 head was fitted using linear transformation and scaling (Brainsight 2.2.12; Rogue Research, Montreal, Canada). During the experiment I monitored the position of the TMS coil and the participant's head with an infrared camera and Brainsight 2.2.12 neuro navigation software.

A normal vector originating in the centre of the figure-of-eight TMS coil described the expected stimulation location in the brain (see **Fig S3.1B**). For participants with fMRI data, stimulation targets were defined as the centre of a region of interest (V1, V3a or LO) in the brain. For participants without fMRI data, V1 was defined as a point 5mm lateral of Oz (10-20 system). For each target, an ideal trajectory was defined approximately normal to the scalp surface. The precision of stimulation during the experiment is described by three coil position parameters (targeting error, angular error and tilt error) which are described relative to this ideal trajectory (see **Fig. 3.2B**). During the experiment, coil position parameters were monitored and recorded (see **Fig. 3.2C**).

Electric field simulation

For the seven participants, for whom all areas of interest were stimulated, I created an electric current model of TMS to investigate whether stimulation successfully targeted V1, V3a and LO. I used simNIBS [2.0] (www.simnibs.org; Thielscher, Antunes, & Saturnino, 2015) to model current distributions with a finite element method. I constructed detailed meshes (1.1 million tetrahedra) from the structural MRI scans and modelled electrical field spread. I assigned electrical conductivities to different tissue types as described by Windhoff, Opitz and Thielscher (2013). Isotropic conductivity in the brain was assumed. A magnetic dipole model for a MagStim 70mm figure-8 coil was provided by simNIBS. I defined coil position and orientation in the simulation as the mean position and orientation recorded during the experiment with neuro navigation. Rate of change of current flow in the stimulator coil, for a given stimulator output, was defined relative to the peak current at 100% stimulator output, as provided by MagStim. Since the output is a sinusoidal waveform, current flow in the coil was calculated as the root mean square of the peak current for a pulse duration of 300μs. For a stimulator output of 60% used in this study, this results in a rate of change of current flow of 20.08 A/μs.

Eye Tracking

I recorded binocular eye movements with an EyeLink 1000 remote video tracker (SR Research). The system has a stated accuracy of 0.25 deg and resolution of 0.01 deg (root mean square). The tracker viewed the participant's eyes through infrared transmitting cold mirrors. At the beginning of each experiment block participants were instructed to keep fixating on a calibration marker, which was used to calibrate a four by four degree area on the screen in which stimuli were presented.

To analyse eye movement data I converted raw gaze positions to degrees of visual angle. Trials during which tracking was lost in one or both eyes were excluded (average proportion of trials per participant 25.7%). This high proportion of lost trials was due to the challenge of tracking both eyes through the mirrors and eye holes of the stereoscope. Time series data were pre-processed by removing any data that corresponded to periods of blinks or saccades, as identified by the EyeLink inbuilt detection functions. I removed an additional 50ms of data before and after blinks to remove large gaze point offsets which were likely caused by eye rotation prior to blinks. Removed data was then linearly interpolated. Finally, eye tracking in a stereoscope sometimes led to erroneous tracking of interior parts of the stereoscope instead of participant's pupils (average proportion of trials per participant 7.9%).

To remove all trials where this occurred, I excluded all trials where gaze position was located outside of a four by four degree window around fixation where stimuli were presented in this study.

I checked whether loosing or removing eye tracking data affected different conditions of the experiment disproportionately. In this experiment the loss of eye tracking data was not significantly different between experiment conditions. This was true for observers where all experiment conditions were tested ($F_{4,24}$=1.07, p=.39), as well as for a larger group of observers for which I replicated the main effect of this study ($F_{2,26}$=1.9, p=.17). However, the amount of eye tracking data which had to be removed due to erroneous tracking differed significantly between experiment conditions (main experiment: $F_{1.9,11.5}$=6.45, p<.05; replication: $F_{2,26}$=10.32, p<.01). This is due to the fact that significantly less erroneous tracking occurred in the condition where no TMS was applied compared to when TMS was applied at any location on the scalp. The best explanation for this is that increased rates of blinking during TMS application (see **Fig. 3.10A**) leave the eye tracker without a pupil and cornea to track, thereby increasing the risk of erroneous tracking. Given that erroneous tracking did not significantly between conditions where TMS was applied, it is unlikely that missing eye tracking data represents a problem with the experiment which could affect the outcome of this study.

I report vergence and horizontal version eye movements during stimulus presentation to check that brain stimulation and lateralized stimulus presentation did not interfere with vergence stability. To quantify changes of vergence through TMS, I fit a linear model to participants' average eye vergence during stimulus presentation. I quantify vergence changes on each trial in terms of the gradient (β) of the best fit (least-squares).

Analysis

Statistical analysis was conducted in SPSS (SPSS Inc, Chicago, Ill). I analysed raw proportion correct values using repeated-measures ANOVAs and applied Greenhouse-Geiser correction where appropriate. For post-hoc analysis, I used Bonferroni corrected t-tests.

3.3 Results

Participants were tested for each polarity condition (black, white or mixed dots) at a range of disparity differences and at a fixed disparity noise level. **Fig. 3.3** shows the psychometric functions that were fitted to the data. I found significant differences for thresholds of psychometric functions for black, white and mixed stimuli ($F_{2,36}$=16.97, p<.01). Participants had significantly better depth perception (lower disparity acuity thresholds) when a mixture of black and white dots was presented compared to only white (t_{18}=-4.25, p<.01) or black (t_{18}=-4.73, p<.01) dots (comparison of 80% correct performance thresholds). Depth discrimination was marginally better for white stimuli compared to black stimuli (t_{18}=-2.36, p=.03). However, this difference was not significant after Bonferroni correction.

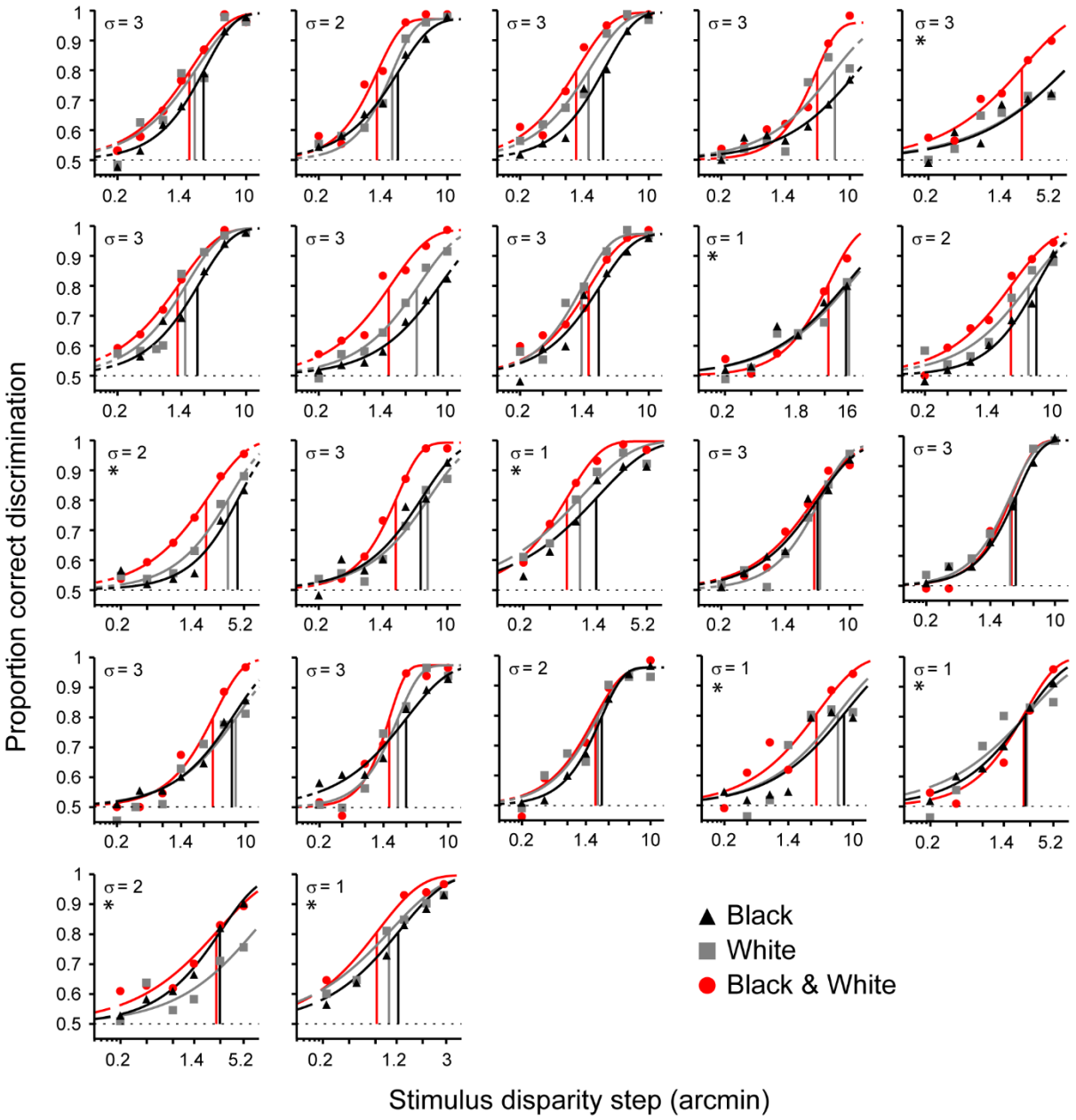

Figure 3.3: Disparity discrimination for mixed and single polarity stimuli. Discrimination performance for RDSs with black dots, white dots and a mixture of black and white dots. Task difficulty is defined by two parameters: The disparity offset in the RDS (x-axis) and the disparity noise assigned to each dot in RDS (sampled from Gaussian with a SD (σ) in arcmin). Psychometric functions were fitted to mean proportion correct responses. For fourteen participants the upper asymptote was set to performance at lapse trials (see Methods). For eight participants no lapse data was available (marked with *) and the upper asymptote was set to the average group lapse rate. Vertical lines mark the threshold where participants performed at 80% correct for each condition.

Next, I applied brain stimulation during the task to locate where in the visual cortex the mixed polarity benefit arises. For seven participants, brain stimulation was applied over all areas of interest in the visual cortex (V1, V3a, LO). The application of TMS did not significantly change disparity discrimination performance for all TMS conditions ($F_{4,24}$=1.74, p=.17), however a significant interaction between TMS site and stimulus dot polarity ($F_{4,24}$=5.8, p<.01) shows that TMS location is a critical factor in affecting the perceptual benefit between mixed and single polarity (see **Fig. 3.4A**). Post hoc comparisons revealed significant improvements in disparity discrimination performance through V1 stimulation compared to control stimulation for mixed polarity stimuli (t_6=3.37, p= .015). For stimulation of higher visual areas V3a and LO I did not observe a significant change in performance for mixed polarity stimuli (V3a: t_6=1.86, p=.11; LO: t_6=0.66, p=.53). For single observer results see **Fig. 3.5A**.

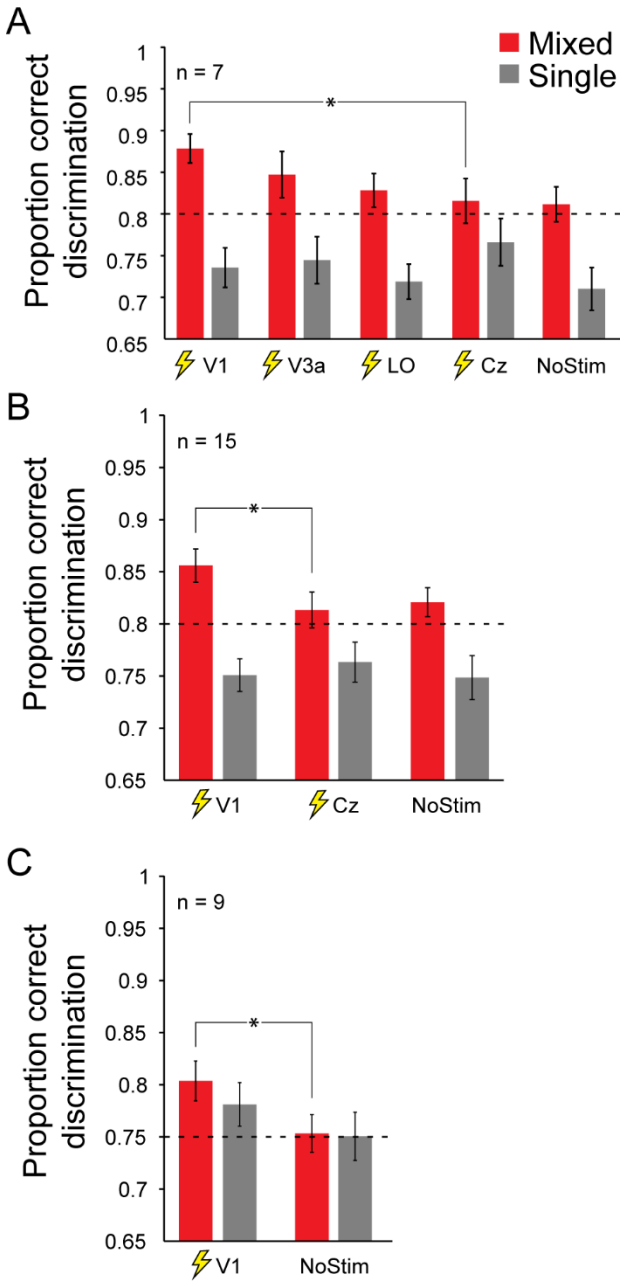

Figure 3.4: Effect of TMS on disparity discrimination for mixed and single polarity stimuli. Mean discrimination performance for different stimulation conditions. Error bars depict one standard error of the mean (SEM). Results are shown for stimulus location left of fixation. Brain stimulation was applied to right hemisphere visual cortex. **A)** Results for all stimulation conditions investigated in this study (n = 7). **B)** Results for V1 stimulation investigated for a larger sample size (n = 15). **C)** Replication of V1 stimulation effect of main experiment (n = 9). Additionally, task difficulty for mixed and single polarity was adjusted so that participants had similar proportions of correct responses for both stimulus conditions prior to brain stimulation. This was done to control whether TMS effects depend on task performance.

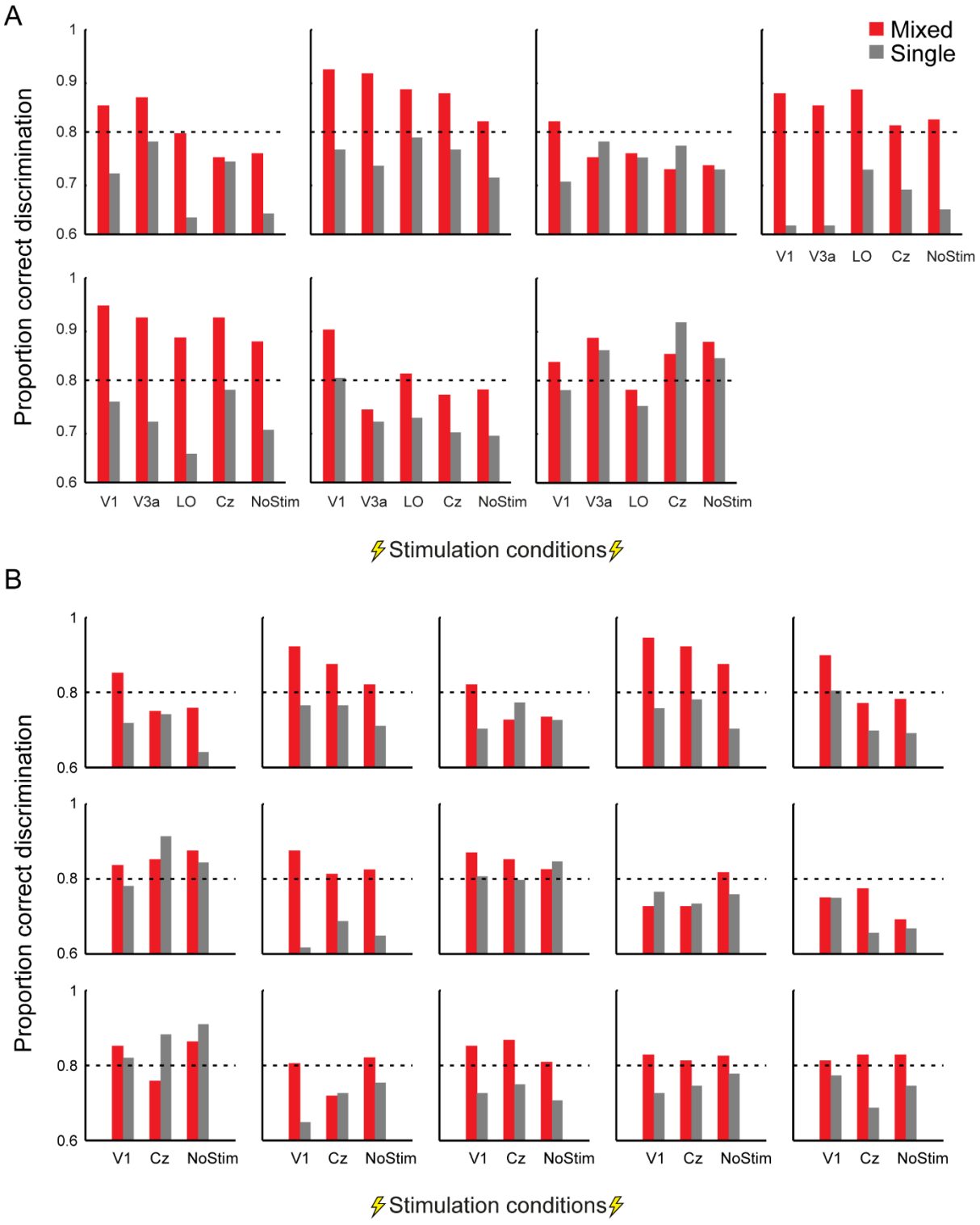

Figure 3.5: Effect of TMS on disparity discrimination for singular observers. Discrimination performance for different stimulation conditions. Results are shown for stimulus location left of fixation. Brain stimulation was applied to right hemisphere visual cortex. **A)** Results for all stimulation conditions investigated in this study (n = 7). **B)** Results for V1 stimulation investigated for a larger sample size (n = 15).

To assess which areas of the visual cortex were critically influenced by TMS, I simulated intensity and spread of the electric field induced by TMS for all participants which were stimulated over V1, V3a and LO (n = 7). **Fig. 3.6** shows representative electric fields in one participant simulated for stimulation of all target areas. Overlaid are the boundaries of functional areas defined by retinotopy and localiser scans. For higher visual areas V3a and LO mean electric field intensity was highest in the targeted area (see **Fig. 3.7A**). Stimulation over V1, on the other hand, may have induced a stronger electric field in area V2d (This was true for all participants). However, while electric field intensities in V2d were similar for stimulation over V1 and V3a, only TMS over V1 produced significant behavioural changes. I therefore calculated a measure of behaviourally relevant electric field intensity by subtracting electric field intensities for stimulation over V1 and V3a. **Fig. 3.7B** shows that this behaviourally relevant electric field component was greatest in V1 and suggests that behaviourally relevant changes of brain activity took place in V1. For Cz control stimulations negligible electric field intensities were induced in all areas of interest.

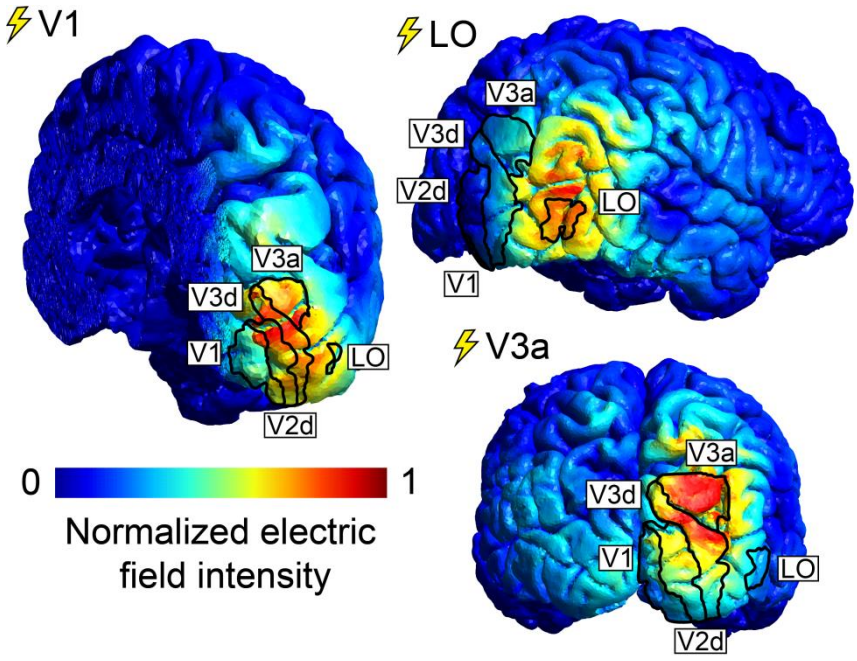

Figure 3.6: Electric field simulations of TMS. Representative electric field intensity (V/m) simulations in one participant for stimulation over V1, V3a and LO. Retinotopic areas and LO, defined from fMRI data, are superimposed. Electric field intensity ranged from 0 to 35 V/m.

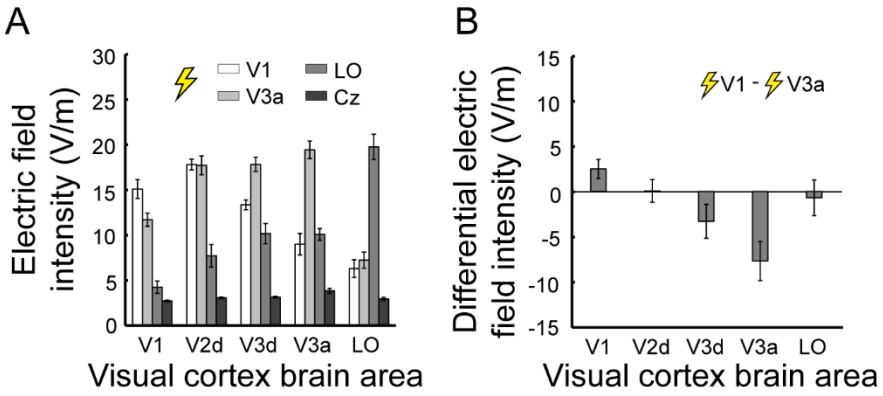

Figure 3.7: Estimated electric field intensities during TMS. A) Mean simulated electric field intensity in functional areas of the visual cortex for stimulation over V1, V3a, LO and Cz. Error bars depict one standard deviation. **B)** Mean contrast of simulated electric field intensity for stimulation over V1 and V3a. Error bars depict one standard deviation. Both stimulation over V1 and V3a produced comparable stimulation over early visual areas outside V1 e.g. V2d, however only V1 stimulation produced significant changes in behaviour. This contrast acts as an estimate of behaviourally meaningful stimulation.

I was surprised by the observation that there were significant improvements in disparity discrimination under V1 stimulation. I sought to ensure that this was true for a larger sample size and therefore continued testing eight additional participants with stimulation over V1. In total, 15 participants were tested for V1 stimulation, Cz control stimulation and a no stimulation condition (see **Fig. 3.4B**). Again, there was no main effect of TMS ($F_{2,28}$=1.13, p=.33) but a significant interaction between TMS and stimulus contrast polarity ($F_{2,28}$=4.32, p=.02). This suggests that it is critical where in the visual system TMS is applied. Stimulation over V1 significantly improved disparity discrimination performance for mixed polarity stimuli compared to control stimulation (t_{14}=3.15, p<.01). For single observer results see **Fig. 3.5B**. No such stimulation effect could be observed for single polarity stimuli (t_{14}=-0.76, p=.46). There was no significant difference in discrimination performance between control stimulation and no stimulation (Single polarity: t_{14}=1.06, p=.31; Mixed polarity: t_{14}=-0.46, p=.65), suggesting that the side effects of TMS were not disruptive for task performance.

I also tested seven participants without neuro-navigation (no MRI data was collected), where V1 stimulation was applied based on scalp landmarks (see Methods). I tested V1 stimulation, Cz control stimulation and a no stimulation condition. While TMS at the visual cortex appears to improve disparity discrimination performance for mixed polarity stimuli, this

change was not significant (t_6=0.94, p=.39). This was mostly likely due to non-optimal stimulation of V1 without neuro-navigation (see Discussion).

To resolve this conflict of the stimulation outcome with and without neuro-navigation, and to decide whether there was an overall effect of stimulation, I performed a single-paper meta-analysis (McShane & Böckenholt, 2017). Results for the initial seven participants and subsequent eight participants with neuro-navigation as well as the seven participants without neuro-navigation were treated as three separate experiments. This meta-analysis confirmed that stimulation over V1 significantly increased observer disparity discrimination performance compared to control stimulation for mixed polarity stimuli (Z=2.98, p<.001).

To test whether task difficulty affects the stimulation outcome, I retested nine participants in the main experiment. Stimulus properties for the mixed and single polarity conditions were adjusted so that participants had matched performance for both conditions prior to brain stimulation. Participants were tested for V1 stimulation and a no stimulation condition (see **Fig. 3.4C**). Similar to the main experiment, stimulation over V1 significantly improved disparity discrimination performance for mixed polarity stimuli (Z=-2.31, p=.02). For single polarity stimuli TMS did slightly improve discrimination performance, however this effect was not significant (Z=-1.36, p=.17).

TMS produces methodological challenges that might affect the experiment outcome. Due to the large size of the coil, stimulation cannot always be applied at an ideal location on the scalp. Additionally, participants will move their head relative to stimulator coil, which makes it difficult to reliably target the same underlying population of neurons. In this study, I monitored coil position, orientation and tilt relative to stimulation targets in the brain. **Fig. 3.2C** shows these control measures for each stimulation condition. For all my measures of coil precision, V1 stimulation was equal or less precise than for V3a and LO stimulation. This makes it unlikely that V1 stimulation effects can be explained by how easily an area can be reached with a TMS coil.

A useful predictor of the success of TMS in the brain is the distance between stimulation target and the centre of the coil during stimulation (Stokes et al., 2013). **Fig. 3.2C** shows that for V1 this distance was lower compared to V3a and LO in my participants. In a previous study, I showed that stimulation of comparable intensity has reliable effects on V3a neural activity (Schaeffner & Welchman, 2017), suggesting that my null result for V3a in this paper is not due to insufficient stimulation intensity. Electric field simulations suggest that stimulation of V3a and LO was, in fact, more successful than V1 stimulation (see **Fig. 3.7A**). This makes it unlikely that the results of this study can be explained by stimulation efficacy, based on the distance to the target brain region.

One challenge of TMS research is that cortical excitability (i.e. how much brain activity is changed by TMS) varies considerably between days due to a variety of factors such as sleep (Huber et al., 2013). Given that in this experiment participants were tested over up to eight sessions on different days, one concern was that differences in cortical excitability might affect the outcome of the experiment. In this experiment the order of conditions was randomized so differences in cortical excitability should not affect the experiment results in a systematic way. I nonetheless controlled whether observer depth discrimination varied between experiment sessions. **Fig. 3.8** shows the discrimination performance of mixed and single polarity stimuli for each experiment session ignoring stimulation condition. Observer's depth discrimination did not differ significantly between experiment sessions (Participants with four experiment sessions: $F_{3,39}$=0.16, p=.93; participants with eight experiment sessions: $F_{7,42}$=2.02, p=.07). Participants did not perform significantly better in the first half compared to the second half of the experiment (Mixed polarity: t_6=-1.75, p=.13; Single polarity: t_6=0.42, p=.69). This suggests that differences in cortical excitability did not systematically affect the outcome of this study. There was a slight increase in discrimination performance over the course of the experiment which is probably due to observers still slightly improving at the task.

However, because TMS conditions were randomized over different experiment sessions, it is still possible that daily differences in cortical excitability affected the outcome of this study. **Fig 3.9.** shows observer depth discrimination for each TMS condition on separate testing days. To check whether daily variations in cortical excitability systematically affected TMS conditions, I compared absolute differences in observer depth discrimination performance between the first and second day of testing for all TMS conditions. No TMS condition showed significant larger differences in experiment results between session one and session 2 of data collection when all TMS conditions were tested ($F_{9,54}$=0.81, p=.61; see **Fig. 3.9A**) as well as in a larger group of observers for which I only tested the main effect of this study ($F_{5,70}$=0.59, p=.71; see **Fig. 3.9B**). This suggests that differences in cortical excitability did not systematically affect the results of this study.

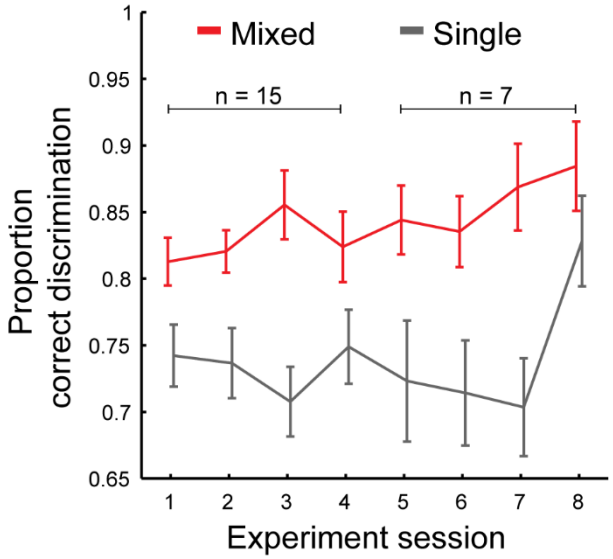

Figure 3.8: Depth discrimination in different experiment sessions. Mean discrimination performance from session one to session eight of testing. Error bars depict one standard error of the mean (SEM). Different stimulation conditions were pooled together for each day of testing. For seven participants data were collected in eight experiment sessions. For another eight participants data were collected in only four experiment sessions.

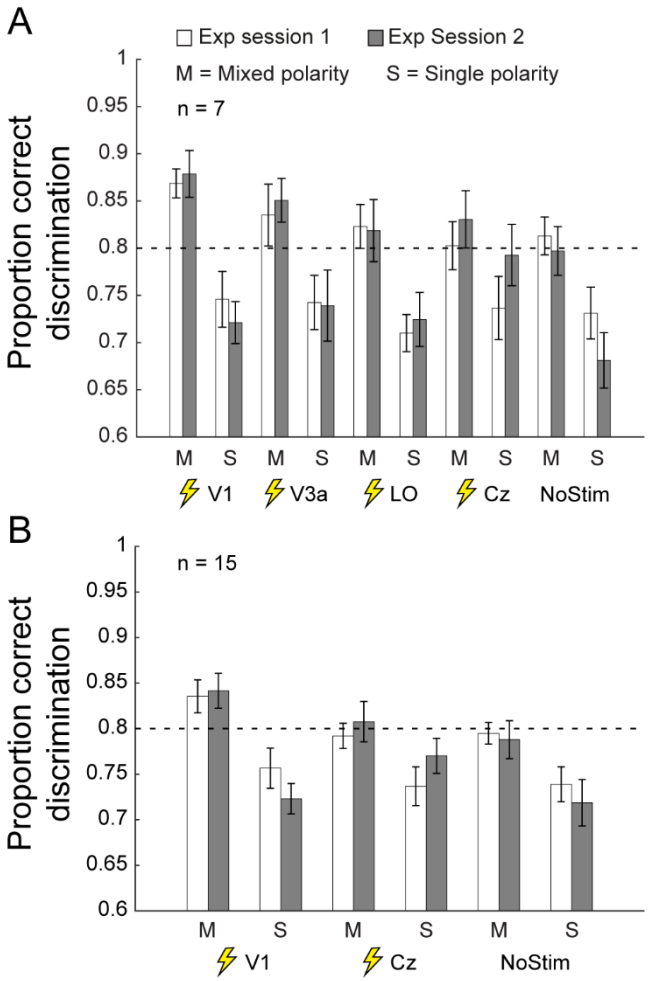

Figure 3.9: Session wise depth discrimination for different TMS conditions. Mean depth discrimination performance in different experiment sessions. Error bars depict one standard error of the mean (SEM). Results are shown for two separate experiment sessions in which data were collected in this experiment. The figure shows depth discrimination performance for mixed and single polarity stimuli during TMS intervention. **A)** Results for all TMS conditions investigated in this study (n = 7). **B)** Results for V1 stimulation investigated for a larger sample size (n = 15).

Another challenge of combining TMS with psychophysical tasks is the fact that stimulation produces muscle twitches on the scalp, which often lead to reflexive blinks. This effectively reduces the exposure time during stimulus presentation. Given that stimulation was applied at different locations on the head, this might systematically affect the behavioural outcome and favour coil locations at the back of the head (e.g. V1), which are furthest away from the eyes. **Fig. 3.10A** shows the number of blinks during stimulus presentation between different stimulation conditions. Participants had to blink more often when stimulation was applied

during the task. However, this did not favour a specific stimulation condition and could therefore not have affected the experiment results in a systematic way. Also, it is conceivable that side effects of stimulation were more detrimental on behaviour for a particular coil position. **Fig. 3.10B** shows the number of proportion of trials that participants missed for each condition based on catch trials for lapses (see Methods). Lapse rates were higher for V1 stimulation (where depth perception improved through stimulation) compared to V3a and LO stimulation. This rules out the possibility that distraction, through stimulation, might have disproportionately affected observers during V3a and LO stimulation.

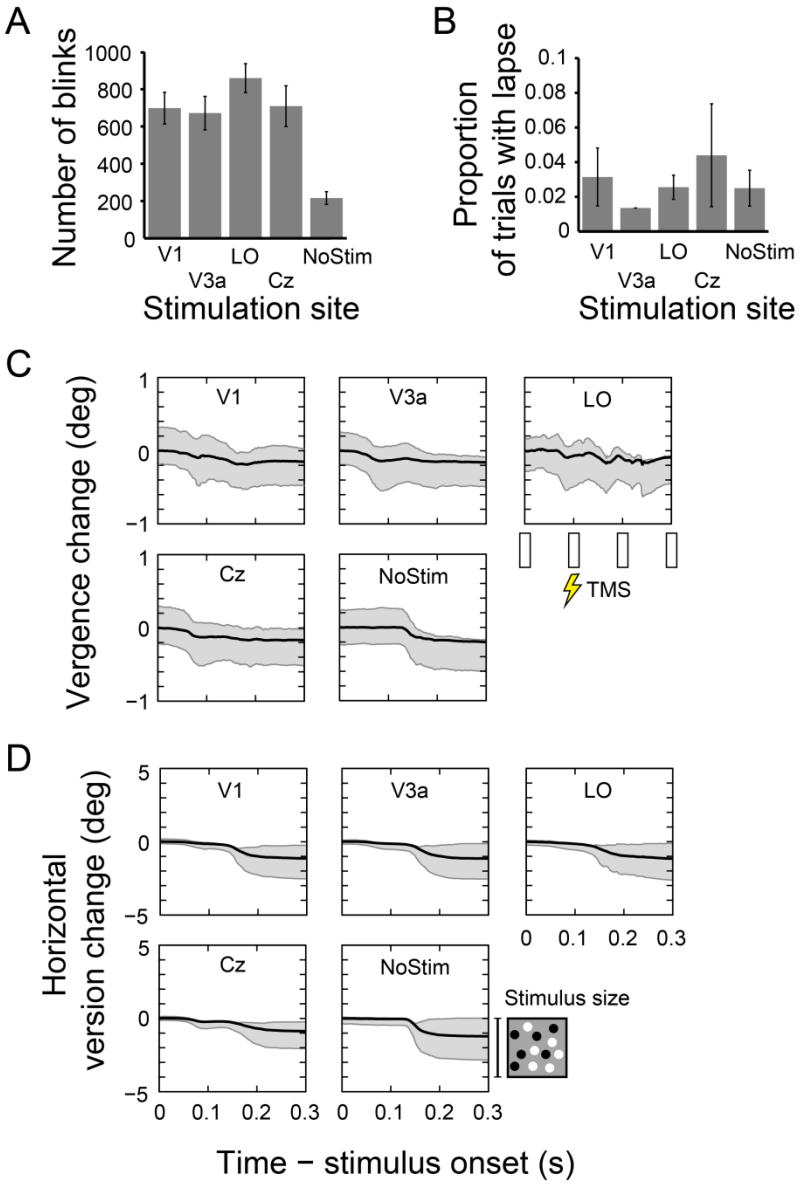

Figure 3.10: Effect of TMS on blink rate, lapse rate, and vergence and version eye movements. A) Number of blinks during stimulus presentation for different stimulation conditions. **B)** Proportion of trials in which participants missed stimulus presentation, based on lapse trials (step size 10/20', σ = 0'). **C)** Vergence and **D)** horizontal version change during stimulus presentation. Shaded area shows 25-75 percentiles. White bars indicate the timing of TMS pulses during stimulus presentation.

Finally, TMS stimulation might have affected the stability of eye vergence during the task. This could be the case for two reasons. First, depending on coil location relative to the eyes, stimulation might actively interfere with extraocular muscles. Secondly, it is possible that TMS affected brain areas involved in control of eye movements such as parietal regions

close to V3a (Pierrot-Deseilligny, Milea, & Müri, 2004). To control for this potential confound, I recorded pupil positions during stimulus presentation. **Fig. 3.10C** shows average vergence eye movements during stimulus presentation for different stimulation conditions. To quantify changes of vergence through TMS, I fitted a linear model to participants' eye vergence during stimulus presentation. Changes in vergence after stimulus onset did not differ significantly for different stimulation conditions ($F_{4,24}$=0.76, p=.56). This confirms that stimulation of different brain regions did not affect vergence during stimulus presentation.

In this study, I presented stimuli at a location lateral to fixation. This was done to maximize stimulus processing in one hemisphere, and therefore increase the chances of TMS intervention which I could only apply to one hemisphere at a time. I found that the lateral position of the stimulus did trigger horizontal version eye movements during stimulus presentation around 150ms after stimulus onset (see **Fig. 3.10D**). Again, to quantify changes of version through TMS, I fitted a linear model to participants' gaze position during stimulus presentation. Horizontal eye movements towards stimulus position did not differ significantly between TMS conditions ($F_{4,24}$=2.39, p=.08). This makes it unlikely that horizontal eye movements can the changes in stereopsis I observed.

3.4 Discussion

In this study, I investigated where in the visual cortex disparity processing benefits from the availability of a mixture of bright and dark visual features and allows for better depth perception. I found that stimulation over V1 with TMS, during stimulus presentation, increased this perceptual benefit. Stimulation of higher visual areas V3a and LO did not change perception. My findings show that disparity processing in early visual cortex gives rise to the mixed polarity benefit. This is consistent with models of stereopsis at the level of V1 which produce a mixed polarity benefit.

Where does the mixed polarity benefit occur?

In this study, I applied TMS over V1, V3a and LO to locate the disparity processing mechanism that produces the mixed polarity benefit. I found that stimulation over V1 significantly improved disparity discrimination for mixed polarity, but not single polarity stimuli (See **Fig. 3.4**). Stimulation of higher visual areas V3a and LO, which are responsive to

binocular disparity (Goncalves et al., 2015; Patten & Welchman, 2015; Preston et al., 2008), did not significantly change perception.

In the main experiment of this study, I report results for 15 participants where I applied neuro-navigated TMS. However, I also tested an additional seven participants where the TMS coil was placed over primary visual cortex based on scalp landmarks because no MRI scan was available. With this approach, TMS over primary visual cortex did slightly improve observer depth perception for mixed polarity stimuli, but the result was not significant. To resolve this conflict of the stimulation outcome with and without neuro-navigation, I performed a single-paper meta-analysis (see Results). This meta-analysis confirms that TMS over primary visual cortex did significantly improve depth perception for mixed polarity stimuli for all 22 participants stimulated in this study. Moreover, I replicated the improved performance in a subsequent control condition that matched behavioural performance in the mixed and single polarity conditions.

There are good reasons why stimulation without neuro-navigation did not produce a similar outcome. It has been shown that coil placement based on scalp landmarks results in far less precise stimulation, and that larger sample sizes are necessary to compensate for this imprecision (Sack et al., 2009). It is possible that with a larger sample size I would obtain a similar result compared to neuro-navigated TMS. Additionally, in the main experiment, neuro-navigation allowed me to optimally adjust the direction of the induced electric current for individual participants. This has been shown to optimize the stimulation outcome (A. M. Janssen et al., 2015; Laakso et al., 2014; Thielscher et al., 2011). Hence, without neuro-navigation stimulation can be expected to be less successful, and this can explain the attenuated effect on observer performance that I found in this study.

Another limitation of TMS research is the unknown volume of brain tissue in which we are affecting neuronal behaviour. **Fig. 3.4A** shows that the effect of TMS starts to emerge as I move the coil from a distant control site (Cz) to area LO and V3a, which are located closer to early visual cortex. It is conceivable that stimulation over V3a caused small changes of neural activity in early visual cortex, which was insufficient to significantly affect perception.

Additionally, TMS related cell activation has been shown to propagate in neural networks and can reach interconnected areas (Bestmann, 2008). In previous research, I showed that TMS related cell activation in V2d, V3d and V3a propagates back to primary visual cortex (Schaeffner & Welchman, 2017). It is possible that in this study TMS induced activation of V3a which propagated back to V1, producing marginal changes in perception.

It is difficult to confirm where in the brain TMS changes neural activity. In this study, I placed the TMS coil to maximize electric field induction in a given target area. However, electric field modelling reveals that, due to anatomical brain structure, TMS over V1 creates the strongest electric field intensity in V2d (see **Fig. 3.7A**) (Salminen-Vaparanta et al., 2014). To control whether stimulation of V2d played a role in this study, I calculated the differential between a behaviourally relevant (TMS over V1) and a behaviourally non-relevant (TMS over V3a) electric field intensity (for both coil positions I found comparable electric field intensities in V2d). This behaviourally relevant electric field component was maximal in V1 (see **Fig. 3.7B**), suggesting that stimulation of V1 neurons underlies the changes in depth perception I observed in this study. However, I cannot rule out the possibility that stimulation of V2d or V3d also played a role.

How does the mixed polarity benefit arise?

It is a long standing observation that the presence of both black and white dots in RDSs improves disparity-based depth judgments (Harris & Parker, 1995; Read et al., 2011). Here I was able to replicate this effect, showing that discrimination thresholds were significantly lower for mixed polarity stimuli compared to single polarity stimuli. The benefit is present for a large range of disparity magnitudes (See **Fig. 3.3**).

One concern about the contrast polarity effect in previous studies was that only small sample sizes of experienced psychophysical observers were tested. It is conceivable that this benefit only arises when the visual system has been trained to maximize the use of binocular disparity as a cue for depth perception. In this study, I specifically tried to test naïve observers who did not have a history of year-long exposure to RDSs. I show that the mixed polarity benefit is present in a sample of naive participants.

Different explanations have been proposed for how the mixed polarity benefit arises. Harris and Parker (1995) suggested that separate ON and OFF channels process bright and dark features in the RDS separately. This would reduce the number of potentially correct dot matches in a mixed polarity RDS by half and double the number of correct dot matches a human observer can sample to get an optimal representation of the stimulus. Separate ON and OFF channels are well established in the early visual system (Jiang, Purushothaman, & Casagrande, 2015; Schiller, 1992, 2010), however our current understanding is that these separate channels converge in V1 onto simple cells (Schiller, 1992) and therefore cannot explain the mixed polarity benefit. Additionally, separate ON and OFF channels produce a doubling in observer performance for tasks that require a global correspondence solution

(Edwards & Badcock, 1994). However, Read et al. (2011) showed that the mixed polarity benefit is not fixed to a doubling of observer performance. This makes it unlikely that the benefit can be explained by separate ON and OFF channels.

Alternatively, the benefit could be explained by different image statistics of mixed and single contrast polarity RDSs. Read and Cumming (2018) showed that stimuli used in this study, and all previous studies, contain higher inter-ocular image correlation at the target disparity if they have mixed contrast polarity compared to a single contrast polarity. A more correlated input drives binocular cells in primary visual cortex more strongly and produces a more reliable binocular disparity signal. This stimulus artefact arises from the way that dots are placed to avoid dot overlap when the RDS is created (for details see Read & Cumming, 2018) and could explain why the mixed polarity benefit only arises when there is no dot overlap in the stimulus (Read et al., 2011). Read and Cumming (2018) showed that the standard binocular energy model produces larger energy peaks at preferred disparities for mixed polarity RDSs. This could explain why the mixed polarity benefit arises.

This difference in inter-ocular image correlation was present in the stimuli used in this study (see **Fig. 3.11A)**. With increasing disparity noise image correlation at target disparity decreases more strongly for single polarity stimuli. From this it follows that, in my experiment, the benefit should be larger for observers that can tolerate higher amounts of disparity noise in the stimulus. In this study, I tested people at one of three Gaussian disparity noise levels, depending on how much noise they could tolerate (see Methods). **Fig. 3.11B** shows the depth discrimination performance for increasing levels of disparity noise. I found a trend that agrees with the prediction by Read and Cumming (2018): With greater disparity noise observers required a larger disparity signals to achieve 80% correct discrimination, and this effect is stronger for single polarity stimuli compared to mixed polarity stimuli. However, this trend was not significant ($F_{1,19}$=2.32, p=.14), and so here I cannot conclude whether this observation is representative.

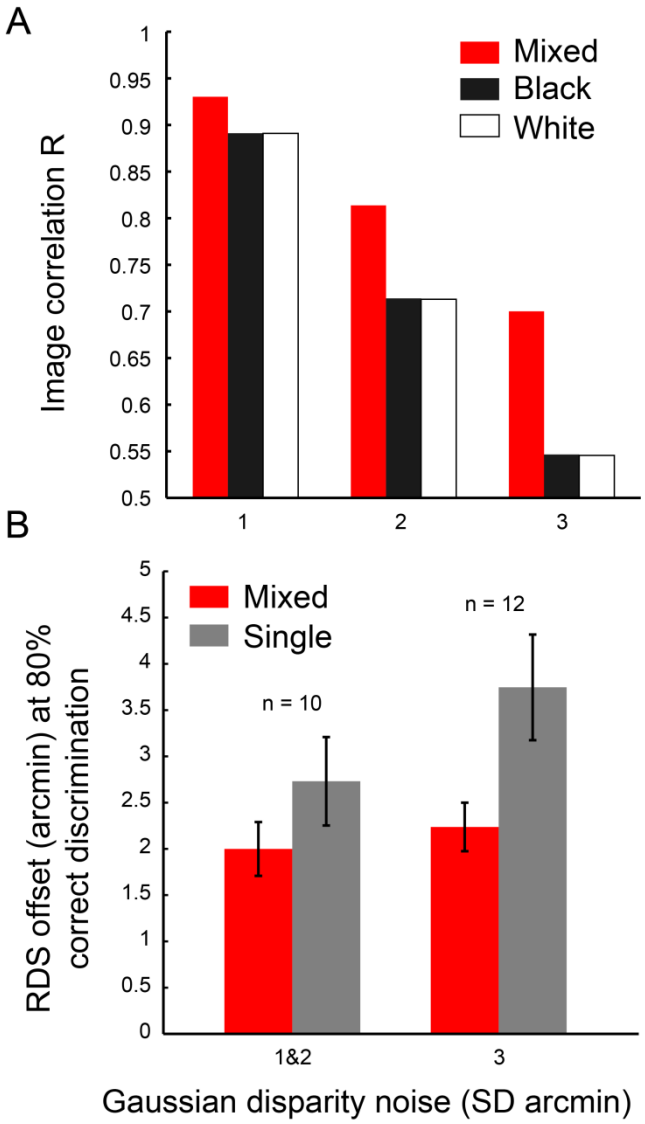

Figure 3.11: The effect of disparity noise on the mixed polarity benefit. A) Binocular image correlation of mixed and single polarity RDSs at target disparity for different amounts of added disparity noise (1000 RDSs per bar). **B)** Mixed polarity benefit with different amounts of disparity noise in the stimulus (for lower disparity noise levels data was pooled). The data shown are RDS offsets where observers achieved correct discrimination in 80% of trials and were taken from psychometric functions in **Fig. 3.3**. Error bars depict one SEM.

Another explanation of the mixed polarity benefit is offered by a recent augmentation of the binocular energy model. Read and Cumming (2007) proposed that the visual system might use opposite contrast polarity of features in the two retinal images to reject false matches and thereby find the true correspondence by a process of elimination. Recently, Goncalves and Welchman (2017) developed a binocular neural network, which is based on an advanced concept of the binocular energy model and uses proscription of unmatched image

information to achieve stereo correspondence. This neural network produces a mixed polarity benefit together with other phenomena of human vision such as Da Vinci stereopsis. Additionally, the network only produces a perceptual benefit if dots did not overlap in the RDS, as is true for human observers (Read et al., 2011).

Why does brain stimulation increase the benefit?

It is surprising that brain stimulation has the potential to improve stereopsis. The best explanation for why TMS amplifies the mixed polarity benefit is that TMS changes neural activity in a sensory processing mechanism through which the benefit arises. I therefore discuss the different potential outcomes of stimulation and consider how they could explain an improvement of depth perception, given the explanations of the mixed polarity benefit which have been proposed above.

TMS has the potential to both drive excitation and increase suppression of neural activity in the brain (Rattay, 1999). While it is possible for TMS to hyperpolarize cells, this only happens under very specific conditions (Rattay, 1999), and it is therefore assumed that cell suppression following TMS results from the activation of inhibitory connections (Moliadze et al., 2003; Murphy et al., 2016). Electrical stimulation of animal neural tissue triggers initial brief excitation (Adrian & Moruzzi, 1939; Patton & Amassian, 1954), followed by two waves of GABA-ergic inhibition (Connors et al., 1988), in the first 100ms after stimulation. This general effect of initial excitation (Boroojerdi et al., 2001; Devanne et al., 1997; C. W. Hess et al., 1987; Ziemann et al., 1996) and subsequent GABA-ergic inhibition (Kujirai et al., 1993; Premoli et al., 2014) has been replicated in the human motor cortex. TMS to primary visual cortex in cats suggests that stimulation predominantly triggers suppression of simple and complex cells in a 100ms window (Moliadze et al., 2005, 2003).

Depending on the structure of a neural network, TMS will trigger a different ratio between activation and inhibition. Also, depending on the role of these networks, activation and inhibition of certain cell sub-populations will have different effects on the behavioural outcome. Accordingly, TMS has been shown to differently affect behavioural tasks and brain areas. TMS has been shown to impair sensory discrimination for visual features such as motion direction (Pascual-Leone et al., 1999), motion speed (McKeefry et al., 2008), object shape (Silson et al., 2013) and local orientation (Rahnev et al., 2012). It has been argued that brain stimulation results in random neural noise, which compromises cell populations that encode the relevant visual features. However, TMS induced activation has also been shown to sum with sensory activation in a meaningful way to improve detection of elusive

stimuli (Abrahamyan et al., 2015; Abrahamyan, Clifford, Arabzadeh, et al., 2011; Miniussi et al., 2013; Schwarzkopf et al., 2011).

So how can we explain an improvement in depth perception for mixed polarity stimuli after TMS that were observed in this study? All variations of the binocular energy model, which describe disparity processing in primary visual cortex, contain a squaring non-linear processing step to match the model output with the strong responses of complex cells to preferred disparities. Read and Cumming (2018) have shown that the binocular energy model produces a stronger population response for mixed compared to single polarity stimuli. This is because inter-ocular image correlations are higher for mixed polarity RDSs, and this difference is further amplified by non-linear processing after summation of simple unit activity. If TMS activates neurons in V1, and thereby drives sensory responses, then we would predict a greater amplification for mixed polarity stimuli due to non-linear processing. In this way, TMS would provide a stronger disparity signal boost to the visual system for mixed polarity stimuli and could thereby improve depth perception.

To test this assumption, I retested nine participants and adjusted task difficulty until observers had similar proportions of correct responses for mixed and single polarity stimuli. These stimuli should produce comparable disparity signals for mixed and single polarity stimuli in primary visual cortex. Similarly to the finding in the main experiment, V1 stimulation significantly improved depth discrimination for mixed polarity stimuli (see **Fig 3C**). For single polarity stimuli, I observed a slight improvement in depth perception, but this increase was not significant. This suggests that the increase of the mixed polarity benefit through TMS cannot be explained solely by an amplification of differentially strong disparity signals in primary visual cortex.

Alternatively, it is possible that TMS drives inhibitory connections, which lead to stronger suppression of binocular mismatches in primary visual cortex. The recently published binocular neural network (Goncalves & Welchman, 2017) makes use of the great number of potential feature mismatches in a RDS by inhibiting the resulting erroneous disparities to support correct stereopsis. This produces a mixed polarity benefit because mixed polarity images contain more contrast mismatch information than single polarity images do. In this study, I applied stimulation in 100ms intervals during stimulus presentations. Animal models of TMS effects in V1 suggest that stimulation in 100ms intervals during stimulus presentation causes inhibition of simple and complex cells (Moliadze et al., 2005, 2003). Given that the visual system is presented with one global solution and far more potential false matches, which would signal incorrect disparities, general inhibition of the full population of simple and complex cells could have a net effect of predominantly suppressing binocular mismatches.

This would support stereopsis and would increase the perceptual benefit of mixed polarity stimuli. For single polarity stimuli this amplification would be less pronounced because less contrast mismatch information is available.

3.5 Conclusion

My results show that a neural mechanism of stereopsis in early visual cortex benefits from the availability of a mixture of contrast polarity and improves depth discrimination. I found that stimulation over V1 with TMS amplifies this mixed polarity benefit, while stimulation of higher visual areas (V3a, LO) had no effect. This finding confirms that the mixed polarity benefit arises during disparity processing in early visual cortex. This is consistent with computational models of stereopsis at the level of V1, which also produce a mixed polarity benefit. The currently most promising explanations for the mixed polarity benefit are that (i) higher inter-ocular image correlation in mixed polarity stereograms drives binocular cells in primary visual cortex more strongly and produces a more reliable binocular disparity signal or that (ii) binocular contrast mismatches, which are available in mixed polarity stimuli, are used to inhibit implausible correspondence solutions and thereby lead to a more reliable disparity signal. Brain stimulation might further increase this perceptual benefit by (i) amplifying responses of binocular cells to mixed polarity stimuli or (ii) by driving the inhibition of binocular contrast mismatches in primary visual cortex. Additional research will be necessary to conclusively answer the question how the mixed polarity benefit arises in stereopsis.

4. The role of parietal cortex in stereopsis

This project was carried out in collaboration with Dr Elizabeth Michael. Dr Michael helped conducting the experiment, performed the initial EEG data cleaning from blink and muscle artefacts and ran the Current Source Density and weighted Phase Lag Index data transformations as discussed in the methods section of this chapter.

4.1 Introduction

Natural scenes often contain complex physical geometries (e.g. the branches of a tree spreading in all directions) and the visual system has to make sense of the resulting noisy binocular disparity in the scene to estimate the distance of a single branch pointing at the observer. Harris and Parker (1992) found that the visual system is surprisingly challenged by this task: Observer ability to distinguish fine depth differences suffers greatly when disparity noise is introduced. It has been suggested that mechanisms of stereopsis in early visual cortex (Schaeffner & Welchman, 2018) which establish stereo correspondence (J. M. Harris & Parker, 1992, 1995; Read & Cumming, 2018; Read et al., 2011) provide an unreliable disparity signal under such conditions. From this emerges the challenge for later stages of stereopsis to correctly construct depth perception based on a noisy disparity signal.

One such mechanism might be located in higher dorsal regions: Researchers have shown that neurons in monkey MT critically support stereopsis for a disparity based signal in disparity noise (signal-in-noise task) (DeAngelis et al., 1998; Uka & DeAngelis, 2003). However, this substrate for disparity signals in noise is not always required by the visual system: After training the discrimination of fine disparity differences, MT neurons are no longer critical for stereopsis with noisy disparity input (Chowdhury & DeAngelis, 2008). Importantly, tuning properties of cells in MT were not changed after training which suggests that the unchanged contribution of this signal-in-noise neural mechanism was no longer used.

Chang, Kourtzi and Welchman (2013) showed that this one-sided learning transfer also exists in human observers. In humans area MT is not sensitive to stimulus position in noisy disparity (Patten & Welchman, 2015). Instead parietal cortex shows strongest sensitivity for noisy disparity based stimuli (Patten & Welchman, 2015) and changing normal neural activity in parietal cortex disrupts the perception of depth in noisy disparity (Chang et al., 2014).

Similar to monkey MT, after fine disparity discrimination training human parietal cortex is no longer critical for processing noisy disparity.

It is currently unclear how this signal-in-noise neural mechanism benefits stereopsis and why this contribution becomes obsolete once the brain learns to distinguish fine disparity differences. There are different potential ways in which the parietal cortex might contribute to depth judgements with noisy disparity information:

One possibility is that neural populations in the dorsal stream, which preferentially respond to large, absolute disparities (Neri et al., 2004; Uka & DeAngelis, 2006; Umeda et al., 2007), support the detection of sufficiently large absolute disparities in smaller disparity noise. Once neural populations in the ventral stream, which encode fine, relative disparities, have been sufficiently engaged by training they could compensate this role in a one-sided learning transfer because relative-disparity-selective neurons can provide information regarding absolute disparities if a zero-disparity reference (fixation cross) is available. However, it has been shown that there is no strict dichotomy between absolute and relative disparity processing in the dorsal and the ventral stream (Cottereau et al., 2011, 2012; Patten & Welchman, 2015).

Alternatively, the signal-in-noise mechanism in human parietal cortex might be involved in 3D shape perception to extract the disparity based shapes in a noisy disparity stimulus. While the ventral visual pathway supports shape discrimination and object recognition (Neri, 2005; Orban, Janssen, & Vogels, 2006; Tyler, 1990), cells in monkey AIP have been shown to be selective to disparity based 3D shape (Srivastava et al., 2009; Theys, Pani, van Loon, Goffin, & Janssen, 2012, 2013). These parietal cells signal 3D structure faster than cells in ventral areas but are less sensitive to small differences in disparities (P. Janssen et al., 2018). It has been proposed that this is beneficial for on-the-fly feedback for motor actions. It is conceivable that an untrained observer would initially rely on quick, but coarse, disparity processing, due to the time constraints of stimulus exposure of classic psychophysical experiments.

Another possibility is that parietal cortex accumulates disparity evidence for discrimination judgements. Parietal cells in monkey LIP accumulate sensory evidence for visual judgements which is read out by motor areas to create an adequate response (de Lafuente, Jazayeri, & Shadlen, 2015; Shadlen & Newsome, 2001). Similar evidence accumulation takes place in human parietal regions (Kelly & O'Connell, 2013; O'Connell et al., 2012). Electrical stimulation of these evidence accumulation circuits disrupts visual judgements in monkeys (Hanks, Ditterich, & Shadlen, 2006; but see also Katz, Yates, Pillow, & Huk, 2016).

Additionally, it has been shown that performance improvements on noisy motion tasks through training are possible through improved representation of sensory evidence in lateral intraparietal sulcus (LIP) (Law & Gold, 2008). In monkey MT cells of this signal-in-noise substrate do not show activity patterns that we associate with evidence accumulation (DeAngelis et al., 1998). However, it is unclear whether neural populations in human parietal cortex could be involved in this process.

Finally, the brain might apply the strategy to exclude unwanted visual input (in this case disparity noise), which it deems irrelevant for a depth judgement. Cueing observer attention to a spatial location, where noisy visual information is presented, has been shown to improve perceptual discrimination (Dosher & Lu, 2000). Results in psychophysics (Hetley, Dosher, & Lu, 2014; Lu & Dosher, 2004; Lu, Lesmes, & Dosher, 2002), monkey single cell recording (Desimone & Duncan, 1995; Haenny & Schiller, 1988; Luck, Chelazzi, Hillyard, & Desimone, 1997; Moran & Desimone, 1985; Treue & Maunsell, 1996) and functional imaging (Kastner, De Weerd, Desimone, & Ungerleider, 1998; Lu, Li, Tjan, Dosher, & Chu, 2011) suggest that spatial attention excludes noise by sharpening selectivity of neurons for the target feature. Importantly, this effect of attention specifically causes noise exclusion and therefore doesn't benefit discrimination of stimuli which do not contain unwanted information (fine feature discrimination). Additionally, the effect of attention on perception is much greater for coarse discrimination compared to fine discrimination (Hetley et al., 2014).

Parietal cortex might play a key role in this attentional noise exclusion. Parietal cortex has been shown to be part of a larger fronto-parietal attention network in both monkeys (Goldberg, Bisley, Powell, Gottlieb, & Kusunoki, 2002) and humans (Corbetta & Shulman, 2002). It has been shown that changes in attention co-occur with changes of activity in this fronto-parietal network, as well as in visual areas which process the attended visual input (Pessoa et al., 2003). Parietal cortex might change sensory processing in visual cortex by (i) cuing sensory areas for relevant features prior to stimulus onset or by (ii) providing top-down feedback during stimulus processing (Pessoa et al., 2003).

All the processes described above have been associated with the parietal cortex and might potentially be compensated by ventral areas. It is challenging to isolate these different parietal contributions: The neural substrates for absolute disparity processing, disparity based shape processing, evidence accumulation and attention overlap spatially in the brain and might all contribute for signal-in-noise discrimination in stereopsis. An alternative approach is to separate them in time: The different contributions of the parietal cortex discussed above are expected to occur at different times between stimulus onset and observer response.

In this study, I recorded EEG during stimulus presentation and disparity processing to disentangle the neural substrates of different potential contributions of the parietal cortex to stereopsis. I combine this approach with TMS to disrupt synaptic transmission in the parietal cortex and reveal which component of parietal processing underlies the discrimination of disparity signals in noise.

I found that parietal TMS produces significant deficits in stereopsis. In the visual cortex parietal TMS attenuates early disparity responses. This is best explained by the disruption of a top-down, inhibitory influence of the parietal. In line with this interpretation, I found that parietal TMS reduces alpha power in visual cortex during stimulus presentation. This suggests that alpha inhibition was reduced in visual cortex following TMS. Additionally, TMS increases a drop in synchronisation after stimulus offset between the parietal and visual cortex. This suggests that, following the disruption of parietal, top-down influences, the contribution of parietal cortex in stereopsis was further suppressed in the visual system. These results suggest that parietal cortex has an early, top-down influence on disparity processing in the visual cortex.

4.2 Methods

Participants

For this study, I screened 79 naïve, right-handed participants. All had normal or corrected-to-normal vision with good visual acuity (between -0.1 and 0.1 LogMAR). I screened participants for good stereo acuity with the demanding depth discrimination task used in this experiment (see Methods). 24 participants successfully passed the screening and were tested for this study. From these 24 participants, two participants had to be excluded because their neuroimaging data was too noisy. Therefore, data from the remaining 22 participants is reported in this study. Before the experiment, participants provided written informed consent and were screened for contraindications to TMS (Rossi et al., 2009; Wassermann, 1998). Procedures were approved by the University of Cambridge ethics committee and were performed in accordance with the ethical standards laid down in the 1964 Declaration of Helsinki.

Stimuli

Participants performed the experiment task with a haploscope in which the two eyes viewed separate 22 inch Samsung (2233) LCD displays through front-silvered mirrors. Viewing distance was 50cm. Stimuli were displayed on 1680 x 1050 pixels at vertical refresh rate of 60 Hz. Participants were instructed to maintain fixation on a square fixation cross with horizontal and vertical nonius lines.

Stimuli were RDS (dot diameter: 0.15 deg, dot density: 6 dots/deg^2, 50/50 ratio black and white dots) depicting a central target (diameter = 6 deg) surrounded by an annulus ("the surround", diameter = 12 deg) on a medium grey background (see **Fig. 4.1A**). Participants judged the position (in front / behind) of the central target relative to the surround. Stimuli were presented for 300ms. The target plane had a disparity of ± 6 arcmin (crossed or uncrossed) and the surround was located at zero disparity in the fixation plane. Task difficulty was adjusted by varying the percentage of dots defining the target relative to noise dots that had a random disparity within ± 12 arcmin. Stimuli were surrounded by a grid of background squares (size = 0.5 deg), designed to provide a background reference and promote stable vergence.

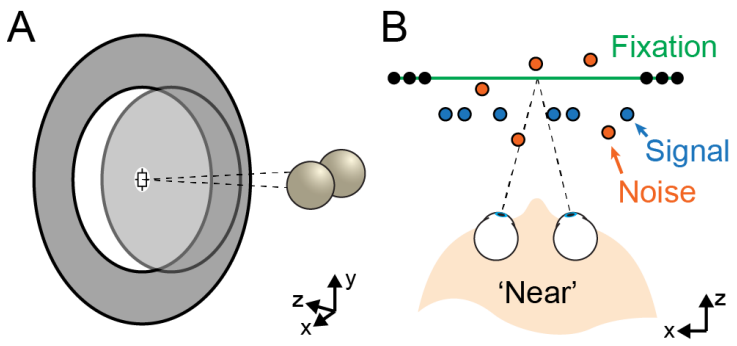

Figure 4.1: Signal-in-noise disparity stimulus. A) Stimulus containing a target centre disc with crossed or uncrossed disparity and with a surrounding annulus and fixation cross at zero disparity. Participants were asked to make a relative near vs. far judgement. **B)** Task difficulty was manipulated by reducing the coherence in the target disc (signal). Dots were randomly replaced in a ± 12 arcmin envelope (noise) around the remaining dots of the target centre disc.

Experiment procedure

Participants were tested for three sessions on separate days. In the first session participants were familiarized with the task and screened for stereo acuity with noisy disparity in four different screening tasks. Feedback was provided after every response. In the first task, participants were asked to discriminate large disparity offsets (+/- 8 arcmin) with no disparity noise. In the second task, participants were asked to discriminate smaller disparity offsets (+/- 0.5, 1, 3, or 6 arcmin). In the third task, participants were asked to discriminate a disparity offset (+/- 6 arcmin) with different amounts of disparity noise (stimulus coherence: 30, 50, 60, or 80%) (see **Fig. 4.1B**). Finally, participants' stereoacuity for noisy disparity discrimination was tested with an adaptive staircase. No feedback on task performance was provided. Participants that could discriminate stimuli with a coherence of 45% or lower correctly 82% of times were included in the main experiment of this study. This matches the performance of participants in previous studies (Chang et al., 2014). The screening was constrained to a total of 460 trials to prevent any training effect for this task. Chang et al. (2014) showed that parietal contributions in this disparity based signal-in-noise task change after task training.

In the remaining two sessions of the experiment participants performed the same task before and after TMS was applied. At the beginning of each session participants performed a 48 training trials with feedback (+/- 6 arcmin, 80% coherence) to allow participants to re-familiarize themselves with the task. During the main experiment participants performed the task with adaptive difficulty (two QUEST staircases each 50 trials). Staircases were designed to converge at a stimulus difficulty that yielded 82% correct observer performance. This design allowed me to obtain a reliable measure of task performance in blocks of 100 trials. Each session contained a total of seven blocks (see **Fig. 4.2**). Three blocks were used to define baseline task performance prior to TMS. Four blocks were run after brain stimulation was applied. TMS was applied either over parietal cortex or a control site (Cz) in a testing session, the order of stimulation sites for the two testing days was counterbalanced.

At the beginning of every test block a full field checkerboard was presented for 15s, reversing contrast at 10Hz (see **Fig. 4.2**). Participants were asked to passively fixate during this period. This was done to assess excitability of the visual cortex at the beginning of each block (see EEG).

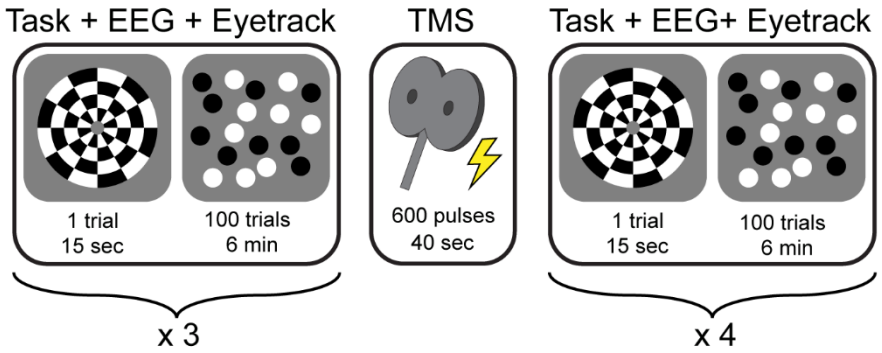

Figure 4.2: Experiment outline. The experiment consisted of blocks in which first a contrast reversing checkerboard was presented for 15 seconds. Afterwards observers performed a depth discrimination task with random dot stereograms as depicted in **Fig. 4.1**. During these blocks I recorded EEG and eyetracking data. Each experiment session consisted of seven experiment blocks. Three blocks were performed prior to TMS application. Next theta burst TMS was applied. Afterwards participants performed four more blocks of the experiment.

Transcranial magnetic stimulation

I applied stimulation with a MagStim Rapid^2 stimulator (MagStim, Whitland, UK), using a figure-of-eight coil (70 mm outer diameter). The TMS coil was placed tangentially on the head aiming at the defined region of interest in the brain. Stimulation was applied to left parietal brain regions (over electrode P3) where TMS was applied successfully in previous studies (Chang et al., 2014). The induced current was directed rostral to caudal with the coil handle facing upwards and towards the front of the head. Control stimulation was applied over electrode Cz with the coil handle facing from front to back with current direction anterior to posterior. Offline repetitive TMS was delivered as a continuous theta burst stimulation (cTBS) protocol (Huang et al., 2005) consisting of 600 pulses at an intensity of 38% of maximum stimulator output.

Electroencephalography

Electroencephalography data were acquired with a 64 channel cap (BrainCap, Brain Products GmbH). Data were recorded using BrainVision Recorder software. Caps were fitted with 61 Ag/AgCl electrodes positioned according to the standard 10-20 system (Fp1 Fp2 F3 F4 C3 C4 P3 P4 O1 O2 F7 F8 T7 T8 P7 P8 Fz Cz Pz IO FC1 FC2 CP1 CP2 FC5 FC6 CP5 CP6 FT9 FT10 F1 F2 C1 C2 P1 P2 AF3 AF4 FC3 FC4 CP3 CP4 PO3 PO4 F5 F6 C5 C6 P5 P6 AF7 AF8 FT7 FT8 TP7 TP8 PO7 PO8 Fpz CPz POz Oz). Electrooculograms were also

acquired, using two pairs of bipolar electrodes placed horizontally and vertically around the left eye. Data were acquired at a sampling rate of 1kHz and filtered online at 0.1Hz. Temporal markers of stimulus onset were sent using a pair of photodiodes attached to the stimulus presentation screen.

Pre-processing and analyses were performed in MATLAB, using the EEGLAB toolbox (Delorme & Makeig, 2004) and custom in-house scripts. Epochs were extracted around the stimulus onset to include a 1s pre- and 3s post-stimulus period. All epochs were visually inspected and artefactual epochs were rejected (excluding eye movements). Channel interpolation was performed on any channels with consistently noisy signal across the entire session. Data were filtered offline with a 1Hz high pass and a 40Hz low pass filter. Data were re-referenced to an average reference across all channels. ICA decomposition was applied for the purpose of artefact identification and resultant ICA components were visually inspected before rejection. Only components reflecting eye movements and other likely muscle artefacts were removed. As a final pre-analysis step, the raw signal amplitudes were converted into Current Source Density (CSD) estimates to minimise the impact of volume conduction effects (Srinivasan, Winter, Ding, & Nunez, 2007; Winter, Nunez, Ding, & Srinivasan, 2007).

Eye tracking

I recorded binocular eye movements with an EyeLink 1000 remote video tracker (SR Research), at a sampling rate of 500 Hz. The system has a stated accuracy of 0.25 deg and resolution of 0.01 deg (root mean square). The tracker viewed participants' eyes through the (infrared transmitting) cold mirrors of the stereoscope. Observers were instructed to maintain their gaze on the fixation marker at all times during the experiment. At the beginning of each experiment block participants were instructed to keep fixating on a calibration marker which was used to calibrate a four by four degree area on the screen in which stimuli were presented.

To analyse eye movement data, I converted raw gaze positions to degrees of visual angle. Trials during which tracking was lost in one or both eyes were excluded (average proportion of trials per participant 16.4%). This high proportion of lost trials was due to the challenge of tracking both eyes through the mirrors and eye holes of the stereoscope. Time series data were pre-processed by removing any data that corresponded to periods of blinks or saccades, as identified by the EyeLink inbuilt detection functions. I removed an additional 50ms of data before and after blinks to remove large gaze point offsets which were likely

caused by eye rotation prior to blinks. Removed data was then linearly interpolated. Finally, eye tracking in a stereoscope sometimes led to erroneous tracking of interior parts of the stereoscope instead of participant's pupils (average proportion of trials per participant 1.8%). To remove all trials where this occurred, I excluded all trials where gaze position was located outside of the stimulus. I checked whether loosing or removing eye tracking data affected different conditions of the experiment disproportionately. In this experiment the loss of eye tracking data was not significantly different between experiment conditions (Z=-0.66, p=.51). Similarly, excluding eye tracking data due to erroneous tracking did not significantly differ between conditions (Z=-0.73, p=.47).

I report vergence and horizontal version eye movements during stimulus presentation to check that brain stimulation and lateralized stimulus presentation did not interfere with vergence stability. To quantify changes of vergence through TMS, I fit a linear model to participants' average eye vergence during stimulus presentation. I quantify vergence changes on each trial in terms of the gradient (β) of the best fit (least-squares).

Event related potentials

Event related potentials (ERP) were computed time-locked to stimulus onset. Group averages were calculated for each task for occipital (Left: O1, PO7; Right: O2, PO8) and centro-parietal (Left: P1, CP1; Right: P2, CP2) electrode groups in both hemispheres. To identify any effect of parietal TMS on the visual evoked response, I concentrated the first analysis on the first components of the visual evoked response. To overcome any between-participant differences in ERP latency, I defined individual participant's P100 and N100 component peak in a 100+/-50ms window after stimulus onset (see **Fig. 4.7**). Individual component peaks were visually inspected to confirm that all cases the correct peak was selected. Additionally, I computed alpha power (8-12Hz) as a measure of local inhibition for occipital (Left: O1, PO7; Right: O2, PO8) electrode groups.(EEGLAB; Delorme and Makeig, 2004)

In addition to the stimulus-locked components, I also compared the amplitude of evoked response in the pre-response period, which has been associated with a decision making role in perceptual judgement paradigms. Data were re-aligned to the response time for each trial, for 100ms pre-response to 500ms post response.

Steady state visual evoked response

The steady state visual evoked response (SSVEP) in response to the contrast-reversing checkerboard was pre-processed in the same way as the task data, using epochs of -2/+18s around the stimulus onset. However, no epochs were discarded due to blinks because this intense checkerboard stimulus causes blinking too frequently. The first two seconds of data were discarded to avoid the onset response, and the subsequent 10s of data were used in the analysis. Data from left hemisphere occipital electrodes (O1, PO7) were averaged together before a fast Fourier Transform was applied. Each participant had a clearly identifiable peak at the expected frequency (see **Results**), matching the reversal rate of 10Hz. The amplitude of the 10Hz peak was referenced to the amplitude within +/-20 frequency bins around the 10Hz peak to estimate the signal-to-noise ratio.

wPLI connectivity measures

To measure the functional connectivity between the parietal stimulation site (P3) and occipital sites, I computed the weighted phase lag index (wPLI; Vinck, Oostenveld, Van Wingerden, Battaglia, & Pennartz, 2011). This measured the phase coherence between the electrode time series, weighted by the imaginary component of the coherency. This measure is intended to be more robust to the spurious signal correlations induced by volume conduction.

To compute the wPLI, I first band-pass filtered the CSD time series at each electrode with a Hilbert transform at 0.5Hz sub-band intervals for the frequency range of interest (Alpha: 8-12 Hz, Theta: 4-8Hz), to calculate the instantaneous phase. The wPLI was calculated for all parietal-occipital pairs at the trial level, and then averaged across all pairs and frequency sub-bands. The wPLI data was smoothed using a Savitzky-Golay filter.

Two time windows of interest were selected, to capture pre-and post-stimulus onset changes in functional connectivity. Blocks 2 and 3 pre-TMS were averaged and used as a reference baseline time series, which was subtracted from each block post-TMS.

Analysis

All data were analysed using repeated-measures ANOVAs, and Greenhouse-Geiser correction was applied where appropriate. For post-hoc analysis I used Bonferroni corrected t-tests.

4.3 Results

Behaviour

Behavioural performance was measured across 7 blocks of trials, using an adaptive procedure to estimate the noise level required to achieve 82% accuracy (see Methods). To measure the impact of TMS, I compared the difference in performance between the target site (P3) and the control site. As these measurements were taken on separate days, the first three experiment blocks on each day prior to stimulation were used as a baseline reference for the remaining four experiment blocks after TMS. However, **Fig. 4.3** shows that during the first testing block of each session participants showed elevated thresholds compared to the second and third baseline testing block. It is likely that participants took longer than expected to reach a stable level of performance at the beginning of a session with this demanding depth judgement task. I therefore excluded data from the first baseline block and collapsed the data from the remaining baseline blocks to obtain a stable measure of baseline performance. Baseline performance before parietal and control stimulation did not differ significantly (t_{21}=-1.75, p=.1). Performance across the four post-TMS blocks (**Fig. 4.4**) is shown relative to the pre-TMS baseline.

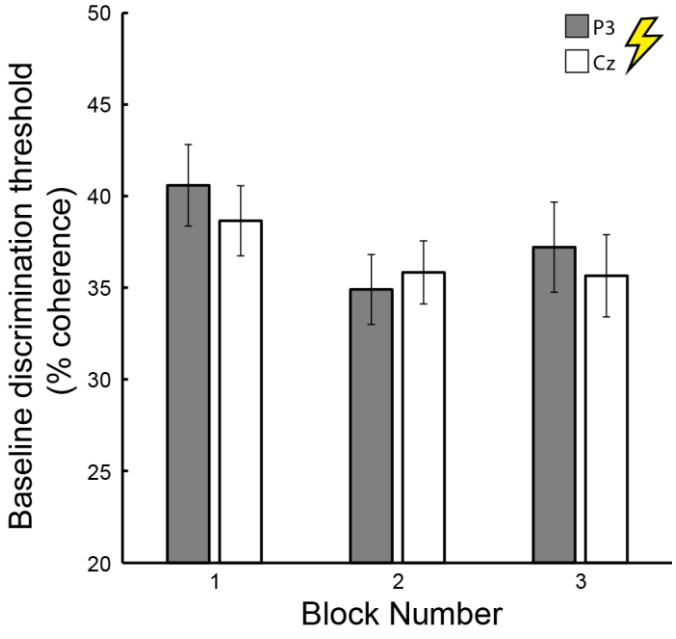

Figure 4.3: Baseline disparity discrimination priori to TMS. Mean baseline disparity discrimination thresholds (% stimulus coherence) prior to TMS application for all participants tested in both the pilot phase and the main experiment of this study (n = 31). Error bars depict one standard error of the mean.

I found that TMS over parietal cortex (P3) significantly affected disparity discrimination performance ($F_{1,21}$=4.96 , p=.04) by increasing disparity thresholds where observers judged visual depth correctly for 82% of trials. Further, a significant interaction, between the stimulation site and the block number, suggests that the impact of TMS on visual depth judgements varied over time ($F_{3,63}$=2.91 , p=.04). Post-hoc paired t-tests revealed that in block two (t_{21}=3.1, p=.005) and block three (t_{21}=2.36, p=.028) after TMS P3 thresholds were significantly increased relative to Cz (see **Fig. 4.4**).

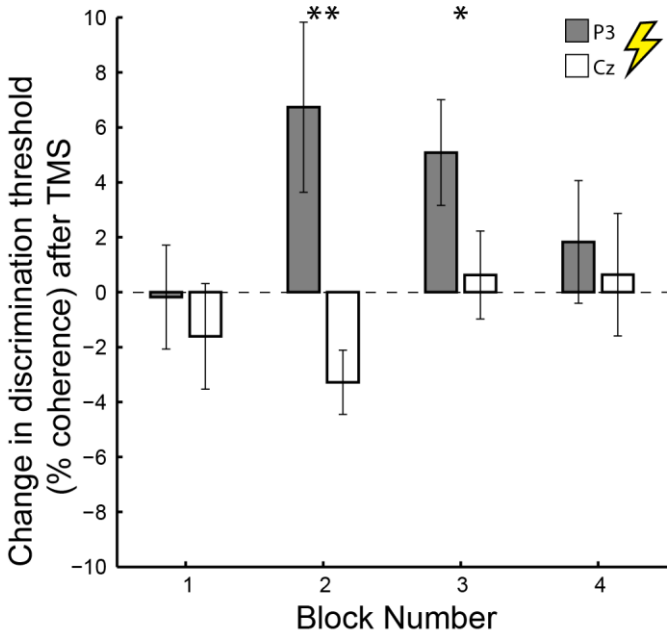

Figure 4.4: Effect of TMS on disparity discrimination. Mean change in disparity discrimination thresholds (% stimulus coherence) after TMS application. Error bars depict one standard error of the mean.

Reaction times did not change significantly after parietal stimulation compared to control stimulation ($F_{1,21}$=0.02, p=.89) (see **Fig. 4.5**). This confirms that the impaired disparity discrimination after TMS was not caused by participants giving more rushed responses.

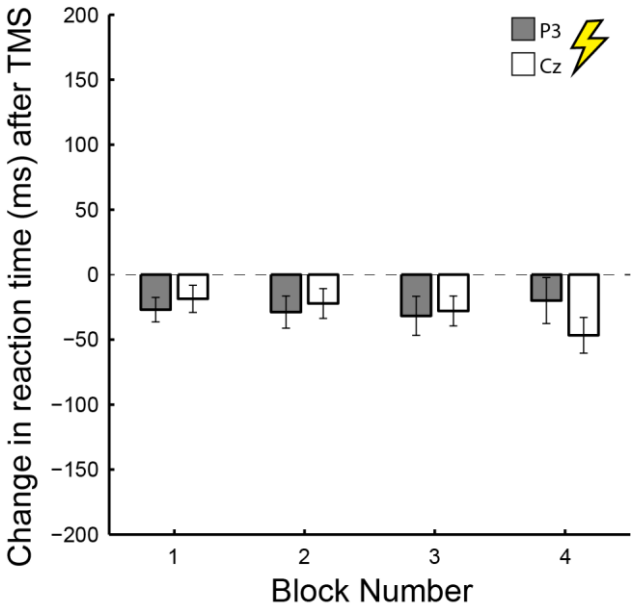

Figure 4.5: Reaction times for disparity discrimination after TMS. Mean changes in reaction time (ms) after TMS application relative to baseline reaction time prior to TMS (n = 22). Error bars depict one standard error of the mean.

Disparity evoked response

Having established that TMS to P3 impairs discrimination in noise performance, I next asked how TMS disrupted task-relevant neural processing. To capture any TMS effect, I mirrored the structure of the behavioural data comparisons – I first subtracted the pre-TMS baseline, and then looked for time windows that showed a significant P3-Cz difference. **Fig. 4.6** shows a full scalp map of changes in neural responses after TMS. I observed changes of early responses (100-200ms after stimulus onset) in the visual cortex of the left, stimulated brain hemisphere. This suggests that parietal TMS affects early processing mechanisms of stereopsis.

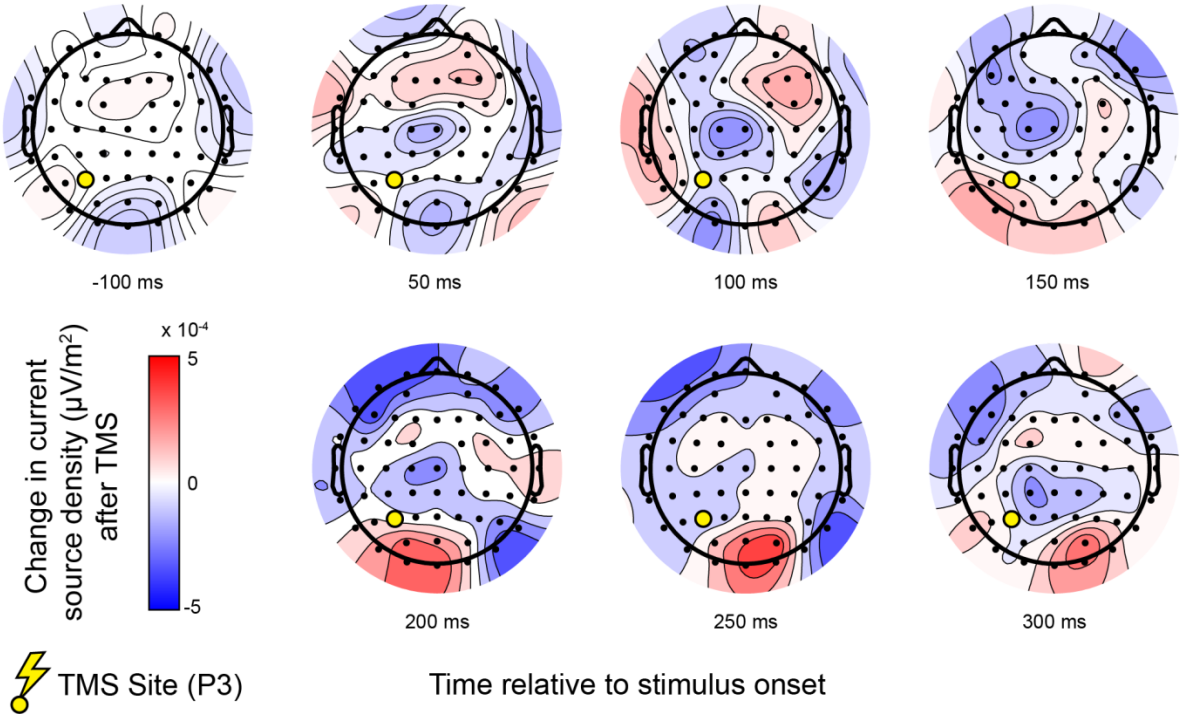

Figure 4.6: Full-brain changes of disparity responses after TMS. Scalp map of the changes in stimulus evoked responses before and after TMS. This figure shows changes after parietal stimulation (P3) relative to control stimulation (Cz). A larger black dot indicates the stimulation site.

Next, I assessed how TMS changed neural responses to the stimulus in visual cortex. **Fig. 4.7** shows individual participant and group average ERP responses to the RDS in the left visual cortex (data from block 3 prior to control stimulation). In a 200ms time window after stimulus onset the RDS produces a prominent P100 and N100 component. I therefore focused on these two components to asses TMS related changes in neural responses. Because the latencies of these components varied amongst participants (see **Fig. 4.7**) I extracted positive and negative peaks in a 100+/-50ms window (greyed area). The resulting peaks were visually inspected to confirm correct selection.

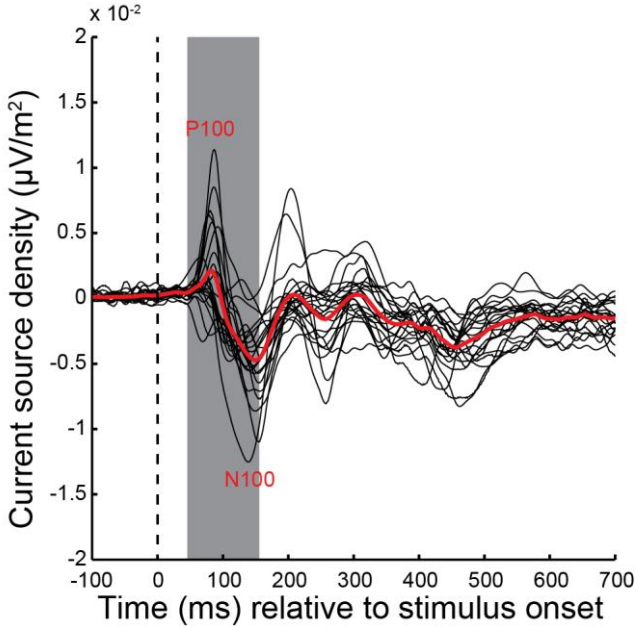

Figure 4.7: Disparity evoked response in visual cortex. Example of stimulus evoked responses in the left visual cortex of individual participants (black lines) and as a group average (red line). This data was recorded prior to control stimulation (Cz) at baseline block three. P100 and N100 component peaks were calculated in a 100+/-50ms window (greyed area) after stimulus onset.

Fig. 4.8 shows the changes in N100 and P100 amplitude after parietal and control TMS. TMS over left parietal cortex significantly decreased N100 amplitudes in the left visual hemisphere ($F_{1,21}$=4.83, p=.04) (see **Fig. 4.8A**). This effect was particularly pronounced at block two after stimulation (t_{21}=3.14, p=.005) where observed the strongest effects of TMS on stereopsis. No such effect was observed in the right, non-stimulated hemisphere ($F_{1,21}$=0.48, p=.5) (see **Fig. 4.8B**). Additionally, I observed a significant decrease of N100 amplitude over the course of the experiment in both the left- ($F_{3,63}$=4.84, p=.004) and right hemisphere ($F_{3,63}$=4.25, p=.023) for both parietal and control stimulation. Similarly, for the P100 component TMS significantly decreased amplitudes in the left visual hemisphere ($F_{1,21}$=5.42, p=.03) (see **Fig. 4.8C**). This effect was strongest at block (t_{21}=-2.34, p=.03) as well as block four (t_{21}=-2.74, p=.012) of the experiment. I did not find any effect of TMS in the right, non-stimulated hemisphere ($F_{1,21}$=0.07, p=.8) (see **Fig. 4.8D**). The P100 component did not change significantly over the course of the experiment (left hemisphere: $F_{3,63}$=0.88, p=.46; right hemisphere: $F_{3,63}$=0.28, p=.84). These changes in N100 and P100 amplitude through parietal stimulation were correlated at block two ($r_s(22)$ = -.53, p = .01) where I observe the strongest effects of TMS on stereopsis (see **Fig. 4.4**).

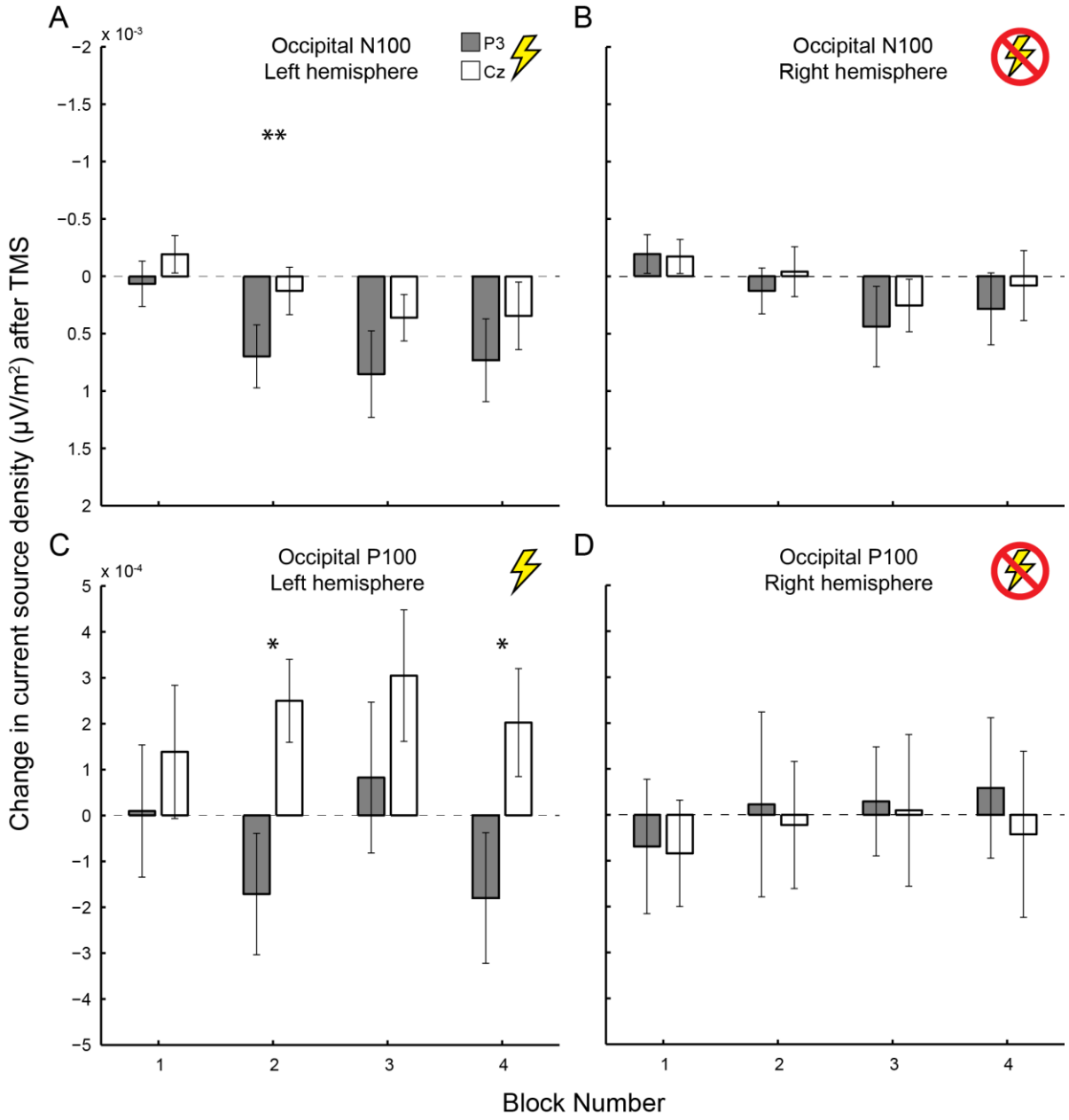

Figure 4.8: Changes of the disparity evoked response in visual cortex after TMS. Mean changes in stimulus evoked responses in the visual cortex after TMS. Error bars depict one standard error of the mean. **A)** and **C)** show changes of the N100 and P100 in the left, stimulated brain hemisphere. **B)** and **D)** show changes of these components in the right, non-stimulated brain hemisphere.

Additionally, I assessed how TMS changed alpha power (8-12Hz) in visual cortex as measure of local inhibition. **Fig. 4.9A** shows individual participant and group average alpha power change in the left visual cortex during stimulus presentation (data from block 3 prior to control stimulation). Alpha power increased during stimulus presentation and dropped below

a pre-stimulus level after stimulus offset. TMS over parietal cortex decreased alpha power approximately 100 to 400ms after stimulus onset in the both the left and right visual cortex (see **Fig. 4.9B**). However, this drop in alpha power was not significantly different ($p<.05$) from control stimulation.

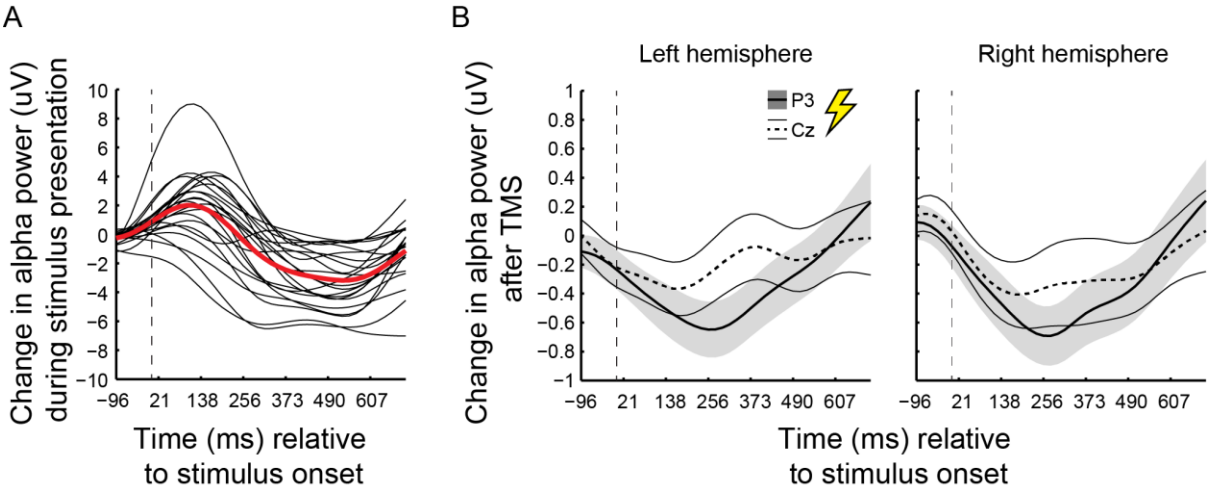

Figure 4.9: Changes in alpha power after TMS. A) Example of stimulus evoked changes in alpha power in the left visual cortex of individual participants (black lines) and as a group average (red line). This data was recorded prior to control stimulation (Cz) at baseline block three. **B)** Changes in alpha power after parietal (P3) and control (Cz) stimulation in the left and right visual cortex.

Given the reported contribution of parietal regions to later, decision-related processing stages, the evoked response at parietal sites was calculated relative to the trial response time. This analysis showed that pre-response, there was a slow increase in amplitude until the time of response, consistent with the process of evidence accumulation reported previously (O'Connell et al., 2012). This increase in parietal response did not significantly differ at any time point between the P3 and control stimulation ($p<.05$), suggesting the P3 stimulation did not impact on later parietal signals.

Steady state visual evoked response

Given the observed change in the amplitude of the stimulus locked evoked response, I next aimed to identify whether this was a task-specific modulation in response amplitude, or

whether TMS over parietal areas induced a broad, nonspecific change in cortical excitability in visual cortex. To do this, I compared the amplitude of the steady state visual evoked response measured in response to a 10Hz contrast-reversing checkerboard at the start of each block (see **Fig. 4.10**).

Fig. 4.11 shows changes cortical excitability of both left and right visual cortex after parietal and control stimulation. I did not find a significant difference in visual cortex excitability after parietal or control stimulation in the left, stimulated hemisphere ($F_{1,21}$=0.51, p=.82) (see **Fig. 4.11A**) or the right, non-stimulated hemisphere ($F_{1,21}$=0.63, p=.44) (see **Fig. 4.11B**). Changes in cortical excitability also did not change over the course of the experiment (left hemisphere: $F_{3,63}$=0.13, p=.94; right hemisphere: $F_{3,63}$=0.53, p=.66).

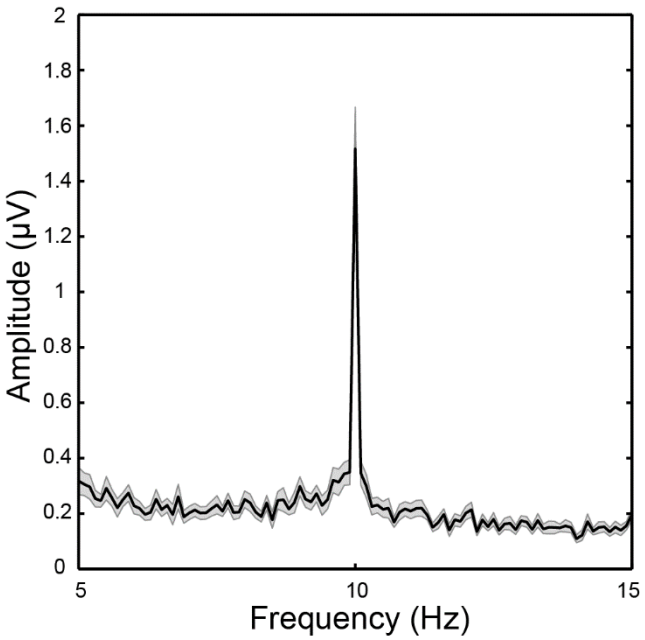

Figure 4.10: Frequency response to flickering checkerboard stimulus. Example of mean steady state visual evoked response to a contrast-reversing checkerboard (10Hz). The shaded area shows the standard error of the mean. The stimulus produces a discernible increase in amplitude at a narrow frequency band around 10 Hz. In this study, I used this response to quantify cortical excitability within the visual cortex. This data was recorded prior to control stimulation (Cz) at baseline block three.

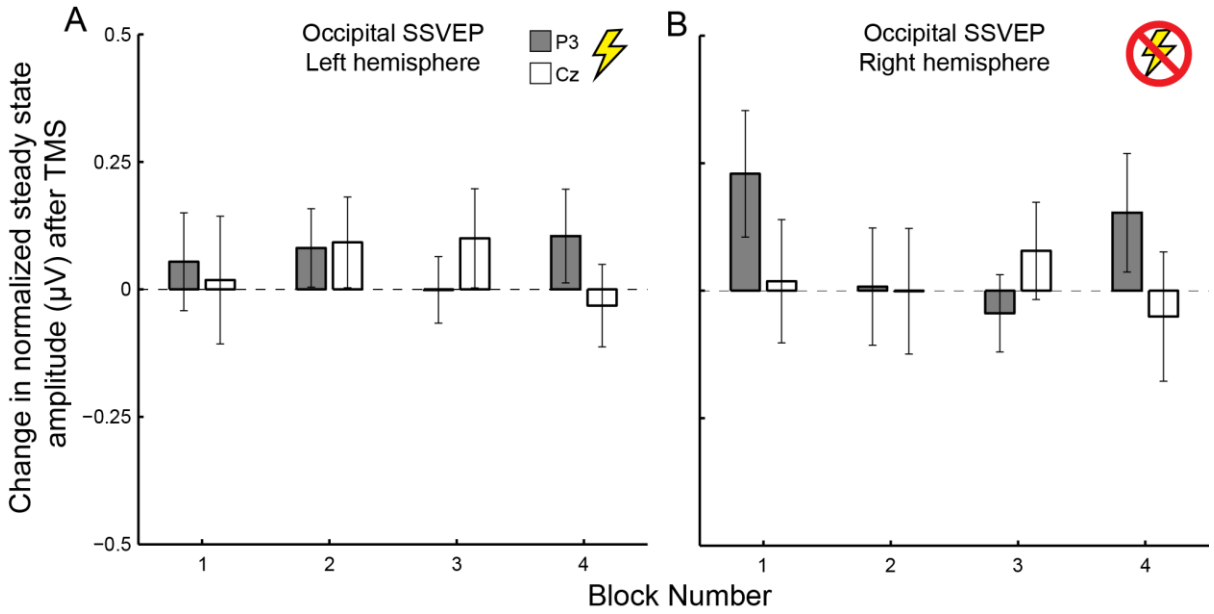

Figure 4.11: Changes in frequency response to flickering checkerboard stimulus after TMS. Mean changes in cortical excitability in visual cortex after TMS application in the left, stimulated (**A**) and the right, non-stimulated brain hemisphere (**B**). Error bars depict one standard error of the mean.

Phase coherence connectivity measures

The described modulation of the early components of the visual evoked response after TMS suggests that parietal stimulation had a functional impact at distal, visual areas. To investigate the mechanism underlying this modulatory influence, I turned to a time-resolved measure of functional connectivity. Specifically, I calculated the wPLI (Vinck, Oostenveld, Van Wingerden, Battaglia, & Pennartz, 2011) within the alpha frequency band (8-12Hz). I was interested in two time windows: pre-stimulus onset (-500-0ms) and post stimulus onset (300-700ms). These time windows capture any pre-stimulus anticipatory effects, and the post-stimulus desynchronisation within the alpha band. **Fig. 4.12A** shows individual participant and group average functional connectivity before and after stimulus onset (data from block 3 prior to control stimulation).

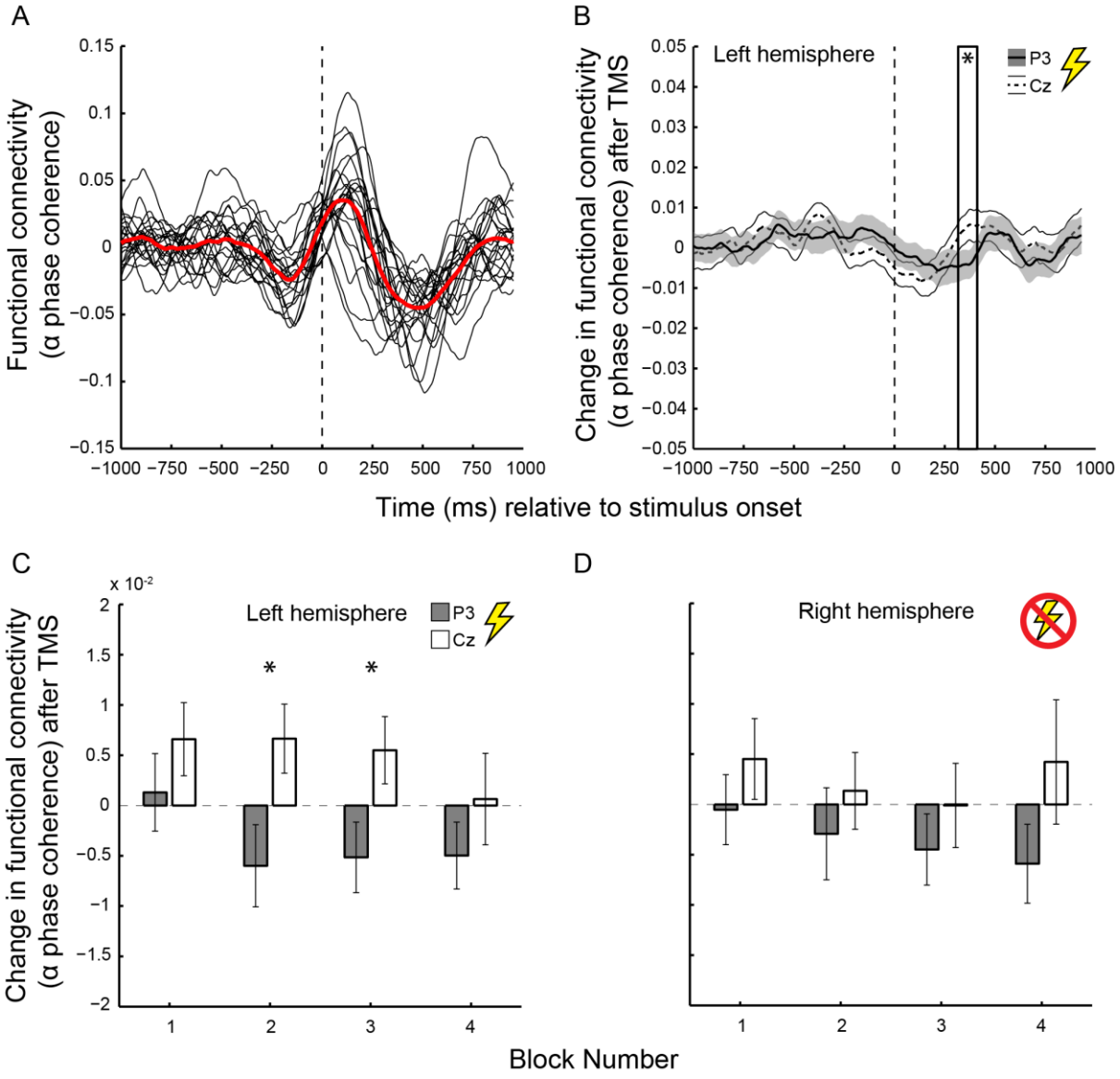

Figure 4.12: Functional connectivity between visual and parietal cortex before and after TMS. A) Example of changes in functional connectivity between parietal- and visual cortex for individual participants (black lines) and a group average (red line). This data was recorded prior to control stimulation (Cz) at baseline block three. **B)** Changes in functional connectivity after parietal (P3) and control (Cz) stimulation before and after stimulus onset. An asterisk marks the time window where functional connectivity differed significantly after parietal and control stimulation ($p<.05$). **C)** and **D)** show changes of functional connectivity in the left, stimulated (**C**) and right, non-stimulated (**D**) brain hemisphere. Error bars depict one standard error of the mean.

First, I identified during which time window (relative to stimulus onset) functional connectivity between parietal and visual cortex changed through stimulation. **Fig. 4.12B** shows changes in functional connectivity in the left hemisphere averaged over all four blocks. I observed significant changes in functional connectivity ($p<.05$) through parietal stimulation in a time window 323-417ms after stimulus onset (highlighted in **Fig. 4.12B**). Next, I compared functional connectivity during this time window for individual blocks:

I found that TMS over the left parietal cortex significantly reduced functional connectivity in the left, stimulated hemisphere ($F_{1,21}$=7.13, p=.01) (see **Fig. 4.12C**). This effect was particularly pronounced at block two (t_{21}=-2.55, p=.02) and block three (t_{21}=-2.25, p=.04) after stimulation where observed the strongest effects of TMS on stereopsis. I did not observe a significant effect on functional connectivity in the right, non-stimulated hemisphere ($F_{1,21}$=1.75, p=.2) (see **Fig. 4.12D**).

To control whether functional connectivity changes were specific to the parietal and visual cortex I also inspected functional connectivity between visual and frontal brain areas. Specifically, I chose the dorso-lateral prefrontal cortex (DLPFC) because this area has been identified as a part of a wider fronto-parietal attention network which can affect sensory processing in visual cortex (Corbetta & Shulman, 2002; Goldberg et al., 2002). **Fig. 4.13A** shows participant's individual and group average functional connectivity before and after stimulus onset (data from block 3 prior to control stimulation). Functional connectivity fluctuations around stimulus onset had a similar profile as visual-parietal connectivity (see **Fig. 4.12A**) but were less pronounced. **Fig. 4.13B** shows that parietal TMS did not induce significant functional connectivity changes between DLPFC and visual cortex.

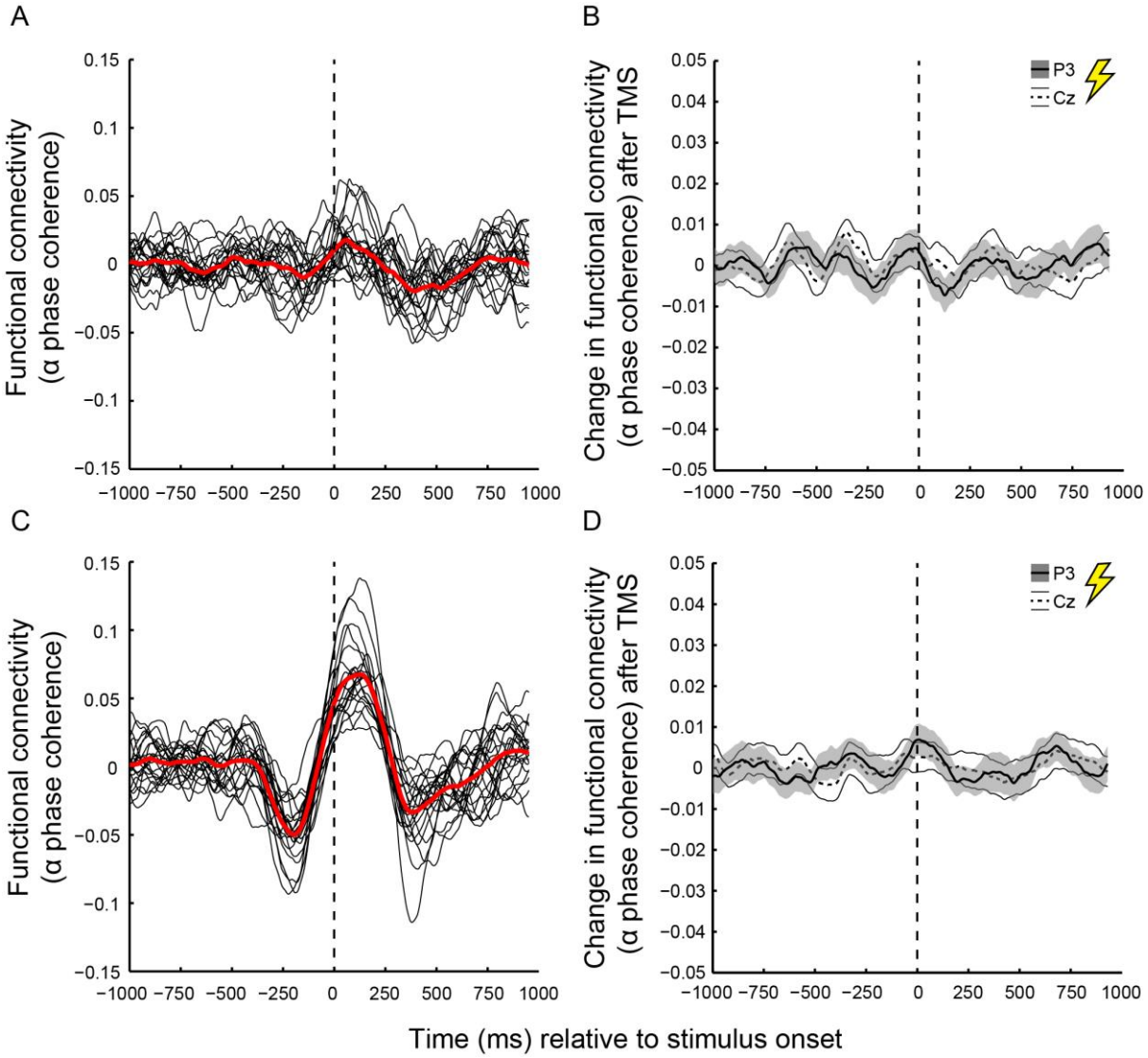

Figure 4.13: Control measures of functional connectivity. A) Example of changes in functional connectivity between DLPFC and visual cortex for individual participants (black lines) and a group average (red line). The data in **A** and **C** was recorded prior to control stimulation (Cz) at baseline block three. **B)** Changes in functional connectivity between DLPFC and visual cortex after parietal (P3) and control (Cz) stimulation before and after stimulus onset. **C)** Example of changes in theta phase coherence between parietal and visual cortex for individual participants (black lines) and a group average (red line). **D)** Changes in theta phase coherence between parietal and visual cortex after parietal (P3) and control (Cz) stimulation before and after stimulus onset.

This analysis focused on the alpha frequency band due to the large body of literature linking visual cortex alpha to sensory processing and parietal cortex alpha activity to attentional and control functions in visual tasks (Klimesch, Sauseng, & Hanslmayr, 2007). To control whether the observed change in connectivity profile was specific to alpha, I performed the same analysis in the theta band, which has also been implicated as a mechanisms to optimise or control task-relevant information (Palva & Palva, 2011).

Fig. 4.13C shows participant's individual and group average theta phase coherence before and after stimulus onset (data from block 3 prior to control stimulation). Phase coherence changes around stimulus onset were even more pronounced than alpha phase coherence changes (see **Fig. 4.12A**). However, parietal TMS did not induce significant theta phase coherence changes between parietal and visual cortex (see **Fig. 4.13D**).

Eye tracking

Finally, to control whether TMS affected vergence eye movements during the experiment, I recorded pupil positions during stimulus presentation. **Fig. 4.14** shows average vergence eye movements during stimulus presentation before and after parietal and control stimulation. To quantify changes of vergence through TMS, I fitted a linear model to participants' eye vergence during stimulus presentation. Eye vergence during stimulus presentation did not differ significantly differ after parietal and control stimulation ($F_{1,12}$=0.12, p=.73). Also, vergence eye movements did not change over the course of the experiment ($F_{3,36}$=0.29, p=.83). This confirms that stimulation of parietal cortex did affect vergence during stimulus presentation.

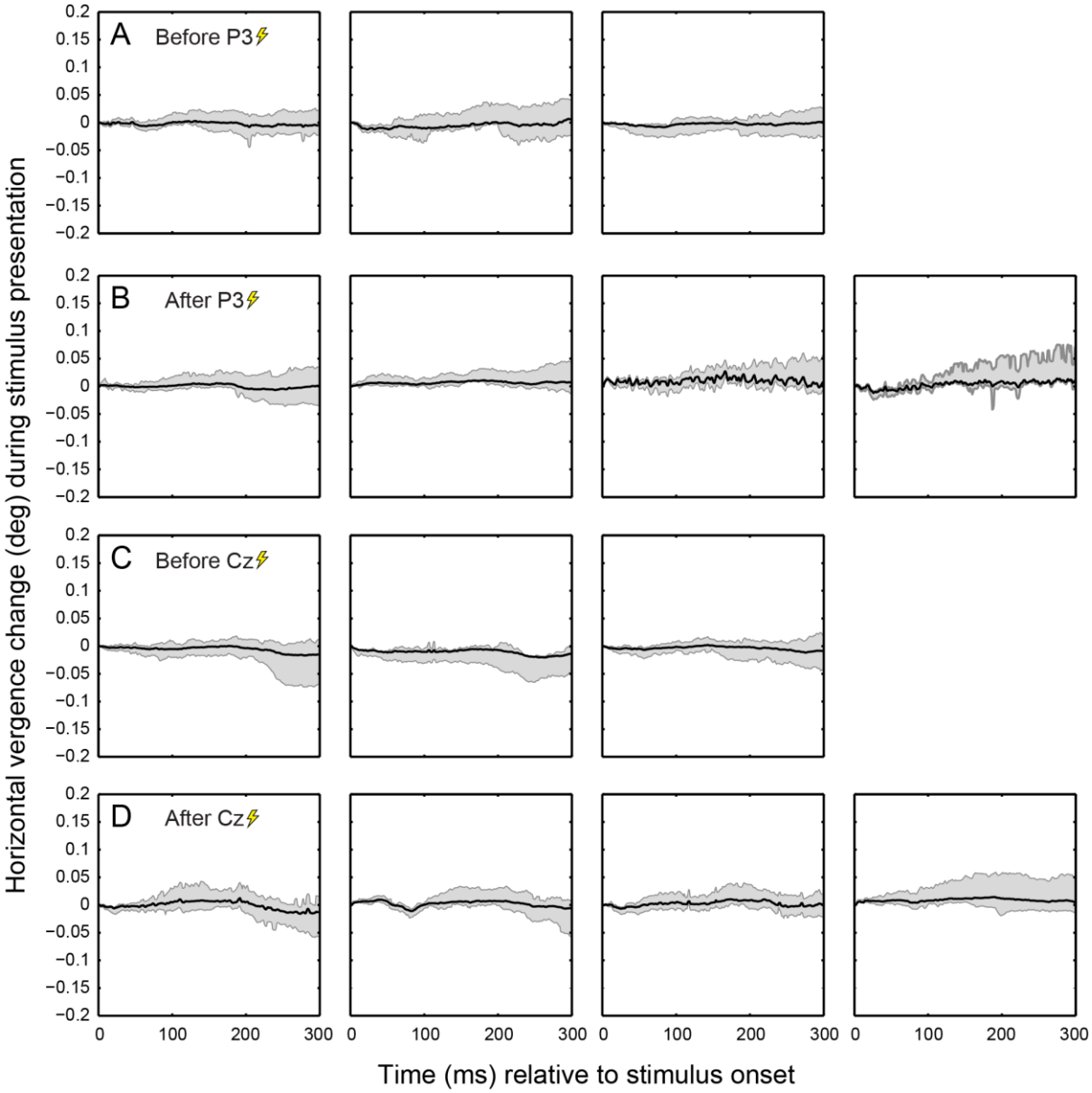

Figure 4.14: Vergence eye movements before and after TMS. Horizontal vergence change during stimulus presentation before (**A**) and after (**B**) parietal (P3) as well as before (**C**) and after (**D**) control (Cz) TMS. Shaded area shows 25-75 percentiles.

4.4 Discussion

In this study, I applied TMS over parietal cortex and subsequently recorded brain activity during a signal-in-noise disparity discrimination task. I found that TMS produced significant deficits in stereopsis. In the visual cortex parietal TMS attenuated early disparity responses alpha power. Additionally, TMS increased a drop in synchronisation after stimulus offset between the parietal and visual cortex.

Effect of parietal TMS on stereopsis

In this study I applied theta burst TMS to change the probability of synaptic transmission within parietal cortex, and between parietal cortex and interconnected areas, for a prolonged period. I found that TMS over parietal cortex (P3) affected the discrimination of depth differences in a disparity-based signal-in-noise task. Specifically, during the time window with the largest TMS effect on stereopsis, the intervention increased discrimination thresholds on average by ~5% stimulus coherence compared to control stimulation (Cz) (see **Fig. 4.4**). This increase matches previous findings which suggest that human parietal cortex plays a critical role when observers have to detect depth differences in noisy disparity signals (Chang et al., 2014).

One limitation of the study was that I used a different TMS intervention from what has previously been used to disrupt parietal cortex. In a previous study Chang et al. (2014) used online TMS over parietal cortex to disrupt depth discrimination for the same signal-in-noise task. Because I recorded brain activity during stimulus processing in this study, I was forced to use theta-burst, offline TMS which can be applied prior to the start of the experiment. Online TMS changes neural activity during application by actively depolarizing neurons and triggering action potentials (Rattay, 1999). Offline TMS, on the other hand, does not directly affect neural activity. Instead it changes the probability of synaptic transmission for a prolonged time after stimulation (Huang et al., 2005). One concern in this study was that online and offline TMS over parietal cortex would not disrupt stereopsis in a comparable way, or that online and offline TMS would interfere with different brain mechanisms in parietal cortex. In this study I found that offline TMS had the same effect on stereopsis as online TMS. Depth discrimination was disrupted and thresholds increased by a similar magnitude of ~5% stimulus coherence as reported for online TMS (Chang et al., 2014). This suggests that the same parietal mechanism was disrupted with both TMS interventions.

In this study the effect of theta burst TMS on stereopsis was unstable over time (see **Fig. 4.4)**. During the first block I did not observe a difference in observer stereopsis for parietal and control stimulation. It has been shown that the maximum effect of theta burst on brain activity in the motor cortex is reached five minutes after stimulation (Huang et al., 2005). In this study testing blocks lasted for approximately six minutes and so it is possible that the effects of TMS only arose in block two of this experiment. Additionally, I used an adaptive staircase method to estimate perceptual thresholds in a testing block and thereby measured the effect of TMS on stereopsis. These adaptive staircases are more sensitive to incorrect responses at the beginning of a block when the staircase varies difficulty more greatly. Given

that the effect of theta burst might build up over the first five minutes, it is possible that only at the beginning of the second block staircases were sensitive enough to capture the effect of TMS.

From block two onwards there was an effect of parietal TMS on observer stereopsis. This effect gradually decreased over time, which is expected for the effect of theta burst stimulation on synaptic efficiency (Huang et al., 2005). In this study I recorded EEG after stimulation which reveals the effect of parietal TMS on brain activity. These measures also showed the strongest differences between parietal and control stimulation at experiment block two (see **Fig. 4.8A&C** and **Fig. 4.12C**). This makes it likely that the effect of TMS on mechanisms of stereopsis was strongest in block two, six minutes after brain stimulation.

Effect of parietal TMS on disparity responses in visual cortex

In this study I recorded EEG during task performance to assess in what way parietal TMS changes noisy disparity processing. A first inspection over the whole scalp revealed that TMS at the parietal stimulation site caused the largest changes in visual cortex (see **Fig. 4.3**). I found that the two earliest ERP components of stimulus processing in visual cortex, the P100 and N100, were attenuated in the left hemisphere after stimulation (see **Fig. 4.8A&C**). The reductions in the P100 and N100 component were correlated which suggests that these changes are connected. The P100 and N100 are the first EEG components which are shaped under top-down control (Klimesch et al., 2007). Specifically, it has been suggested that top-down, alpha inhibition synchronizes sensory responses in the visual cortex and thereby amplifies the ERPs I observe (von Stein, Chiang, & Konig, 2000).

To test this hypothesis, I analysed alpha power in the visual cortex during stimulus presentation. **Fig. 4.9A** shows that alpha power increased during stimulus presentation and dropped off after stimulus offset. This agrees with our hypothesis that top-down-controlled alpha inhibition supports disparity processing in visual cortex. If this was true, then we would expect parietal TMS to disrupt alpha inhibition in visual cortex, and alpha power should decrease. This is what I found in this study: Parietal TMS attenuated the rise in alpha power during stimulus presentation (see **Fig. 4.9B**). However, this effect was present in both the stimulated, left hemisphere and the non-stimulated, right hemisphere. Also, the attenuation of alpha power after parietal TMS was not significantly different from alpha power changes after control stimulation. I can therefore not say with certainty whether attenuated responses to disparity in visual cortex after parietal TMS are connected to changes in alpha inhibition.

One concern in this study was that TMS over parietal cortex does not affect top-down inhibition in the visual cortex, but rather changes cortical excitability in the visual cortex directly. Studies which combine TMS with fMRI have shown that TMS does not only affect brain activity locally but also in distant, interconnected areas. Given the strong association of parietal and visual cortex for our task it is conceivable that theta burst TMS could spread to visual areas and reduce cortical excitability directly. To rule out this explanation I measured visual cortex excitability with a flickering checkerboard stimulus at the beginning of each experiment block. After parietal and control stimulation I did not observe a significant change in task-independent visual cortex excitability. This makes it unlikely that TMS interfered with visual cortex function directly.

To control whether evidence accumulation was affected in parietal cortex I also analysed response locked ERPs. I found no difference in parietal brain activity leading up to observer responses between parietal and control stimulation. This suggests that later, decision-related functions of parietal cortex were not affected by stimulation. However, it has been suggested that ERPs recorded from classic psychophysical tasks which involve stimulus presentation and a subsequent response are not sensitive to the gradual build-up of evidence in parietal regions (O'Connell et al., 2012). I therefore cannot rule out that also decision-related mechanisms were affected by TMS.

Neither the changes in early disparity responses nor the changes in alpha power, which I report in this study, were significantly correlated with the observed deficits in stereopsis after parietal TMS. One possible explanation for this could be the relatively small sample size of 22 participants for a correlation analysis. Alternatively, it is possible that disrupted brain signals of disparity only explain deficits in stereopsis at later, decision-related processing stages. In this study I did not observe any differences in response-locked, parietal brain activity after TMS. This could suggest that TMS did not disrupt evidence accumulation, however, as mentioned above, this experiment was not perfectly suited to investigate decision-related mechanisms of stereopsis. I therefore cannot rule out the explanation that later disparity processing, based on a disrupted disparity signal, might better explain the deficits of stereopsis I observed in this study.

Effect of parietal TMS on functional interactions between parietal and visual cortex during disparity processing

In this experiment I applied theta burst TMS which has the potential to change the probability of synaptic transmission both within the parietal cortex, and between the parietal cortex and interconnected sites (Huang et al., 2007). So far, I have shown that parietal TMS indirectly causes changes in visual brain activity. To assess whether interactions between parietal and visual cortex were affected after TMS I analysed phase coherence between these two areas as a measure of functional connectivity (Vinck et al., 2011). Alpha phase coherence has been shown to increase between visual cortex and other task relevant sites during stimulus processing (Mima, Oluwatimilehin, Hiraoka, & Hallett, 2001; Varela, Lachaux, Rodriguez, & Martinerie, 2001). It has been suggested that this alignment increases the likelihood of information transfer and suppresses other, task irrelevant input (Palva & Palva, 2011).

I observed a pronounced increase in alpha phase coherence between parietal and visual cortex during stimulus presentation (see **Fig. 4.12A**). The strongest interactions between these areas fall in a 0-200ms window after stimulus onset which agrees with the idea that parietal top-down modulation shapes early disparity processing in visual cortex. After stimulus offset the two areas desynchronize, potentially because the feedback is now no longer required. In fact coherence levels drop below the level of connectivity prior to stimulus onset.

Parietal TMS caused a significant decrease in functional connectivity between parietal and visual cortex. However, while changes in stimulus evoked visual components suggest that TMS disrupted early, top-down mechanisms of stereopsis, changes in functional connectivity between parietal and visual cortex occurred 300ms after stimulus onset (see **Fig. 4.12B**). Specifically, the drop in alpha phase coherence which occurs after stimulus offset was more pronounced after parietal stimulation. This could suggest that parietal TMS and its potential effect on visual cortex inhibition leads amplifies the desynchronization of parietal and visual cortex after stimulus presentation. This could be due to a reduction of alpha power in visual cortex which could reduce phase coherence. Alternatively, it is possible that the connectivity to parietal cortex is further reduced (and parietal, top-down influence further suppressed) because it´s contribution has been compromised by TMS.

Similar to changes of disparity responses in visual cortex, changes in functional connectivity after TMS did not correlate significantly with the deficits of stereopsis that I observed in this study. As discussed above, this could be because early interactions between parietal and visual cortex might not be strongly associated with later, decision-related mechanisms.

In this study I investigated the role of parietal cortex in processing noisy binocular disparity. I found that parietal cortex shows increased alpha phase synchronisation with the visual cortex during stimulus presentation which suggests that parietal cortex involved in noisy disparity processing. However, research suggests that parietal cortex is part of a larger fronto-parietal network which controls spatial attention and modulates visual processing (Corbetta & Shulman, 2002; Goldberg et al., 2002). Based on the close, functional interaction between frontal and parietal structures in top-down feedback for sensory processing we should expect parietal TMS to also affect functional connectivity between frontal and visual cortex during disparity processing. I therefore also analysed alpha phase coherence between the visual cortex and the dorsolateral prefrontal cortex (which is a frontal part of the fronto-parietal network) during stimulus processing. Stimulus evoked changes in functional connectivity between visual and frontal cortex during stimulus processing had a similar profile as parieto-visual connectivity, but was less pronounced (see **Fig. 4.13C**). TMS did not cause any changes in alpha phase coherence between frontal and visual cortex (see **Fig. 4.13D**). This could suggest that deficits in disparity processing after parietal TMS are mainly due to the disruption of parietal cortex and not a larger fronto-parietal network. However, more research is needed to conclusively answer this question.

Additionally, different fronto-parietal networks with different contributions to perception have been proposed. One network between the posterior parietal cortex and the frontal cortex has been suggested to be involved in the cognitive selection of information and the anticipation of incoming information (Corbetta & Shulman, 2002; Pessoa et al., 2003). Here, I have suggested that this network might play a role in top-down modulation of stereopsis. However, researchers have also identified another, spatially close network between the temporal parietal cortex and the frontal cortex (Corbetta & Shulman, 2002). This network could be involved in the detection of sensory events which are salient but unattended. Additionally, it has been proposed that the two networks interact, namely that the latter can overrule the former when relevant information is presented outside of the focus of attention. This could serve to force attention to the newly encountered source of information. In this study I propose that TMS over parietal cortex affects attentional top-down modulation of visual cortex mechanisms of stereopsis. A potential limitation of this interpretation is that also detection of most informative parts of a RDS stimulus could have been affected in the temporal parietal cortex. However, this is unlikely because the attentional detection network between the temporal parietal cortex and the frontal cortex is strongly lateralized in the right hemisphere. In this study, TMS was applied over the left hemisphere which makes it unlikely that the TMS intervention affected this brain network.

In this study I focused on the alpha frequency band which has been shown to play an important role in parietal, attentional top-down modulation of sensory processing (Klimesch et al., 2007). Another frequency band which often has been associated with the interaction between different brain areas is theta frequency band (Palva & Palva, 2011). To confirm that parietal top-down modulation of visual cortex is in fact best captured by alpha phase coherence I also analysed theta phase coherence between these two sites (see **Fig. 4.13A**). Theta phase coherence did show a similar stimulus evoked profile change which suggests that also in theta band frequency there was a stimulus related interaction between parietal and visual cortex. However, parietal TMS did not change theta phase coherence (see **Fig. 4.13B**) which suggests that the disruption of stereopsis I observed in this study is not associated with any parieto-visual interaction in theta band frequency.

Effect of parietal TMS on eye movements

Finally, one concern in this study was that TMS might affect the stability of eye vergence during the task. Parietal brain regions have been shown to be involved in the control of eye movements (Pierrot-Deseilligny et al., 2004). A change in vergence stability during stimulus presentation could affect stereopsis negatively and thereby create a spurious result of parietal TMS affecting disparity processing. In this study I recorded vergence eye movements to control for this potential confound (see **Fig. 4.14**). I did not find any changes in vergence eye movements after parietal or control stimulation. This suggests that our TMS effect on stereopsis cannot be explained by a change in vergence stability.

4.5 Conclusion

In this study, I investigated the role of parietal cortex in stereopsis. I applied TMS over parietal cortex and subsequently recorded brain activity during a signal-in-noise disparity discrimination task. I found that TMS produced significant deficits in stereopsis. In the visual cortex parietal TMS attenuated early disparity responses. This is best explained by the disruption of a top-down, inhibitory influence of the parietal. In line with this interpretation, I found that parietal TMS reduced alpha power in visual cortex during stimulus presentation. This suggests that alpha inhibition was reduced in visual cortex following TMS. Additionally, TMS increased a drop in synchronisation after stimulus offset between the parietal and visual cortex. This suggests that, following the disruption of parietal, top-down influences, the

contribution of parietal cortex in stereopsis was further suppressed in the visual system. These results suggest that parietal cortex has an early, top-down influence on disparity processing in the visual cortex.

5. Discussion

In this thesis, I present my experimental studies, which used non-invasive brain stimulation, to advance our understanding of the neural computations of stereopsis. In the final part of this thesis I will discuss implications, limitations and potential future research that follow from the results of my studies.

5.1 Assessing where in the visual brain TMS can be used to study perception

In **Chapter 2**, I investigated where in the visual cortex TMS can be used to change neural activity in a way that is sufficient to study mechanisms of perception. TMS is a powerful research tool that allows researchers to establish causal relationships between brain areas and functional mechanisms of perception. However, TMS research is currently challenged by a high rate of uninterpretable null results (De Graaf & Sack, 2011). If we want to be more successful at probing brain mechanisms with TMS, then we need to get a better understanding of what happens in the brain during stimulation. At the single neuron level this problem has been well researched: Brain stimulation can directly change neural activity during application (Moliadze et al., 2003; Rattay, 1999) or change the probability of synaptic transmission for a prolonged period of time after stimulation (Huang et al., 2007, 2005). TMS should, in principle, work similarly for any part of grey matter tissue in the brain (Histed et al., 2009). Therefore, if we observe no effect on behaviour after TMS, we have to assume that some neural activity was changed, but the net effect was not substantial enough to affect the brain mechanism that we are trying to study. In **Chapter 2**, I therefore investigated where in the visual cortex TMS can cause changes in neural activity that result in measurable effects on perception. As a marker of sufficient stimulation, I defined phosphenes, which are a direct outcome of TMS-induced changes of neural activity in the visual cortex. I found that TMS over dorsal (V3a, V3) and early (V1, V2d, V2v) visual cortex can reliably induce phosphenes. Researchers who want to study these brain areas and their role in perception with TMS can therefore be confident that stimulation is likely to induce changes in neural activity.

What change in brain activity causes phosphenes?

Previous research has indicated that activity changes in primary visual cortex should underlie phosphenes (Kammer et al., 2005; Tehovnik & Slocum, 2013). However, my results show that TMS induces phosphene even more frequently over dorsal visual areas. This suggests that activity changes which propagate back to the primary visual cortex are most suited to produce phosphenes. A similar suggestion has previously been made by (Pascual-Leone & Walsh, 2001) who showed that it is necessary for brain activity changes, which are cause by TMS over parietal cortex, to propagate back to the primary visual cortex to induce phosphenes. This emphasizes the role of afferent connections from dorsal to primary visual cortex for phosphenes and suggests that phosphenes could be connected to brain mechanisms for which this connection exists, e.g. higher visual areas providing top-down feedback to primary visual cortex during stimulus processing. By studying the different ways in which dorsal visual cortex provides input to primary visual cortex researchers could get a better understanding of what brain mechanism ultimately produces a phosphene through TMS application.

Additionally, the observation that TMS induces brain activity spreads so readily from dorsal to primary visual cortex poses a challenge to how TMS experiments are designed today. fMRI research has already informed us that TMS does not only cause local changes in brain activity but also causes BOLD changes at distant, interconnected brain areas (Caparelli et al., 2010). However, generally it is assumed that a TMS intervention will always be most potent at the location where it is applied because here the magnetic field is strongest. Contrary to this assumption, my results have shown that TMS over dorsal visual cortex are even more likely to induce phosphenes than TMS directly over primary visual cortex. This suggests that, in the context of phosphene research, TMS over dorsal visual areas stimulates primary visual cortex more strongly than TMS directly over the primary visual cortex. Consequently, we might have to abandon the assumption that TMS effects will always be strongest in the brain tissue directly underneath the TMS coil. It is conceivable that distant, TMS-induced brain activity, which travels through interconnected brain areas, cumulates to a stronger effect on perception than local TMS effects. Future research could consider this possibility and provide evidence (e.g. through concurrent neuro-imaging) that TMS effects were in fact strongest in a region of interest in the brain. This will allow researchers to more reliably connect changes in behaviour after TMS to functional regions in the brain.

One limitation of this study is that we still don't have a good understanding of what change in brain activity produces phosphenes. We know that muscle twitches (the classic metric of motor cortex stimulation) are caused by the excitation of interneurons and pyramidal cells in the motor cortex (Rothwell, 1997). It is currently unclear whether phosphenes are caused by excitation, inhibition (through interneurons) or hyperpolarization of neurons (Kammer et al., 2005). Answering this question would be useful because researchers could formulate more sophisticated a priori hypotheses about the effect of TMS on an area in the visual cortex, after it has been established that stimulation of this area induces phosphenes.

To get a better understanding of how phosphenes occur, researchers could combine TMS with neuroimaging techniques to investigate what type of neural activity change underlies the perception of phosphenes. This has already been done with fMRI. The occurrence of phosphenes is associated with blood-oxygen-level dependent signal (BOLD) increases at the stimulation site and distant interconnected sites (Caparelli et al., 2010). However, it has been suggested that BOLD changes do not reliably capture neural activity changes that are induced by TMS (for a detailed summary see section ‘Can TMS be used in every part of the neocortex to study brain function?’).

A more promising approach would be to combine TMS with electrophysiology. It is possible to clean electrophysiological recordings from the artefacts induced by a single TMS pulse and recover the underlying recording of neural activity (Mueller et al., 2014; Rogasch et al., 2014). TMS could be combined with single cell recording in animals to understand how cell activity changes in different parts of the brain during phosphene perception. One apparent challenge would be to teach monkeys or cats to accurately report the position of phosphenes in their visual field. However, an elegant solution to this problem has been proposed by (Tehovnik & Slocum, 2013) and would allow researchers to detect phosphenes psychophysically. Phosphenes have been shown to interfere with visual information that is presented at their visual field location (Kammer, 1999). Consequently, animals show a delayed saccadic response to visual stimuli presented at the location of the phosphene, which is called the 'delay field' (Tehovnik & Slocum, 2013). This would allow a researcher to confirm the occurrence of a phosphene during stimulation and map out the exact location of the phosphene in the visual field of the observer.

In humans TMS can be combined with EEG to record larger neuron population responses during phosphene perception. While this technique lacks the spatial specificity to infer how the activity of individual neurons changed, there are some ways to categorize different changes in neural activity. For example, in the visual cortex alpha power is a well-

established measure of local inhibition. This could allow researchers to investigate whether TMS primarily drives local excitation or inhibition during phosphene perception.

TMS induces phosphenes unreliably

Another limitation of phosphene research is that not every observer will report phosphenes after stimulation. This is likely a consequence of choosing a conservatively safe stimulator output which is common practise in brain stimulation research (Rossi et al., 2009; Wassermann, 1998). In **Chapter 2**, I screened a large number of participants of which 30% did not report phosphenes after single pulse stimulation. In line with previous reports (Boroojerdi et al., 2002; Ray et al., 1998) a large proportion of these 'non-perceivers' reliably reported phosphenes when I stimulated them with a longer lasting train of TMS pulses. This suggests that the vast majority of participants should be capable of perceiving phosphenes with brain stimulation and that the challenge of phosphene research lies in finding participants that are capable of spotting these elusive and short-lived percepts.

A goal of future phosphene research could therefore be to design a testing environment or task which makes it easier for participants to spot phosphenes. One characteristic of phosphenes, which is currently (to my knowledge) not explored to increase the likelihood of phosphene detection, is the observation that phosphenes interfere with visual information presented at the same location in the visual field (Kammer, 1999). Future research could use stimuli with repetitive patterns which cover the participant's whole visual field. It might be easier for the participant to detect distortion in these patterns compared to detecting spots of light in a dark room.

Locating the effects of TMS in the brain

Finally, a further limitation of this study is the challenge to accurately estimate the location of TMS effects in the brain without concurrent neuroimaging. The deciding factor, of whether neurons get activated by stimulation or not, is a sufficiently strong electric field and the geometry of neurons relative to the electric current produced by TMS (Rattay, 1999). Given that the electric field is always strongest directly under the TMS coil, I assume that neurons in the target location are most likely stimulated by TMS. However, sometimes neurons further distant from the coil centre are more ideally situated and will experience the strongest effect of stimulation (Opitz, Windhoff, Heidemann, Turner, & Thielscher, 2011; Thielscher et al., 2011). In **Chapter 2**, I used a vector projection method to estimate the location of

strongest TMS effects in the brain for a given coil position. I validated this approach with a more sophisticated electric field model (SimNIBS; Thielscher, Antunes, & Saturnino, 2015). However, both vector projection and electric field simulation are simplified models of the true effect of TMS on neural activity. This approach cannot give us full certainty where TMS-induced effects were located in the brain.

A future approach, which would overcome this limitation, could be to combine visual field maps of phosphenes, retinotopic maps of the visual cortex and electric field simulations. We know that the location of the phosphene in the participant's visual field follows the logic of retinotopy, e.g. stimulation of the dorsal visual cortex will produce phosphenes in the lower visual hemifield and vice versa (Kammer et al., 2005). In previous studies researchers have used individual participant retinotopic maps to explore whether neighbouring areas in primary visual cortex, which respond to information in different visual field locations, can be stimulated separately (Kammer et al., 2005; Salminen-Vaparanta et al., 2014). An interesting future approach could be to validate TMS effect localisations in the visual cortex by combining electric field simulations and the retinotopic organisation of the visual cortex to predict the location of phosphenes in the visual field. A similar study has successfully validated electric field model predictions of TMS effect locations in the motor cortex (Opitz, Zafar, Bockermann, Rohde, & Paulus, 2014). This could infirm whether phosphenes can be induced by any subpopulation of neurons in the visual cortex. Additionally, such an experiment could validate electric field models as good estimators for TMS effects in the visual brain.

Can TMS be used in every part of the neocortex to study brain function?

To the broader researcher readership the question remains whether TMS can be reliably applied outside of motor and visual cortex. Generally, we know how neurons should behave in electric currents (Rattay, 1999), and we can therefore safely assume that TMS will always trigger some changes in neural activity in a given portion of the cortex. However, it is a common observation that stimulation, which produces reliable effects in motor cortex, produces no observable effect on human behaviour when applied somewhere else in the brain (De Graaf & Sack, 2011). The critical question is whether TMS can trigger activity changes in large populations of neurons to have a substantial impact on neural processing, and subsequently human behaviour. To answer this question researchers have started to combine TMS with different neuroimaging techniques to get a better understanding of what happens during brain stimulation.

TMS has been successfully combined with fMRI, where stimulation is applied during a scan session (Bergmann, Karabanov, Hartwigsen, Thielscher, & Siebner, 2016). TMS triggers local BOLD increases in motor (Bestmann, Baudewig, Siebner, Rothwell, & Frahm, 2004) and visual (Caparelli et al., 2010) cortex. BOLD changes could be used as a readout to quantify TMS effects on brain activity. A convergent observation is that participants who can perceive phosphenes through TMS show larger BOLD changes than participants who cannot (Caparelli et al., 2010). However, BOLD change after primary motor cortex (M1) stimulation does not correlate with motor evoked potentials (MEPs) amplitude (Turi, Paulus, & Antal, 2012). BOLD signal changes might therefore not always capture the same aspects of TMS related changes in brain activity.

Additionally, TMS often triggers widespread BOLD changes in the brain, including in distant, interconnected areas (Hartwigsen et al., 2013; Turi et al., 2012; Volman, Roelofs, Koch, Verhagen, & Toni, 2011). This would rely on the idea that TMS induced activation might spread via axonal connections. However, sometimes changes in BOLD signal due to TMS can only be observed in distant brain sites (Dowdle, Brown, George, & Hanlon, 2018; Ruff et al., 2006). While it is conceivable that TMS might change brain activity in areas next to the stimulation site, the focality of TMS is generally too good to cause stimulation effects in distant, contra-hemispheric areas while leaving the local site unaffected (Opitz et al., 2011; Thielscher et al., 2011). The only current explanation is that BOLD signals are more sensitive to pick up TMS effects for certain brain mechanisms. This suggests that the widely distributed BOLD changes in different parts of the brain after TMS cannot be treated equally. These limitations currently make it challenging to use fMRI to validate TMS effects.

Another technique we can record brain activity with, while applying brain stimulation, is EEG. TMS-evoked-potentials (TEP) are neuron population activity directly driven by TMS which can be recorded with EEG. TEPs can be reliably triggered for many different TMS coil locations on the scalp (Lioumis, Kičić, Savolainen, Mäkelä, & Kähkönen, 2009) suggesting that TMS induced neural activation can be observed all over the brain. However, the spatial specificity of EEG is not good enough to be certain that TEPs are driven by the underlying brain region of interest when stimulated by TMS. While this approach allows us to conclude that frontal cortex activity can be altered with TMS (Rogasch et al., 2014), it would not allow us to distinguish whether the population response was driven by DLPFC or orbitofrontal cortex (OFC).

Finally, a promising, alternative approach is the use of calcium imaging to reveal the effects of TMS on brain activity. This involves the injection of fluorescent substances which signal calcium concentrations in nervous tissue and allows researchers to record the release of

neurotransmitters at the synapses as a measure of neuron activity. While this technique is currently not available for use in healthy humans, it allows researcher to observe how single neurons, as well as larger neural networks, change their activity through TMS (Murphy et al., 2016). This approach has the potential to answer the question why some brain mechanisms are prone to TMS intervention, while others are not.

It would be useful to have a metric brain stimulation effects which can be used in any part of the brain. However, the techniques used to observe brain activity in healthy humans do currently not provide a reliable marker of TMS effects. Unfortunately, this means that researchers will, for now, be forced to continue exploratory TMS research outside of the motor and visual cortex. Null results cannot be interpreted and TMS related changes in human behaviour will require a post hoc explanation.

5.2 Locating where the mixed polarity benefit of stereopsis arises

In **Chapter 3**, I investigated where in the visual cortex disparity processing benefits from the availability of a mixture of bright and dark visual features, allowing for better depth perception. This mixed polarity benefit, which was first discovered by Harris and Parker (1995), serves as a great opportunity to validate computational models of stereopsis. Any model that aims to describe the neural mechanisms of disparity processing in humans should be capable of producing such a benefit. Both the standard binocular energy model (Read & Cumming, 2018) and more advanced versions of it (Goncalves & Welchman, 2017) have been shown to produce a mixed polarity benefit. This suggests that disparity processing in early visual cortex can produce such a benefit. However, an important addition to this observation should be that we have empirical evidence which suggests where in the brain the mixed polarity benefit arises. Here, I applied brain stimulation to early (V1) and higher (V3a & LO) visual brain areas. These areas have been shown to be extensively involved in disparity processing (Goncalves et al., 2015; Patten & Welchman, 2015; Preston et al., 2008) and were therefore good candidates for a location where the mixed polarity benefit might arise. I found that stimulation over V1 increased the mixed polarity benefit. Stimulation of higher visual areas V3a and LO did not change perception. This finding shows that disparity processing in early visual cortex gives rise to the mixed polarity benefit.

Subsequently, this emphasizes that computational models of disparity processing in early visual cortex should produce such a mixed polarity benefit if we want to consider that they

employ similar computations as neural networks in the brain. My findings here provide the necessary basis for this approach. Further, the mixed polarity benefit relies on certain characteristics such as no dot overlap in the RDS or a sufficiently high dot density. These characteristics either categorically allow or disallow a benefit or change the strength of benefit magnitude. Researchers could use these facts to further assess how close computational models of stereopsis behave compared to human observers. Ideally, researchers could put together a range of phenomena of human depth vision (e.g. Da Vinci stereopsis) which model of stereopsis should successfully mimic. This will allow us to identify the models which most likely resemble the computation of stereopsis in the brain from a large number of proposed models which are all suitable to detect disparity but might not be biologically implemented.

How does the mixed polarity benefit arise?

Different models of stereopsis inspire different explanations for the mixed polarity benefit. The Binocular Energy Model describes how a mixed polarity benefit can arise purely through differently strong image correlation in mixed- and single contrast polarity stereo images (Read & Cumming, 2018). The binocular neural network, on the other hand, suggests that the mixed polarity benefit arises through the inhibition of unmatched binocular information (Goncalves & Welchman, 2017). Both explanations could in principle explain the mixed polarity benefit. Also, these explanations are not mutually exclusive, meaning that benefit might actually be explained by a combination of both. Ultimately, all current models are likely to be a simplified version of the real solution that the brain applies. It is therefore possible that a completely different form of binocular disparity processing is implemented in the brain. The phenomenon of the mixed polarity benefit therefore has the potential to validate which model does best at describing disparity processing in the brain.

A future experiment might help to confirm whether the mixed polarity benefit arises as predicted by the standard binocular energy model. Read and Cumming (2018) showed that the binocular energy model produces a mixed polarity benefit for noisy- but not for consistent disparity discrimination. Specifically, binocular image correlation is reduced in noisy disparity profiles and, because this effect is stronger in single polarity stereo images, a mixed polarity benefit could arise. Importantly, this reduction in image correlation is constrained to a given pixel shift (i.e. disparity offset) dependent on the dot density on the RDS. In a future experiment, we could make use of this insight. Rather than using noisy disparity profile to challenge the observer, a discrimination task could employ dots at just two disparities which appear as two transparent depth planes. Given the binocular image correlation profile for a

stimulus with a given dot density we would be able to predict at what disparity offset, between the two transparent disparity planes, stimulus energy is reduced. At this point observer performance should drop below their predicted stereo acuity as a function of disparity offset magnitude. Additionally, given the shape of the binocular image correlation profile, as the two transparent disparity planes converge and approach 0 disparity, the discrimination performance should start to recover to the normal stereo acuity function. If observer performance for mixed and single polarity RDSs are exactly the same for larger offsets of the transparent planes discrimination task, and the benefit only starts to arise once the plane offset reaches the disparity magnitude predicted by the binocular image correlation profile, then we can conclude that the binocular energy model can completely explain the mixed polarity benefit. However if the benefit exists outside of this sweet spot, then we must conclude that other aspects (e.g. inhibition of incorrect correspondence) also contribute to the benefit.

Another way to explore which model of early disparity processing correctly describes how the mixed polarity benefit arises would be to add the effect of brain stimulation to the model. If we can replicate the amplification of the mixed polarity benefit through external stimulation then this would be strong evidence that the model produces the benefit in a similar way as human brains do. While this approach is intuitive, there are certain pitfalls with this idea: With enough modifications it might be possible to achieve almost any desired change in the behaviour of the standard binocular energy model. We would need an a priori assumption of how the model units, which resemble simple and complex cells, should change their behaviour during TMS. For this, we would need to record single cell responses to mixed and single polarity RDSs during TMS application. These data would have to be recorded in animals. Unfortunately, the changes in neuron activity we might observe during TMS application would not be directly transferrable to humans due to different stimulation parameters such as brain size. Neuroimaging techniques that can safely be used with human observers do not allow us to infer changes in the activity of either simple or complex cells during stimulation. Given these constraints, I think it is unlikely that researchers will follow this approach.

5.3 The role of parietal cortex in stereopsis

In **Chapter 4**, I investigated the role of parietal cortex in stereopsis. Researchers have found that dorsal area MT in monkeys (DeAngelis et al., 1998) and parietal cortex in humans (Chang et al., 2014) play a critical role for stereopsis. Specifically, parietal cortex seems to

be involved in processing disparity signals in disparity noise. However, it was previously unclear in what way parietal cortex contributes to stereopsis. There are many documented roles of the parietal cortex in perception which might be involved, such as primarily processing absolute disparity (Neri et al., 2004; Uka & DeAngelis, 2006; Umeda et al., 2007), supporting 3D shape perception (Srivastava et al., 2009; Theys et al., 2012, 2013), accumulating evidence for perceptual decisions (de Lafuente et al., 2015; Kelly & O'Connell, 2013; O'Connell et al., 2012; Shadlen & Newsome, 2001) and suppressing unwanted information (Pessoa et al., 2003). Here, I applied brain stimulation to disrupt the contribution of parietal cortex to stereopsis and recorded EEG to investigate how disparity processing is affected when the parietal contribution is reduced. I found that TMS produced significant deficits in stereopsis. In the visual cortex parietal TMS attenuated early disparity responses.

My findings suggest that TMS over parietal cortex disrupts an early, top-down influence of parietal cortex on disparity processing in visual cortex. Specifically, top-down input could inhibit noisy disparity at disparity magnitudes which are irrelevant for depth discrimination and therefore should not be attended. In line with this interpretation, I found that parietal TMS reduced alpha power in visual cortex during stimulus presentation. This suggests that alpha inhibition was reduced in visual cortex following TMS. Additionally, TMS increased a drop in synchronisation after stimulus offset between the parietal and visual cortex. This suggests that, following the disruption of parietal, top-down influences, the contribution of parietal cortex in stereopsis was further suppressed in the visual system.

Is the contribution of the parietal cortex to stereopsis specific to signal-in-noise tasks?

One open question is how general the contribution of parietal cortex is to stereopsis. The results of this study suggest that the parietal cortex provides top-down inhibition during early disparity processing in visual cortex. It is possible that this inhibition serves to suppress disparity noise. However, as discussed in the introduction of this thesis, the strategy of suppressing disparity noise is specific to signal-in-noise task. Other forms of disparity noise might require a different strategy to minimize the influence of disparity noise on the observer's depth estimate. All the studies which investigated the role of monkey MT (DeAngelis et al., 1998) and human parietal cortex (Chang et al., 2014) in stereopsis have used this exact signal-in-noise task. It is an open question whether the parietal cortex is still involved with different forms of disparity noise, which might require different strategies of disparity processing.

In a future study, researchers could address this question using tasks that employ noisy disparity discrimination, but don't allow the observer to use a strategy in which noise is suppressed. In **Chapter 3**, I used an RDS stimulus where I introduced disparity noise by adding random (randomly distributed around zero) disparity shifts to each dot in the stimulus. Here, to nullify the effect of disparity noise, an observer should try to integrate all depth information into a mean estimate which will match the true underlying disparity signal. If parietal cortex exclusively serves to suppress information, we would expect no parietal contribution and disruption of parietal activity should not affect stereopsis. Alternatively, we could modify the task which was used in this study. Rather than changing stimulus coherence (the number of dots that is replaced) to manipulate task difficulty we could change the disparity magnitude of the signal in the stimulus. Here, I expect no or a delayed parietal contribution because at stimulus onset it is unclear to the observer where the disparity signal will be located in depth. Such an experiment could answer the question whether parietal cortex is primarily engaged in the suppression of disparity noise in a signal-in-noise task or whether this area provides a more general contribution to stereopsis.

My findings in this study suggest that parietal cortex has an early, top-down influence on disparity processing in the visual cortex. The timing of this top-down influence matches that of early, attentional modulation of perception (Lu, Jeon, & Dosher, 2004). My results suggest that attention does in fact aid the processing of certain disparity magnitude ranges and suppresses clutter at different visual depth. This contribution would make sense as it has been proposed that depth-based figure-ground-segmentation is one of the mayor benefits of stereopsis (Bredfeldt & Cumming, 2006; Julesz, 1971). Recent studies have found that the fronto-parietal network plays a critical role not only in two-dimensional but also three-dimensional detection tasks (Ogawa & Macaluso, 2015). This suggests that the contribution of parietal cortex does in fact go beyond tasks where observers need to detect disparity signals in disparity noise. Future research could combine classic experimental paradigms for studying two-dimensional spatial attention (e.g. priming the observer for spatial locations and subsequently measuring detection accuracy; Dosher and Lu, 2000) with stereoscopic research. This will allow us to investigate how well our understanding of two-dimensional spatial attention describes attentional effects in three-dimensional space.

Does parietal cortex also contribute to evidence accumulation for decisions of depth discrimination?

Another limitation of this study is that the results are less sensitive to decision related mechanisms of stereopsis. During the experiment I kept observer performance almost

constant and recorded task difficulty as a measure of observer depth acuity. Specifically, in each experiment block I used adaptive staircases which converged at 82% correct performance. It was necessary to obtain quick, reliable estimates of observer depth acuity in short blocks because it was to be expected that the effect of TMS would decay over time. This means that for a majority of the trials observers performed at 82% correct performance and decision related mechanisms of stereopsis should have received similar amounts of evidence for either a 'near' or 'far' depth judgement. Importantly, this means that decision related areas still received the same amount of evidence after parietal TMS when observer depth acuity was affected. This could suggest that this experiment was not sensitive enough to detect any changes of decision related activity in parietal cortex after stimulation.

How directly does TMS cause changes of disparity responses in visual cortex?

Another limitation is that it is not clear whether the different effects of TMS on neural activity that we observe in this study are separate effects or rather causing each other. Given that TMS over parietal cortex did not directly change cortical excitability in visual cortex, we can be confident that TMS changed brain activity outside the visual cortex which in turn affected early disparity responses in visual cortex. However, it is unclear whether TMS also caused the decrease in local inhibition during stimulus presentation and the observed functional connectivity drop between parietal and visual cortex after stimulus offset. These effects could also be of a secondary nature and primarily caused by the changes in early disparity responses. All of these effects happen at different time windows relative to stimulus onset. If these effects are in fact signatures of different steps of disparity processing, then future experiments could aim at disentangling each of these different steps individually. Additionally, if these time windows contain different steps of disparity processing, it would be interesting to know which disruption of what steps underlies the changes in observer stereo acuity.

One way a future experiment could answer this question is by interfering with parietal brain activity at different time points during disparity processing. The results of this study could be used to define time windows in which TMS can be used to directly change neural activity in parietal cortex, as has previously been done by (Chang et al., 2014). Additionally, it is possible to clean EEG from the artefacts of single pulse of online TMS, which in turn would allow us to record changes in disparity responses in visual cortex. The effect of a single pulse is very constrained in time. Any effects on disparity responses that occur more than 200ms after TMS can be expected to be secondary effects driven by a preceding TMS effect (De Graaf, Koivisto, Jacobs, & Sack, 2014). This will allow researchers to confirm exactly at

what time a parietal, top-down contribution is critical to stereopsis and will show whether disruption of parietal cortex causes longer lasting changes of disparity responses in visual cortex.

References

Abrahamyan, A., Clifford, C. W. G., Arabzadeh, E., & Harris, J. A. (2011). Improving visual sensitivity with subthreshold transcranial magnetic stimulation. *Journal of Neuroscience*, *31*(9), 3290–3294. http://doi.org/10.1523/JNEUROSCI.6256-10.2011

Abrahamyan, A., Clifford, C. W. G., Arabzadeh, E., & Harris, J. A. (2015). Low intensity TMS enhances perception of visual stimuli. *Brain Stimulation*, *8*(6), 1175–1182. http://doi.org/10.1016/j.brs.2015.06.012

Abrahamyan, A., Clifford, C. W. G., Ruzzoli, M., Phillips, D., Arabzadeh, E., & Harris, J. A. (2011). Accurate and Rapid Estimation of Phosphene Thresholds (REPT). *PLoS ONE*, *6*(7). http://doi.org/10.1371/journal.pone.0022342

Adrian, E. D., & Moruzzi, G. (1939). Impulses in the pyramidal tract. *The Journal of Physiology*, *97*(2), 153–199.

Allman, J. (2000). *Evolving brains*. New York: Scientific American Library W. H. Freeman.

Antal, A., Nitsche, M. A., Kincses, T. Z., Lampe, C., & Paulus, W. (2004). No correlation between moving phosphene and motor thresholds: a transcranial magnetic stimulation study. *Neuroreport*, *15*(2), 297–302. http://doi.org/10.1097/01.wnr.0000099600.41403.ec

Anzai, A., Ohzawa, I., & Freeman, R. D. (1997). Neural mechanisms underlying binocular fusion and stereopsis: position vs. phase. *Proceedings of the National Academy of Sciences of the United States of America*, *94*(10), 5438–5443. http://doi.org/10.1073/pnas.94.10.5438

Anzai, A., Ohzawa, I., & Freeman, R. D. (1999a). Neural mechanisms for encoding binocular disparity: receptive field position versus phase. *Journal of Neurophysiology*, *82*(2), 874–890.

Anzai, A., Ohzawa, I., & Freeman, R. D. (1999b). Neural Mechanisms for Processing Binocular Information I. Simple Cells. *Journal of Neurophysiology*, *82*(2), 891–908.

Anzai, A., Ohzawa, I., & Freeman, R. D. (1999c). Neural Mechanisms for Processing Binocular Information II. Complex Cells. *Journal of Neurophysiology*, *82*(2), 909–924. http://doi.org/10.1016/j.tins.2013.04.006

Arcaro, M. J., & Kastner, S. (2015). Topographic organization of areas V3 and V4 and its relation to supra-areal organization of the primate visual system. *Visual Neuroscience*, *32*. http://doi.org/10.1017/S0952523815000115

Barker, A. T., Jalinous, R., & Freeston, I. L. (1985). Non-Invasive Magnetic Stimulation of Human Motor Cortex. *The Lancet*, *325*(8437), 1106–1107. http://doi.org/10.1016/S0140-6736(85)92413-4

Barlow, H. B., Blakemore, C., & Pettigrew, J. D. (1967). The neural mechanism of binocular depth discrimination. *The Journal of Physiology*, *193*(2), 327–342. http://doi.org/10.1113/jphysiol.1967.sp008360

Bergmann, T. O., Karabanov, A., Hartwigsen, G., Thielscher, A., & Siebner, H. R. (2016). Combining non-invasive transcranial brain stimulation with neuroimaging and electrophysiology: Current approaches and future perspectives. *NeuroImage*, *140*, 4–

19. http://doi.org/10.1016/j.neuroimage.2016.02.012

Berman, N. J., Douglas, R. J., Martin, K. A., & Whitteridge, D. (1991). Mechanisms of inhibition in cat visual cortex. *The Journal of Physiology*, *440*(1), 697–722.

Bestmann, S. (2008). The physiological basis of transcranial magnetic stimulation. *Trends in Cognitive Sciences*, *12*(3), 217–221. http://doi.org/10.1016/j.tics.2007.12.002

Bestmann, S., Baudewig, J., Siebner, H. R., Rothwell, J. C., & Frahm, J. (2004). Functional MRI of the immediate impact of transcranial magnetic stimulation on cortical and subcortical motor circuits. *European Journal of Neuroscience*, *19*(7), 1950–1962. http://doi.org/10.1111/j.1460-9568.2004.03277.x

Bestmann, S., de Berker, A. O., & Bonaiuto, J. (2015). Understanding the behavioural consequences of noninvasive brain stimulation. *Trends in Cognitive Sciences*, *19*(1), 13–20. http://doi.org/10.1016/j.tics.2014.10.003

Blake, A., & Bülthoff, H. (1990). Does the brain know the physics of specular reflection? *Nature*, *343*(6254), 165–168. http://doi.org/10.1038/343165a0

Blakemore, C. (1970). The range and scope of binocular depth discrimination in man. *The Journal of Physiology*, *211*(3), 599–622. http://doi.org/10.1113/jphysiol.1970.sp009296

Boroojerdi, B., Battaglia, F., Muellbacher, W., & Cohen, L. G. (2001). Mechanisms influencing stimulus-response properties of the human corticospinal system. *Clinical Neurophysiology*, *112*(5), 931–937. http://doi.org/10.1016/S1388-2457(01)00523-5

Boroojerdi, B., Meister, I. G., Foltys, H., Sparing, R., Cohen, L. G., & Töpper, R. (2002). Visual and motor cortex excitability: a transcranial magnetic stimulation study. *Clinical Neurophysiology*, *113*(9), 1501–1504. http://doi.org/10.1016/S1388-2457(02)00198-0

Brasil-Neto, J. P., Cohen, L. G., Panizza, M., Nilsson, J., Roth, B. J., & Hallett, M. (1992). Optimal Focal Transcranial Magnetic Activation of the Human Motor Cortex. *Journal of Clinical Neurophysiology*, *9*(1), 132–136. http://doi.org/10.1097/00004691-199201000-00014

Brasil-Neto, J. P., McShane, L. M., Fuhr, P., Hallett, M., & Cohen, L. G. (1992). Topographic mapping of the human motor cortex with magnetic stimulation: factors affecting accuracy and reproducibility. *Electroencephalography and Clinical Neurophysiology*, *85*(1), 9–16. http://doi.org/10.1016/0168-5597(92)90095-S

Bredfeldt, C. E., & Cumming, B. G. (2006). A Simple Account of Cyclopean Edge Responses in Macaque V2. *Journal of Neuroscience*, *26*(29), 7581–7596. http://doi.org/10.1523/JNEUROSCI.5308-05.2006

Bresadola, M. (1998). Medicine and science in the life of Luigi Galvani (1737-1798). *Brain Research Bulletin*, *46*(5), 367–380.

Cai, W., George, J. S., Chambers, C. D., Stokes, M. G., Verbruggen, F., & Aron, A. R. (2012). Stimulating deep cortical structures with the batwing coil: How to determine the intensity for transcranial magnetic stimulation using coil-cortex distance. *Journal of Neuroscience Methods*, *204*(2), 238–241. http://doi.org/10.1016/j.jneumeth.2011.11.020

Caparelli, E. C., Backus, W., Telang, F., Wang, G.-J., Maloney, T., Goldstein, R. Z., … Henn, F. (2010). Simultaneous TMS-fMRI of the Visual Cortex Reveals Functional Network, Even in Absence of Phosphene Sensation. *The Open Neuroimaging Journal*, *4*(631), 100–110. http://doi.org/10.2174/1874440001004010100

Cartmill, M. (2005). New views on primate origins. *Evolutionary Anthropology: Issues, News, and Reviews*, *1*(3), 105–111. http://doi.org/10.1002/evan.1360010308

Chang, D. H. F., Kourtzi, Z., & Welchman, A. E. (2013). Mechanisms for Extracting a Signal from Noise as Revealed through the Specificity and Generality of Task Training. *Journal of Neuroscience*, *33*(27), 10962–10971. http://doi.org/10.1523/JNEUROSCI.0101-13.2013

Chang, D. H. F., Mevorach, C., Kourtzi, Z., & Welchman, A. E. (2014). Training transfers the limits on perception from parietal to ventral cortex. *Current Biology*, *24*(20), 2445–2450. http://doi.org/10.1016/j.cub.2014.08.058

Changizi, M. A., & Shimojo, S. (2008). "X-ray vision" and the evolution of forward-facing eyes. *Journal of Theoretical Biology*, *254*(4), 756–767. http://doi.org/10.1016/j.jtbi.2008.07.011

Chowdhury, S. A., & DeAngelis, G. C. (2008). Fine Discrimination Training Alters the Causal Contribution of Macaque Area MT to Depth Perception. *Neuron*, *60*(2), 367–377. http://doi.org/10.1016/j.neuron.2008.08.023

Chung, S., & Ferster, D. (1998). Strength and orientation tuning of the thalamic input to simple cells revealed by electrically evoked cortical supression. *Neuron*, *20*(6), 1177–1189.

Colby, C. L., Duhamel, J. R., & Goldberg, M. E. (1993). Ventral intraparietal area of the macaque: anatomic location and visual response properties. *Journal of Neurophysiology*, *69*(3), 902–914. http://doi.org/10.1152/jn.1993.69.3.902

Connors, B. W., Malenka, R. C., & Silva, L. R. (1988). Two inhibitory postsynaptic potentials, and GABAA and GABAB receptor-mediated responses in neocortex of rat and cat. *The Journal of Physiology*, *406*, 443–68.

Corbetta, M., & Shulman, G. L. (2002). Control of goal-directed and stimulus-driven attention in the brain. *Nature Reviews Neuroscience*, *3*(3), 201–215. http://doi.org/10.1038/nrn755

Cottereau, B. R., McKee, S. P., Ales, J. M., & Norcia, A. M. (2011). Disparity-Tuned Population Responses from Human Visual Cortex. *Journal of Neuroscience*, *31*(3), 954–965. http://doi.org/10.1523/JNEUROSCI.3795-10.2011

Cottereau, B. R., McKee, S. P., Ales, J. M., & Norcia, A. M. (2012). Disparity-Specific Spatial Interactions: Evidence from EEG Source Imaging. *Journal of Neuroscience*, *32*(3), 826–840. http://doi.org/10.1523/JNEUROSCI.2709-11.2012

Cowey, A., & Walsh, V. (2000). Magnetically induced phosphenes in sighted, blind and blindsighted observers. *Neuroreport*, *11*(14), 3269–73.

Creutzfeldt, O. D., Watanabe, S., & Lux, H. D. (1966). Relations between EEG phenomena and potentials of single cortical cells. I. Evoked responses after thalamic and epicortical stimulation. *Electroencephalography and Clinical Neurophysiology*, *20*(1), 1–18. http://doi.org/10.1016/0013-4694(66)90136-2

Cumming, B. G. (1997). Stereopsis: how the brain sees depth. *Current Biology*, *7*(10), 645–647. http://doi.org/10.1016/S0960-9822(06)00324-1

Cumming, B. G., & Parker, A. J. (1997). Responses of primary visual cortical neurons to binocular disparity without depth perception. *Nature*, *389*(6648), 280–283. http://doi.org/10.1038/38487

Cumming, B. G., & Parker, A. J. (2000). Local disparity not perceived depth is signaled by binocular neurons in cortical area V1 of the Macaque. *Journal of Neuroscience*, *20*(12), 4758–4767.

Datto, C. J. (2000). Side effects of electroconvulsive therapy. *Depression and Anxiety*, *12*(3), 130–134.

De Graaf, T. A., Koivisto, M., Jacobs, C., & Sack, A. T. (2014). The chronometry of visual perception: Review of occipital TMS masking studies. *Neuroscience and Biobehavioral Reviews*, *45*, 295–304. http://doi.org/10.1016/j.neubiorev.2014.06.017

De Graaf, T. A., & Sack, A. T. (2011). Null results in TMS: From absence of evidence to evidence of absence. *Neuroscience and Biobehavioral Reviews*, *35*(3), 871–877. http://doi.org/10.1016/j.neubiorev.2010.10.006

De Graaf, T. A., & Sack, A. T. (2014). Using brain stimulation to disentangle neural correlates of conscious vision. *Frontiers in Psychology*, *5*. http://doi.org/10.3389/fpsyg.2014.01019

de Haan, E. H. F., & Cowey, A. (2011). On the usefulness of “what” and “where” pathways in vision. *Trends in Cognitive Sciences*, *15*(10), 460–466. http://doi.org/10.1016/j.tics.2011.08.005

de Lafuente, V., Jazayeri, M., & Shadlen, M. N. (2015). Representation of Accumulating Evidence for a Decision in Two Parietal Areas. *Journal of Neuroscience*, *35*(10), 4306–4318. http://doi.org/10.1523/JNEUROSCI.2451-14.2015

DeAngelis, G. C., Cumming, B. G., & Newsome, W. T. (1998). Cortical area MT and the perception of stereoscopic depth. *Nature*, *394*(6694), 677–680. http://doi.org/10.1038/29299

DeAngelis, G. C., & Newsome, W. T. (1999). Organization of disparity-selective neurons in macaque area MT. *Journal of Neuroscience*, *19*(4), 1398–1415.

DeAngelis, G. C., Ohzawa, I., & Freeman, R. D. (1991). Depth is encoded in the visual cortex by a specialized receptive field structure. *Nature*, *352*(6331), 156–159. http://doi.org/10.1038/352156a0

Delorme, A., & Makeig, S. (2004). EEGLAB: an open source toolbox for analysis of single-trial EEG dynamics including independent component analysis. *Journal of Neuroscience Methods*, *134*(1), 9–21. http://doi.org/10.1016/j.jneumeth.2003.10.009

Desimone, R., & Duncan, J. (1995). Neural Mechanisms of Selective Visual. *Annual Review of Neuroscience*, *18*(1), 193–222. http://doi.org/10.1146/annurev.ne.18.030195.001205

Dev, P. (1975). Perception of depth surfaces in random-dot stereograms : a neural model. *International Journal of Man-Machine Studies*, *7*(4), 511–528. http://doi.org/10.1016/S0020-7373(75)80030-7

Devanand, D. P., Fitzsimons, L., Prudic, J., & Sackeim, H. A. (1995). Subjective side effects during electroconvulsive therapy. *Convulsive Therapy*, *11*(4), 232–240.

Devanne, H., Lavoie, B. A., & Capaday, C. (1997). Input-output properties and gain changes in the human corticospinal pathway. *Experimental Brain Research*, *114*(2), 329–338. http://doi.org/10.1007/PL00005641

Diekhoff, S., Uludag, K., Sparing, R., Tittgemeyer, M., Cavusoglu, M., Von Cramon, D. Y., & Grefkes, C. (2011). Functional localization in the human brain: Gradient-echo, spin-

echo, and arterial spin-labeling fMRI compared with neuronavigated TMS. *Human Brain Mapping*, *32*(3), 341–357. http://doi.org/10.1002/hbm.21024

Dosher, B. A., & Lu, Z.-L. (2000). Noise exclusion in spatial attention. *Psychological Science*, *11*(2), 139–146.

Dove, H. W. (1841). *Bericht über die zur bekanntmachung geeigneten verhandlungen der königlich preußischen akademie der wissenschaften zu berlin. ueber die combination der eindruecke beider ohren und beider augen zu einem eindrueck.* Berlin: Verlag der Königlichen Akademie der Wissenschaften.

Dove, H. W. (1860). Ueber stereoskopie. *Annalen Der Physik*, *186*(7), 494–498.

Dowdle, L. T., Brown, T. R., George, M. S., & Hanlon, C. A. (2018). Single pulse TMS to the DLPFC, compared to a matched sham control, induces a direct, causal increase in caudate, cingulate, and thalamic BOLD signal. *Brain Stimulation*, *11*(4), 789–796. http://doi.org/10.1016/j.brs.2018.02.014

Edwards, M., & Badcock, D. R. (1994). Global motion perception: Interaction of the ON and OFF pathways. *Vision Research*, *34*(21), 2849–2858. http://doi.org/10.1016/0042-6989(94)90054-X

Eifuku, S., & Wurtz, R. H. (1999). Response to motion in extrastriate area MSTl: disparity sensitivity. *Journal of Neurophysiology*, *82*(1), 2462–2475. http://doi.org/10.1152/jn.1998.80.1.282

Elkin-Frankston, S., Fried, P. J., Pascual-Leone, A., Rushmore, R. J., & Valero-Cabre, A. (2010). A novel approach for documenting phosphenes induced by transcranial magnetic stimulation. *Journal of Visualized Experiments : JoVE*, (38), 1–4. http://doi.org/10.3791/1762

Felleman, D. J., & Van Essen, D. C. (1991). Distributed hierachical processing in the primate cerebral cortex. *Cerebral Cortex*, *1*, 1–47.

Ferraina, S., Paré, M., & Wurtz, R. H. (2000). Disparity sensitivity of frontal eye field neurons. *Journal of Neurophysiology*, *83*(1), 625–629. http://doi.org/10.1152/jn.2000.83.1.625

Ferster, D. (1981). A comparison of binocular depth mechanisms in areas 17 and 18 of the cat visual cortex. *The Journal of Physiology*, *311*, 623–655.

Fried, P. J., Elkin-Frankston, S., Rushmore, R. J., Hilgetag, C. C., & Valero-Cabre, A. (2011). Characterization of visual percepts evoked by noninvasive stimulation of the human posterior parietal cortex. *PloS One*, *6*(11). http://doi.org/10.1371/journal.pone.0027204

Fritsch, G., & Hitzig, E. (1870). Ueber die elektrische Erregbarkeit des Grosshirns. *Archiv Für Anatomie, Physiologie Und Wissenschaftliche Medicin*. http://doi.org/10.1016/j.yebeh.2009.03.001

Froc, D. J., Chapman, A., Trepel, C., & Racine, R. J. (2000). Long-Term Depression and Depotentiation in the Sensorimotor Cortex of the Freely Moving Rat. *Journal of Neuroscience*, *20*(1), 438–445.

Fründ, I., Haenel, N. V., & Wichmann, F. A. (2011). Inference for psychometric functions in the presence of nonstationary behavior. *Journal of Vision*, *11*(6), 1–19. http://doi.org/10.1167/11.6.16.Introduction

Genç, E., Schölvinck, M. L., Bergmann, J., Singer, W., & Kohler, A. (2016). Functional Connectivity Patterns of Visual Cortex Reflect its Anatomical Organization. *Cerebral Cortex*, *26*(9), 3719–3731. http://doi.org/10.1093/cercor/bhv175

Genovesio, A. (2004). Integration of Retinal Disparity and Fixation-Distance Related Signals Toward an Egocentric Coding of Distance in the Posterior Parietal Cortex of Primates. *Journal of Neurophysiology*, *91*(6), 2670–2684. http://doi.org/10.1152/jn.00712.2003

Gerwig, M., Kastrup, O., Meyer, B.-U., & Niehaus, L. (2003). Evaluation of cortical excitability by motor and phosphene thresholds in transcranial magnetic stimulation. *Journal of the Neurological Sciences*, *215*, 75–78. http://doi.org/10.1016/S0022-510X(03)00228-4

Goebel, R., Esposito, F., & Formisano, E. (2006). Analysis of FIAC data with BrainVoyager QX : From single - subject to cortically aligned group GLM analysis and self - organizing group ICA. *Human Brain Mapping*, *27*(5), 392–401.

Goldberg, M. E., Bisley, J., Powell, K. D., Gottlieb, J., & Kusunoki, M. (2002). The role of the lateral intraparietal area of the monkey in the generation of saccades and visuospatial attention. *Annals of the New York Academy of Sciences*, *956*, 205–215. http://doi.org/10.1111/j.1749-6632.2002.tb02820.x

Goncalves, N. R., Ban, H., Sanchez-Panchuelo, R. M., Francis, S. T., Schluppeck, D., & Welchman, A. E. (2015). 7 Tesla fMRI Reveals Systematic Functional Organization for Binocular Disparity in Dorsal Visual Cortex. *Journal of Neuroscience*, *35*(7), 3056–3072. http://doi.org/10.1523/JNEUROSCI.3047-14.2015

Goncalves, N. R., & Welchman, A. E. (2017). “What Not” Detectors Help the Brain See in Depth. *Current Biology*, *27*(10), 1403–1412. http://doi.org/10.1016/j.cub.2017.03.074

Goodale, M. A., & Milner, A. D. (1992). Separate visual pathways for perception and action. *Trends in Neurosciences*, *15*(1), 20–25. http://doi.org/10.1016/0166-2236(92)90344-8

Gothe, J., Brandt, S. A., Irlbacher, K., Roricht, S., Sabel, B. A., & Meyer, B.-U. (2002). Changes in visual cortex excitability in blind subjects as demonstrated by transcranial magnetic stimulation. *Brain*, *125*(3), 479–490. http://doi.org/10.1093/brain/awf045

Grimson, W. E. L. (1981). A Computer Implementation of a Theory of Human Stereo Vision. *Philosophical Transactions of the Royal Society B: Biological Sciences*, *292*(1058), 217–253. http://doi.org/10.1098/rstb.1981.0031

Guzman-Lopez, J., Silvanto, J., Yousif, N., Nousi, S., Quadir, S., & Seemungal, B. M. (2011). Probing V5/MT excitability with transcranial magnetic stimulation following visual motion adaptation to random and coherent motion. *Annals of the New York Academy of Sciences*, *1233*, 200–207. http://doi.org/10.1111/j.1749-6632.2011.06179.x

Haenny, P. E., & Schiller, P. H. (1988). State dependent activity in monkey visual cortex. I. Single cell activity in V1 and V4 on visual tasks. *Experimental Brain Research*, *69*(2), 225–244. http://doi.org/10.1007/BF00247569

Hamada, M., Murase, N., Hasan, A., Balaratnam, M., & Rothwell, J. C. (2013). The role of interneuron networks in driving human motor cortical plasticity. *Cerebral Cortex*, *23*(7), 1593–1605. http://doi.org/10.1093/cercor/bhs147

Hanks, T. D., Ditterich, J., & Shadlen, M. N. (2006). Microstimulation of macaque area LIP affects decision-making in a motion discrimination task. *Nature Neuroscience*, *9*(5), 682–689. http://doi.org/10.1038/nn1683

Harris, J. A., Clifford, C. W. G., & Miniussi, C. (2008). The functional effect of transcranial

magnetic stimulation: signal suppression or neural noise generation? *Journal of Cognitive Neuroscience*, *20*(4), 734–40. http://doi.org/10.1162/jocn.2008.20048

Harris, J. M., & Parker, A. J. (1992). Efficiency of stereopsis in random-dot stereograms. *Journal of the Optical Society of America*, *9*(1), 14–24. http://doi.org/10.1364/JOSAA.9.001135

Harris, J. M., & Parker, A. J. (1995). Independent neural mechanisms for bright and dark information in binocular stereopsis. *Nature*, *374*(6525), 808–811. http://doi.org/10.1038/374808a0

Hartwigsen, G., Saur, D., Price, C. J., Ulmer, S., Baumgaertner, A., & Siebner, H. R. (2013). Perturbation of the left inferior frontal gyrus triggers adaptive plasticity in the right homologous area during speech production. *Proceedings of the National Academy of Sciences*, *110*(41), 16402–16407. http://doi.org/10.1073/pnas.1310190110

Hasan, A., Hamada, M., Nitsche, M. A., Ruge, D., Galea, J. M., Wobrock, T., & Rothwell, J. C. (2012). Direct-current-dependent shift of theta-burst-induced plasticity in the human motor cortex. *Experimental Brain Research*, *217*(1), 15–23. http://doi.org/10.1007/s00221-011-2968-5

Heinzle, J., Kahnt, T., & Haynes, J. D. (2011). Topographically specific functional connectivity between visual field maps in the human brain. *NeuroImage*, *56*(3), 1426–1436. http://doi.org/10.1016/j.neuroimage.2011.02.077

Hess, C. W., Mills, K. R., & Murray, N. M. (1987). Responses in small hand muscles from magnetic stimulation of the human brain. *The Journal of Physiology*, *388*, 397–419.

Hess, G., & Donoghue, J. P. (1996). Long-term potentiation and long-term depression of horizontal connections in rat motor cortex. *Acta Neurobiologiae Experimentalis*, *56*(1), 397–405.

Hetley, R., Dosher, B. A., & Lu, Z.-L. (2014). Generating a taxonomy of spatially cued attention for visual discrimination: effects of judgment precision and set size on attention. *Attention, Perception, and Psychophysics*, *76*(8), 2286–2304. http://doi.org/10.3758/s13414-014-0705-4

Histed, M. H., Bonin, V., & Reid, R. C. (2009). Direct Activation of Sparse, Distributed Populations of Cortical Neurons by Electrical Microstimulation. *Neuron*, *63*(4), 508–522. http://doi.org/10.1016/j.neuron.2009.07.016

Hodgkin, A. L., & Huxley, A. F. (1952). A quantitative description of membrane current and its application to conduction and excitation in nerve. *The Journal of Physiology*, *117*, 500–544.

Hordacre, B., Goldsworthy, M. R., Vallence, A. M., Darvishi, S., Moezzi, B., Hamada, M., … Ridding, M. C. (2016). Variability in neural excitability and plasticity induction in the human cortex: A brain stimulation study. *Brain Stimulation*, *10*(3), 588–595. http://doi.org/10.1016/j.brs.2016.12.001

Howard, I. P., & Rogers, B. J. (2008). *Seeing in Depth*. Ontario, Canada: Oxford University Press. http://doi.org/10.1093/acprof:oso/9780195367607.001.0001

Huang, Y. Z., Chen, R., Rothwell, J., & Wen, H. (2007). The after-effect of human theta burst stimulation is NMDA receptor dependent. *Clinical Neurophysiology*, *118*(5), 1028–1032. http://doi.org/10.1016/j.clinph.2007.01.021

Huang, Y. Z., Edwards, M. J., Rounis, E., Bhatia, K. P., & Rothwell, J. C. (2005). Theta burst

stimulation of the human motor cortex. *Neuron*, *45*(2), 201–206. http://doi.org/10.1016/j.neuron.2004.12.033

Hubel, D. H., & Wiesel, T. N. (1959). Receptive fields of single neurones in the cat's striate cortex. *The Journal of Physiology*, *148*(28), 574–591. http://doi.org/10.1113/jphysiol.1959.sp006308

Hubel, D. H., & Wiesel, T. N. (1962). Receptive fields, binocular interaction and functional architecture in the cat's visual cortex. *The Journal of Physiology*, *160*(1), 106–154.2. http://doi.org/10.1523/JNEUROSCI.1991-09.2009

Hubel, D. H., & Wiesel, T. N. (1968). Receptive fields and functional architecture of monkey striate cortex. *The Journal of Physiology*, *195*, 215–243. http://doi.org/10.1113/jphysiol.1968.sp008455

Hubel, D. H., & Wiesel, T. N. (1970). Stereoscopic vision in macaque monkey: Cells sensitive to binocular depth in area 18 of the macaque monkey cortex. *Nature*, *225*(5227), 41–42. http://doi.org/10.1038/225041a0

Huber, R., Mäki, H., Rosanova, M., Casarotto, S., Canali, P., Casali, A. G., … Massimini, M. (2013). Human cortical excitability increases with time awake. *Cerebral Cortex*. http://doi.org/10.1093/cercor/bhs014

Janssen, A. M., Oostendorp, T. F., & Stegeman, D. F. (2015). The coil orientation dependency of the electric field induced by TMS for M1 and other brain areas. *Journal of Neuroengineering and Rehabilitation*, *12*(47). http://doi.org/10.1186/s12984-015-0036-2

Janssen, P., Verhoef, B.-E., & Premereur, E. (2018). Functional interactions between the macaque dorsal and ventral visual pathways during three-dimensional object vision. *Cortex*, *98*, 218–227. http://doi.org/10.1016/j.cortex.2017.01.021

Janssen, P., Vogels, R., Liu, Y., & Orban, G. A. (2003). At Least at the Level of Inferior Temporal Cortex, the Stereo Correspondence Problem Is Solved. *Neuron*, *37*(4), 693–701. http://doi.org/10.1016/S0896-6273(03)00023-0

Janssen, P., Vogels, R., & Orban, G. A. (1999). Macaque inferior temporal neurons are selective for disparity-defined three-dimensional shapes. *Proceedings of the National Academy of Sciences*, *96*(14), 8217–8222. http://doi.org/10.1073/pnas.96.14.8217

Janssen, P., Vogels, R., & Orban, G. A. (2000). Three-dimensional shape coding in inferior temporal cortex. *Neuron*, *27*(2), 385–397. http://doi.org/S0896-6273(00)00045-3

Jiang, Y., Purushothaman, G., & Casagrande, V. A. (2015). The functional asymmetry of ON and OFF channels in the perception of contrast. *Journal of Neurophysiology*, *114*(5), 2816–2829. http://doi.org/10.1152/jn.00560.2015

Julesz, B. (1964). Binocular Depth Perception Without Familiarity Cues. *Science*, *145*(3630), 356–362. http://doi.org/10.1126/science.145.3630.356

Julesz, B. (1971). *Foundations of cyclopean perception*. Oxford: University of Chicago Press. http://doi.org/10.1097/OPX.0b013e318155ab62

Kammer, T. (1999). Phosphenes and transient scotomas induced by magnetic stimulation of the occipital lobe: their topographic relationship. *Neuropsychologia*, *37*(2), 191–198. http://doi.org/10.1016/S0028-3932(98)00093-1

Kammer, T., & Baumann, L. W. (2010). Phosphene thresholds evoked with single and

double TMS pulses. *Clinical Neurophysiology*, *121*(3), 376–379. http://doi.org/10.1016/j.clinph.2009.12.002

Kammer, T., Beck, S., Erb, M., & Grodd, W. (2001). The influence of current direction on phosphene thresholds evoked by transcranial magnetic stimulation. *Clinical Neurophysiology*, *112*(11), 2015–2021. http://doi.org/10.1016/S1388-2457(01)00673-3

Kammer, T., Beck, S., Thielscher, A., Laubis-Herrmann, U., & Topka, H. (2001). Motor thresholds in humans: a transcranial magnetic stimulation study comparing different pulse waveforms, current directions and stimulator types. *Clinical Neurophysiology*, *112*(2), 250–258. http://doi.org/10.1016/S1388-2457(00)00513-7

Kammer, T., Puls, K., Erb, M., & Grodd, W. (2005). Transcranial magnetic stimulation in the visual system. II. Characterization of induced phosphenes and scotomas. *Experimental Brain Research*, *160*(1), 129–140. http://doi.org/10.1007/s00221-004-1992-0

Kammer, T., Vorwerg, M., & Herrnberger, B. (2007). Anisotropy in the visual cortex investigated by neuronavigated transcranial magnetic stimulation. *NeuroImage*, *36*(2), 313–321. http://doi.org/10.1016/j.neuroimage.2007.03.001

Kara, P., Pezaris, J. S., Yurgenson, S., & Reid, R. C. (2002). The spatial receptive field of thalamic inputs to single cortical simple cells revealed by the interaction of visual and electrical stimulation. *Proceedings of the National Academy of Sciences*, *99*(25), 16261–16266. http://doi.org/10.1073/pnas.242625499

Kastner, S., De Weerd, P., Desimone, R., & Ungerleider, L. G. (1998). Mechanisms of directed attention in the human extrastriate cortex as revealed by functional MRI. *Science*, *282*(5386), 108–111.

Katz, L. N., Yates, J. L., Pillow, J. W., & Huk, A. C. (2016). Dissociated functional significance of decision-related activity in the primate dorsal stream. *Nature*, *535*(7611), 285–288. http://doi.org/10.1038/nature18617

Kaufman, L. (1964). On the Nature of Binocular Disparity. *The American Journal of Psychology*, *77*(3), 393–402. http://doi.org/10.2307/1421009

Kaufman, L., & Pitblado, C. (1965). Further Observations on the Nature of Effective Binocular Disparities. *The American Journal of Psychology*, *78*(3), 379–391. http://doi.org/10.2307/1420572

Kelly, S. P., & O'Connell, R. G. (2013). Internal and External Influences on the Rate of Sensory Evidence Accumulation in the Human Brain. *Journal of Neuroscience*, *33*(50), 19434–19441. http://doi.org/10.1523/JNEUROSCI.3355-13.2013

Kiers, L., Cros, D., Chiappa, K. H., & Fang, J. (1993). Variability of motor potentials evoked by transcranial magnetic stimulation. *Electroencephalography and Clinical Neurophysiology/ Evoked Potentials*, *89*(6), 415–423. http://doi.org/10.1016/0168-5597(93)90115-6

Klimesch, W., Sauseng, P., & Hanslmayr, S. (2007). EEG alpha oscillations: The inhibition-timing hypothesis. *Brain Research Reviews*, *53*(1), 63–88. http://doi.org/10.1016/j.brainresrev.2006.06.003

Kourtzi, Z., Betts, L. R., Sarkheil, P., & Welchman, A. E. (2005). Distributed neural plasticity for shape learning in the human visual cortex. *PLoS Biology*, *3*(7), 1317–1327. http://doi.org/10.1371/journal.pbio.0030204

Kriegeskorte, N., & Goebel, R. (2001). An Efficient Algorithm for Topologically Correct

Segmentation of the Cortical Sheet in Anatomical MR Volumes. *NeuroImage*, *14*(2), 329–346. http://doi.org/10.1006/nimg.2001.0831

Kujirai, T., Caramia, M. D., Rothwell, J. C., Day, B. L., Thompson, P. D., Ferbert, A., … Marsden, C. D. (1993). Corticocortical inhibition in human motor cortex. *The Journal of Physiology*, *471*(1), 501–519. http://doi.org/10.1113/jphysiol.1993.sp019912

Laakso, I., Hirata, A., & Ugawa, Y. (2014). Effects of coil orientation on the electric field induced by TMS over the hand motor area. *Physics in Medicine and Biology*, *59*, 203–218. http://doi.org/10.1088/0031-9155/59/1/203

Larson, J., & Lynch, G. (1986). Induction of synaptic potentiation in hippocampus by patterned stimulation involves two events. *Science*, *232*(4753), 985–988. http://doi.org/10.1126/science.3704635

Law, C. T., & Gold, J. I. (2008). Neural correlates of perceptual learning in a sensory-motor, but not a sensory, cortical area. *Nature Neuroscience*, *11*(4), 505–513. http://doi.org/10.1038/nn2070

Le Gros Clark, W. E. (1934). *Early forerunners of man. A morphological study of the evolutionary origin of the primates*. Baltimore: W.Wood and Company.

Lehky, S. R., Pouget, A., & Sejnowski, T. J. (1990). Neural models of binocular depth perception. *Cold Spring Harbor Symposia on Quantitative Biology*, *55*, 765–777. http://doi.org/10.1101/SQB.1990.055.01.072

Lehky, S. R., & Sejnowski, T. J. (1990). Neural model of stereoacuity and depth interpolation based on a distributed representation of stereo disparity. *Journal of Neuroscience*, *10*(7), 2281–2299.

Lioumis, P., Kičić, D., Savolainen, P., Mäkelä, J. P., & Kähkönen, S. (2009). Reproducibility of TMS-Evoked EEG responses. *Human Brain Mapping*, *30*(4), 1387–1396. http://doi.org/10.1002/hbm.20608

Lu, Z.-L., & Dosher, B. A. (2004). Spatial attention excludes external noise without changing the spatial frequency tuning of the perceptual template. *Journal of Vision*, *4*(10), 955–966. http://doi.org/10.1167/4.10.10

Lu, Z.-L., Jeon, S. T., & Dosher, B. A. (2004). Temporal tuning characteristics of the perceptual template and endogenous cuing of spatial attention. *Vision Research*, *44*(12), 1333–1350. http://doi.org/10.1016/j.visres.2003.12.017

Lu, Z.-L., Lesmes, L. A., & Dosher, B. A. (2002). Spatial attention excludes external noise at the target location. *Journal of Vision*, *2*(4), 312–323. http://doi.org/10.1167/2.4.4

Lu, Z.-L., Li, X., Tjan, B. S., Dosher, B. A., & Chu, W. (2011). Attention extracts signal in external noise: A BOLD fMRI study. *Journal of Cognitive Neuroscience*, *23*(5), 1148–1159. http://doi.org/10.1162/jocn.2010.21511

Luck, S. J., Chelazzi, L., Hillyard, S. A., & Desimone, R. (1997). Neural mechanisms of spatial selective attention in areas V1, V2, and V4 of macaque visual cortex. *Journal of Neurophysiology*, *77*(1), 24–42.

Marg, E., & Rudiak, D. (1994). Phosphenes Induced by Magnetic Stimulation Over the Occipital Brain: Description and Probable Site of Stimulation. *Optometry and Vision Science*, *71*(5), 301–311.

Markov, N. T., Ercsey-Ravasz, M. M., Ribeiro Gomes, A. R., Lamy, C., Magrou, L., Vezoli,

J., … Kennedy, H. (2014). A weighted and directed interareal connectivity matrix for macaque cerebral cortex. *Cerebral Cortex*, *24*(1), 17–36. http://doi.org/10.1093/cercor/bhs270

Marr, D., & Poggio, T. (1976). Cooperative computation of stereo disparity. *Science*, *194*(4262), 283–287. http://doi.org/10.1126/science.968482

Marr, D., & Poggio, T. (1979). A computational theory of human stereo vision. *Proceedings of the Royal Society of London. Series B*, *204*(1156), 301–328.

Martin, R. D. (1990). *Primate Origins and Evolution: A Phylogenetic Reconstruction*. Princeton, N.J.: Princeton University Press.

Mayhew, J. E. W., & Frisby, J. P. (1981). Psychophysical and computational studies towards a theory of human stereopsis. *Artificial Intelligence*, *17*(1–3), 349–385. http://doi.org/10.1016/0004-3702(81)90029-1

McFarlane, I. (1976). A practical approach to animal behavior. In M. E. Ensminger (Ed.), *Beef Cattle Science Handbook* (13th ed., pp. 420–426). Clovis, California: Agriservices Foundation.

McKeefry, D. J., Burton, M. P., Vakrou, C., Barrett, B. T., & Morland, A. B. (2008). Induced Deficits in Speed Perception by Transcranial Magnetic Stimulation of Human Cortical Areas V5/MT+ and V3A. *Journal of Neuroscience*, *28*(27), 6848–6857. http://doi.org/10.1523/JNEUROSCI.1287-08.2008

McShane, B. B., & Böckenholt, U. (2017). Single Paper Meta-analysis: Benefits for Study Summary, Theory-testing, and Replicability. *Journal of Consumer Research*, *43*, 1048–1063. http://doi.org/10.1093/jcr/ucw085

Meister, I. G., Weidemann, J., Dambeck, N., Foltys, H., Sparing, R., Krings, T., … Boroojerdi, B. (2003). Neural correlates of phosphene perception. In *Supplements to Clinical Neurophysiology* (pp. 305–311). http://doi.org/10.1016/S1567-424X(09)70234-X

Mills, K. R., Boniface, S. J., & Schubert, M. (1992). Magnetic brain stimulation with a double coil: the importance of coil orientation. *Electroencephalography and Clinical Neurophysiology/Evoked Potentials Section*, *85*(1), 17–21. http://doi.org/10.1016/0168-5597(92)90096-T

Mima, T., Oluwatimilehin, T., Hiraoka, T., & Hallett, M. (2001). Transient interhemispheric neuronal synchrony correlates with object recognition. *Journal of Neuroscience*, *21*(11), 3942–3948. http://doi.org/21/11/3942 [pii] ET - 2001/05/23

Miniussi, C., Harris, J. A., & Ruzzoli, M. (2013). Modelling non-invasive brain stimulation in cognitive neuroscience. *Neuroscience and Biobehavioral Reviews*, *37*(8), 1702–1712. http://doi.org/10.1016/j.neubiorev.2013.06.014

Mishkin, M., Ungerleider, L. G., & Macko, K. A. (1983). Object vision and spatial vision: two cortical pathways. *Trends in Neurosciences*, *6*, 414–417. http://doi.org/10.1016/0166-2236(83)90190-X

Moliadze, V., Giannikopoulos, D., Eysel, U. T., & Funke, K. (2005). Paired-pulse transcranial magnetic stimulation protocol applied to visual cortex of anaesthetized cat: effects on visually evoked single-unit activity. *The Journal of Physiology*, *566*(3), 955–965. http://doi.org/10.1113/jphysiol.2005.086090

Moliadze, V., Zhao, Y., Eysel, U., & Funke, K. (2003). Effect of transcranial magnetic

stimulation on single-unit activity in the cat primary visual cortex. *The Journal of Physiology*, *553*(2), 665–679. http://doi.org/10.1113/jphysiol.2003.050153

Moran, J., & Desimone, R. (1985). Selective attention gates visual processing in the extrastriate cortex. *Science*, *229*(4715), 782–784.

Movshon, J. A., Thompson, I. D., & Tolhurst, D. J. (1978). Spatial summation in the receptive fields of simple cells in the cat's striate cortex. *The Journal of Physiology*, *283*, 53–77.

Mueller, J. K., Grigsby, E. M., Prevosto, V., Petraglia, F. W., Rao, H., Deng, Z.-D., … Grill, W. M. (2014). Simultaneous transcranial magnetic stimulation and single-neuron recording in alert non-human primates. *Nature Neuroscience*, *17*(8), 1130–1136. http://doi.org/10.1038/nn.3751

Mulckhuyse, M., Kelley, T. A., Theeuwes, J., Walsh, V., & Lavie, N. (2011). Enhanced visual perception with occipital transcranial magnetic stimulation. *European Journal of Neuroscience*, *34*(8), 1320–1325. http://doi.org/10.1111/j.1460-9568.2011.07814.x

Murphy, S. C., Palmer, L. M., Nyffeler, T., Müri, R. M., & Larkum, M. E. (2016). Transcranial magnetic stimulation (TMS) inhibits cortical dendrites. *ELife*, *5*, 1–12. http://doi.org/10.7554/eLife.13598

Najib, U., Horvath, J. C., Silvanto, J., & Pascual-Leone, A. (2010). State-dependency effects on TMS: a look at motive phosphene behavior. *Journal of Visualized Experiments : JoVE*, (46), 5–8. http://doi.org/10.3791/2273

Nelson, J. I. (1975). Globality and stereoscopic fusion in binocular vision. *Journal of Theoretical Biology*, *49*(1), 1–88. http://doi.org/10.1016/S0022-5193(75)80020-8

Neri, P. (2005). A Stereoscopic Look at Visual Cortex. *Journal of Neurophysiology*, *93*(4), 1823–1826. http://doi.org/10.1152/jn.01068.2004

Neri, P., Bridge, H., & Heeger, D. J. (2004). Stereoscopic Processing of Absolute and Relative Disparity in Human Visual Cortex. *Journal of Neurophysiology*, *92*(3), 1880–1891. http://doi.org/10.1152/jn.01042.2003

Nguyenkim, J. D., & DeAngelis, G. C. (2003). Disparity-based coding of three-dimensional surface orientation by macaque middle temporal neurons. *Journal of Neuroscience*, *23*(18), 7117–7128.

Nikara, T., Bishop, P. O., & Pettigrew, J. D. (1968). Analysis of retinal correspondence by studying receptive fields of binocular single units in cat striate cortex. *Experimental Brain Research*, *6*, 353–372. http://doi.org/10.1007/BF00233184

Nitsche, M. A., & Paulus, W. (2001). Sustained excitability elevations induced by transcranial DC motor cortex stimulation in humans. *Neurology*, *57*(10), 1899–1901. http://doi.org/10.1212/WNL.57.10.1899

O'Connell, R. G., Dockree, P. M., & Kelly, S. P. (2012). A supramodal accumulation-to-bound signal that determines perceptual decisions in humans. *Nature Neuroscience*, *15*(12), 1729–1735. http://doi.org/10.1038/nn.3248

Ogawa, A., & Macaluso, E. (2015). Orienting of visuo-spatial attention in complex 3D space: Search and detection. *Human Brain Mapping*. http://doi.org/10.1002/hbm.22767

Ohzawa, I., DeAngelis, G. C., & Freeman, R. D. (1990). Stereoscopic depth discrimination in the visual cortex: neurons ideally suited as disparity detectors. *Science*, *249*(4972), 1037–1041.

Ohzawa, I., DeAngelis, G. C., & Freeman, R. D. (1997). Encoding of Binocular Disparity by Complex Cells in the Cat's Visual Cortex. *Journal of Neurophysiology*, *77*(6), 2879–2909. http://doi.org/10.1152/jn.1997.77.6.2879

Ohzawa, I., & Freeman, R. D. (1986). The binocular organization of complex cells in the cat's visual cortex. *Journal of Neurophysiology*, *56*(1), 243–259. http://doi.org/10.1152/jn.1986.56.1.243

Okamoto, M., & Dan, I. (2005). Automated cortical projection of head-surface locations for transcranial functional brain mapping. *NeuroImage*, *26*(1), 18–28. http://doi.org/10.1016/j.neuroimage.2005.01.018

Opitz, A., Legon, W., Rowlands, A., Bickel, W. K., Paulus, W., & Tyler, W. J. (2013). Physiological observations validate finite element models for estimating subject-specific electric field distributions induced by transcranial magnetic stimulation of the human motor cortex. *NeuroImage*, *81*, 253–264. http://doi.org/10.1016/j.neuroimage.2013.04.067

Opitz, A., Windhoff, M., Heidemann, R. M., Turner, R., & Thielscher, A. (2011). How the brain tissue shapes the electric field induced by transcranial magnetic stimulation. *NeuroImage*, *58*(3), 849–859. http://doi.org/10.1016/j.neuroimage.2011.06.069

Opitz, A., Zafar, N., Bockermann, V., Rohde, V., & Paulus, W. (2014). Validating computationally predicted TMS stimulation areas using direct electrical stimulation in patients with brain tumors near precentral regions. *NeuroImage: Clinical*, *4*, 500–507. http://doi.org/10.1016/j.nicl.2014.03.004

Orban, G. A., Janssen, P., & Vogels, R. (2006). Extracting 3D structure from disparity. *Trends in Neurosciences*, *29*(8), 466–473. http://doi.org/10.1016/j.tins.2006.06.012

Palva, S., & Palva, J. M. (2011). Functional roles of alpha-band phase synchronization in local and large-scale cortical networks. *Frontiers in Psychology*, *2*. http://doi.org/10.3389/fpsyg.2011.00204

Parker, A. J. (2007). Binocular depth perception and the cerebral cortex. *Nature Reviews Neuroscience*, *8*(5), 379–391. http://doi.org/10.1038/nrn2131

Pascual-Leone, A., Bartres-Faz, D., & Keenan, J. P. (1999). Transcranial magnetic stimulation: studying the brain-behaviour relationship by induction of "virtual lesions". *Philosophical Transactions of the Royal Society of London B: Biological Sciences*, *354*(1387), 1229–1238. http://doi.org/10.1098/rstb.1999.0476

Pascual-Leone, A., & Walsh, V. (2001). Fast backprojections from the motion to the primary visual area necessary for visual awareness. *Science*, *292*(5516), 510–512. http://doi.org/10.1126/science.1057099

Pascual-Leone, A., Walsh, V., & Rothwell, J. (2000). Transcranial magnetic stimulation in cognitive neuroscience--virtual lesion, chronometry, and functional connectivity. *Current Opinion in Neurobiology*, *10*(2), 232–237. http://doi.org/10.1016/S0959-4388(00)00081-7

Patten, M. L., & Welchman, A. E. (2015). fMRI Activity in Posterior Parietal Cortex Relates to the Perceptual Use of Binocular Disparity for Both Signal-In-Noise and Feature Difference Tasks. *PLOS ONE*, *10*(11). http://doi.org/10.1371/journal.pone.0140696

Patton, H. D., & Amassian, E. (1954). Single- and multiple-unit analysis of cortical stage of pyramidal tract activation. *Journal of Neurophysiology*, *17*(4), 345–363.

Pessoa, L., Kastner, S., & Ungerleider, L. G. (2003). Neuroimaging studies of attention: from modulation of sensory processing to top-down control. *Journal of Neuroscience*, *23*(10), 3990–3998.

Pettigrew, J. D., Nikara, T., & Bishop, P. O. (1968). Binocular interaction on single units in cat striate cortex: Simultaneous stimulation by single moving slit with receptive fields in correspondence. *Experimental Brain Research*, *6*(4), 391–410. http://doi.org/10.1007/BF00233186

Pierrot-Deseilligny, C., Milea, D., & Müri, R. M. (2004). Eye movement control by the cerebral cortex. *Current Opinion in Neurology*, *17*(1), 17–25. http://doi.org/10.1097/01.wco.0000113942.12823.e0

Poggio, G. F., & Fischer, B. (1977). Binocular interaction and depth sensitivity in striate and prestriate cortex of behaving rhesus monkey. *Journal of Neurophysiology*, *40*(6), 1392–1405. http://doi.org/10.1152/jn.1977.40.6.1392

Poggio, G. F., Gonzalez, F., & Krause, F. (1988). Stereoscopic mechanisms in monkey visual cortex: binocular correlation and disparity selectivity. *Journal of Neuroscience*, *8*(12), 4531–4550.

Poggio, G. F., & Poggio, T. (1984). The Analysis of Stereopsis. *Annual Review of Neuroscience*, *7*(1), 379–412. http://doi.org/10.1146/annurev.ne.07.030184.002115

Poggio, G. F., & Talbot, W. H. (1981). Mechanisms of static and dynamic stereopsis in foveal cortex of the rhesus monkey. *The Journal of Physiology*, *315*, 469–492.

Ponce, C. R., & Born, R. T. (2008). Stereopsis. *Current Biology*, *18*(18), 845–850. http://doi.org/10.1016/j.cub.2008.07.006

Premoli, I., Castellanos, N., Rivolta, D., Belardinelli, P., Bajo, R., Zipser, C., … Ziemann, U. (2014). TMS-EEG Signatures of GABAergic Neurotransmission in the Human Cortex. *Journal of Neuroscience*, *34*(16), 5603–5612. http://doi.org/10.1523/JNEUROSCI.5089-13.2014

Preston, T. J., Li, S., Kourtzi, Z., & Welchman, A. E. (2008). Multivoxel pattern selectivity for perceptually relevant binocular disparities in the human brain. *Journal of Neuroscience*, *28*(44), 11315–11327. http://doi.org/10.1523/JNEUROSCI.2728-08.2008

Prince, J. H. (1970). The eye and vision. In M. J. Swenson (Ed.), *Dukes Physiology of Domestic Animals* (pp. 1135–1159). New York: Wiley.

Prince, S. J. D., Cumming, B. G., & Parker, A. J. (2002). Range and mechanism of encoding of horizontal disparity in macaque V1. *Journal of Neurophysiology*, *87*(1), 209–221. http://doi.org/10.1152/jn.00466.2000.

Qian, N. (1994). Computing Stereo Disparity and Motion with Known Binocular Cell Properties. *Neural Computation*, *6*(3), 390–404. http://doi.org/10.1162/neco.1994.6.3.390

Qian, N., & Zhu, Y. (1997). Physiological computation of binocular disparity. *Vision Research*, *37*(13), 1811–1827. http://doi.org/10.1016/S0042-6989(96)00331-8

Rahnev, D., Maniscalco, B., Luber, B., Lau, H., & Lisanby, S. H. (2012). Direct injection of noise to the visual cortex decreases accuracy but increases decision confidence. *Journal of Neurophysiology*, *107*(6), 1556–1563. http://doi.org/10.1152/jn.00985.2011

Ramachandran, V. S., Madhusudhan Rao, V., & Vidyasagar, T. R. (1973). The role of

contours in stereopsis. *Nature*, *242*(5397), 412–414. http://doi.org/10.1038/242412a0

Ramachandran, V. S., & Nelson, J. I. (1976). Global grouping overrides point-to-point disparities. *Perception*, *5*, 125–128.

Ramos-Estebanez, C., Merabet, L. B., Machii, K., Fregni, F., Thut, G., Wagner, T. A., … Pascual-Leone, A. (2007). Visual Phosphene Perception Modulated by Subthreshold Crossmodal Sensory Stimulation. *Journal of Neuroscience*, *27*(15), 4178–4181. http://doi.org/10.1523/JNEUROSCI.5468-06.2007

Rattay, F. (1999). The basic mechanism for the electrical stimulation of the nervous system. *Neuroscience*, *89*(2), 335–346. http://doi.org/10.1016/S0306-4522(98)00330-3

Ray, P. G., Meador, K. J., Epstein, C. M., Loring, D. W., & Day, L. J. (1998). Magnetic Stimulation of Visual Cortex: Factors Influencing the Perception of Phosphenes. *Journal of Clinical Neurophysiology*, *15*(4), 351–357. http://doi.org/10.1097/00004691-199807000-00007

Read, J. C. A., & Cumming, B. G. (2007). Sensors for impossible stimuli may solve the stereo correspondence problem. *Nature Neuroscience*, *10*(10), 1322–1328. http://doi.org/10.1038/nn1951

Read, J. C. A., & Cumming, B. G. (2018). A stimulus artefact undermines the evidence for independent ON and OFF channels in stereopsis. *BioRxiv*. http://doi.org/10.1101/295618

Read, J. C. A., Parker, A. J., & Cumming, B. G. (2002). A simple model accounts for the response of disparity-tuned V1 neurons to anticorrelated images. *Visual Neuroscience*, *19*(6), 735–753. http://doi.org/10.1017/S0952523802196052

Read, J. C. A., Vaz, X. A., & Serrano-Pedraza, I. (2011). Independent mechanisms for bright and dark image features in a stereo correspondence task. *Journal of Vision*, *11*(12), 1–14. http://doi.org/10.1167/11.12.4

Ridding, M. C., & Rothwell, J. C. (2007). Is there a future for therapeutic use of transcranial magnetic stimulation? *Nature Reviews Neuroscience*, *8*(7), 559–567. http://doi.org/10.1038/nrn2169

Robertson, E. M., Théoret, H., & Pascual-Leone, A. (2003). Studies in cognition: the problems solved and created by transcranial magnetic stimulation. *Journal of Cognitive Neuroscience*, *15*, 948–960. http://doi.org/10.1162/089892903770007344

Rogasch, N. C., Thomson, R. H., Farzan, F., Fitzgibbon, B. M., Bailey, N. W., Hernandez-Pavon, J. C., … Fitzgerald, P. B. (2014). Removing artefacts from TMS-EEG recordings using independent component analysis: Importance for assessing prefrontal and motor cortex network properties. *NeuroImage*, *101*, 425–439. http://doi.org/10.1016/j.neuroimage.2014.07.037

Rosenberg, A., Cowan, N. J., & Angelaki, D. E. (2013). The Visual Representation of 3D Object Orientation in Parietal Cortex. *Journal of Neuroscience*, *33*(49), 19352–19361. http://doi.org/10.1523/JNEUROSCI.3174-13.2013

Rossi, S., Hallett, M., Rossini, P. M., & Pascual-Leone, A. (2009). Safety, ethical considerations, and application guidelines for the use of transcranial magnetic stimulation in clinical practice and research. *Clinical Neurophysiology*, *120*(12), 323–330. http://doi.org/10.1016/j.clinph.2009.08.016.Rossi

Rothwell, J. C. (1997). Techniques and mechanisms of action of transcranial stimulation of

the human motor cortex. *Journal of Neuroscience Methods*, *74*(2), 113–122. http://doi.org/10.1016/S0165-0270(97)02242-5

Ruff, C. C., Blankenburg, F., Bjoertomt, O., Bestmann, S., Freeman, E., Haynes, J. D., … Driver, J. (2006). Concurrent TMS-fMRI and Psychophysics Reveal Frontal Influences on Human Retinotopic Visual Cortex. *Current Biology*, *16*(15), 1479–1488. http://doi.org/10.1016/j.cub.2006.06.057

Sack, A. T., Cohen Kadosh, R., Schuhmann, T., Moerel, M., Walsh, V., Goebel, R., … Cohen Kadosh, R. (2009). Optimizing functional accuracy of TMS in cognitive studies: a comparison of methods. *Journal of Cognitive Neuroscience*, *21*(2), 207–221. http://doi.org/10.1162/jocn.2009.21126

Salminen-Vaparanta, N., Noreika, V., Revonsuo, A., Koivisto, M., & Vanni, S. (2012). Is selective primary visual cortex stimulation achievable with TMS? *Human Brain Mapping*, *33*(3), 652–665. http://doi.org/10.1002/hbm.21237

Salminen-Vaparanta, N., Vanni, S., Noreika, V., Valiulis, V., Móró, L., & Revonsuo, A. (2014). Subjective Characteristics of TMS-Induced Phosphenes Originating in Human V1 and V2. *Cerebral Cortex*, *24*(10), 2751–2760. http://doi.org/10.1093/cercor/bht131

Sandrini, M., Umilta, C., & Rusconi, E. (2011). The use of transcranial magnetic stimulation in cognitive neuroscience: A new synthesis of methodological issues. *Neuroscience and Biobehavioral Reviews*, *35*(3), 516–536. http://doi.org/10.1016/j.neubiorev.2010.06.005

Schaeffner, L. F., & Welchman, A. E. (2017). Mapping the visual brain areas susceptible to phosphene induction through brain stimulation. *Experimental Brain Research*, *235*(1), 205–217. http://doi.org/10.1007/s00221-016-4784-4

Schaeffner, L. F., & Welchman, A. E. (2018). The mixed polarity benefit of stereopsis arises in early visual cortex, Manuscript submitted for publication.

Schenk, T., & McIntosh, R. D. (2010). Do we have independent visual streams for perception and action? *Cognitive Neuroscience*, *1*(1), 52–62. http://doi.org/10.1080/17588920903388950

Schiller, P. H. (1992). The ON and OFF channels of the visual system. *Trends in Neurosciences*, *15*(3), 86–92.

Schiller, P. H. (2010). Parallel information processing channels created in the retina. *Proceedings of the National Academy of Sciences*, *107*(40), 17087–17094. http://doi.org/10.1073/pnas.1011782107

Schwarzkopf, D. S., Silvanto, J., & Rees, G. (2011). Stochastic Resonance Effects Reveal the Neural Mechanisms of Transcranial Magnetic Stimulation. *Journal of Neuroscience*, *31*(9), 3143–3147. http://doi.org/10.1523/JNEUROSCI.4863-10.2011

Shadlen, N. N., & Newsome, W. T. (2001). Neural Basis of a Perceptual Decision in the Parietal Cortex (Area LIP) of the Rhesus Monkey. *Journal of Neurophysiology*, *86*(4), 1916–1936.

Shiozaki, H. M., Tanabe, S., Doi, T., & Fujita, I. (2012). Neural Activity in Cortical Area V4 Underlies Fine Disparity Discrimination. *Journal of Neuroscience*, *32*(11), 3830–3841. http://doi.org/10.1523/JNEUROSCI.5083-11.2012

Silson, E. H., McKeefry, D. J., Rodgers, J., Gouws, A. D., Hymers, M., & Morland, A. B. (2013). Specialized and independent processing of orientation and shape in visual field

maps LO1 and LO2. *Nature Neuroscience*, *16*(3), 267–269. http://doi.org/10.1038/nn.3327

Silvanto, J. (2013). Transcranial magnetic stimulation and vision. In *Handbook of Clinical Neurology* (pp. 655–669). http://doi.org/10.1016/B978-0-444-53497-2.00052-8

Sinha, P., & Adelson, E. (1993). Recovering reflectance and illumination in a world of painted polyhedra. *1993 (4th) International Conference on Computer Vision*, 156–163. http://doi.org/10.1109/ICCV.1993.378224

Smith, S. M. (2002). Fast robust automated brain extraction. *Human Brain Mapping*, *17*(3), 143–155. http://doi.org/10.1002/hbm.10062

Sperling, G. (1970). Binocular vision: A physical and neural theory. *American Journal of Psychology*, *83*(4), 461–534. http://doi.org/10.2307/1420686

Srinivasan, R., Winter, W. R., Ding, J., & Nunez, P. L. (2007). EEG and MEG coherence: Measures of functional connectivity at distinct spatial scales of neocortical dynamics. *Journal of Neuroscience Methods*, *166*(1), 41–52. http://doi.org/10.1016/j.jneumeth.2007.06.026

Srivastava, S., Orban, G. A., De Maziere, P. A., & Janssen, P. (2009). A Distinct Representation of Three-Dimensional Shape in Macaque Anterior Intraparietal Area: Fast, Metric, and Coarse. *Journal of Neuroscience*, *29*(34), 10613–10626. http://doi.org/10.1523/JNEUROSCI.6016-08.2009

Stokes, M. G., Barker, A. T., Dervinis, M., Verbruggen, F., Maizey, L., Adams, R. C., & Chambers, C. D. (2013). Biophysical determinants of transcranial magnetic stimulation: effects of excitability and depth of targeted area. *Journal of Neurophysiology*, *109*(2), 437–444. http://doi.org/10.1152/jn.00510.2012

Stokes, M. G., Chambers, C. D., Gould, I. C., Henderson, T. R., Janko, N. E., Allen, N. B., … Jason, B. (2005). Simple Metric For Scaling Motor Threshold Based on Scalp-Cortex Distance : Application to Studies Using Transcranial Magnetic Stimulation. *Journal of Neurophysiology*, *94*(6), 4520–4527. http://doi.org/10.1152/jn.00067.2005

Tanabe, S., Doi, T., Umeda, K., & Fujita, I. (2005). Disparity-Tuning Characteristics of Neuronal Responses to Dynamic Random-Dot Stereograms in Macaque Visual Area V4. *Journal of Neurophysiology*, *94*(4), 2683–2699. http://doi.org/10.1152/jn.00319.2005

Taylor, P. C. J., Walsh, V., & Eimer, M. (2010). The neural signature of phosphene perception. *Human Brain Mapping*, *31*(9), 1408–1417. http://doi.org/10.1002/hbm.20941

Tehovnik, E. J., & Slocum, W. M. (2013). Electrical induction of vision. *Neuroscience and Biobehavioral Reviews*, *37*(5), 803–818. http://doi.org/10.1016/j.neubiorev.2013.03.012

Theys, T., Pani, P., van Loon, J., Goffin, J., & Janssen, P. (2012). Selectivity for Three-Dimensional Shape and Grasping-Related Activity in the Macaque Ventral Premotor Cortex. *Journal of Neuroscience*, *32*(35), 12038–12050. http://doi.org/10.1523/JNEUROSCI.1790-12.2012

Theys, T., Pani, P., van Loon, J., Goffin, J., & Janssen, P. (2013). Three-dimensional Shape Coding in Grasping Circuits: A Comparison between the Anterior Intraparietal Area and Ventral Premotor Area F5a. *Journal of Cognitive Neuroscience*, *25*(3), 352–364. http://doi.org/10.1162/jocn_a_00332

Thielscher, A., Antunes, A., & Saturnino, G. B. (2015). Field modeling for transcranial magnetic stimulation: A useful tool to understand the physiological effects of TMS? In *2015 37th Annual International Conference of the IEEE Engineering in Medicine and Biology Society (EMBC)* (pp. 222–225). IEEE. http://doi.org/10.1109/EMBC.2015.7318340

Thielscher, A., Opitz, A., & Windhoff, M. (2011). Impact of the gyral geometry on the electric field induced by transcranial magnetic stimulation. *NeuroImage*, *54*(1), 234–243. http://doi.org/10.1016/j.neuroimage.2010.07.061

Thomas, O. M., Cumming, B. G., & Parker, A. J. (2002). A specialization for relative disparity in v2. *Nature Neuroscience*, *5*(5), 472–478. http://doi.org/10.1038/nn837

Thompson, P. D., Day, B. L., Rothwell, J. C., Dressler, D., Noordhout, A. M. de, & Marsden, C. D. (1991). Further observations on the facilitation of muscle responses to cortical stimulation by voluntary contraction. *Electroencephalography and Clinical Neurophysiology/ Evoked Potentials*, *81*(5), 397–402. http://doi.org/10.1016/0168-5597(91)90029-W

Trepel, C. (1998). Long-term potentiation in the neocortex of the adult, freely moving rat. *Cerebral Cortex*, *8*(8), 719–729. http://doi.org/10.1093/cercor/8.8.719

Treue, S., & Maunsell, J. (1996). Attentional modulation of visual motion processing in cortical areas MT and MST. *Nature*, *382*(6591), 539–541. http://doi.org/10.1038/382539a0

Tsao, D. Y., Conway, B. R., & Livingstone, M. S. (2003). Receptive fields of disparity-tuned simple cells in macaque V1. *Neuron*, *38*(1), 103–114. http://doi.org/10.1016/S0896-6273(03)00150-8

Turi, Z., Paulus, W., & Antal, A. (2012). Functional neuroimaging and transcranial electrical stimulation. *Clinical EEG and Neuroscience*, *43*(3), 200–208. http://doi.org/10.1177/1550059412444978

Tyler, C. W. (1990). A stereoscopic view of visual processing streams. *Vision Research*, *30*(11), 1877–1895. http://doi.org/10.1016/0042-6989(90)90165-H

Uka, T., & DeAngelis, G. C. (2003). Contribution of middle temporal area to coarse depth discrimination: comparison of neuronal and psychophysical sensitivity. *Journal of Neuroscience*, *23*(8), 3515–3530. http://doi.org/23/8/3515

Uka, T., & DeAngelis, G. C. (2006). Linking neural representation to function in stereoscopic depth perception: roles of area MT in coarse vs. fine disparity discrimination. *Journal of Neuroscience*, *26*(25), 6791–6802.

Uka, T., Tanaka, H., Yoshiyama, K., Kato, M., & Fujita, I. (2000). Disparity Selectivity of Neurons in Monkey Inferior Temporal Cortex. *Journal of Neurophysiology*, *84*(1), 120–132. http://doi.org/10.1152/jn.2000.84.1.120

Umeda, K., Tanabe, S., & Fujita, I. (2007). Representation of Stereoscopic Depth Based on Relative Disparity in Macaque Area V4. *Journal of Neurophysiology*, *98*(1), 241–252. http://doi.org/10.1152/jn.01336.2006

Varela, F., Lachaux, J. P., Rodriguez, E., & Martinerie, J. (2001). The brainweb: phase synchronization and large-scale integration. *Nature Reviews. Neuroscience*, *2*(4), 229–239. http://doi.org/10.1038/35067550

Verhoef, B.-E., Vogels, R., & Janssen, P. (2010). Contribution of Inferior Temporal and

Posterior Parietal Activity to Three-Dimensional Shape Perception. *Current Biology*, *20*(10), 909–913. http://doi.org/10.1016/j.cub.2010.03.058

Verhoef, B.-E., Vogels, R., & Janssen, P. (2012). Inferotemporal Cortex Subserves Three-Dimensional Structure Categorization. *Neuron*, *73*(1), 171–182. http://doi.org/10.1016/j.neuron.2011.10.031

Verhoef, B.-E., Vogels, R., & Janssen, P. (2015). Effects of Microstimulation in the Anterior Intraparietal Area during Three-Dimensional Shape Categorization. *PloS One*, *10*(8). http://doi.org/10.1371/journal.pone.0136543

Vinck, M., Oostenveld, R., Van Wingerden, M., Battaglia, F., & Pennartz, C. M. A. (2011). An improved index of phase-synchronization for electrophysiological data in the presence of volume-conduction, noise and sample-size bias. *NeuroImage*, *55*(4), 1548–1565. http://doi.org/10.1016/j.neuroimage.2011.01.055

Volman, I., Roelofs, K., Koch, S., Verhagen, L., & Toni, I. (2011). Anterior prefrontal cortex inhibition impairs control over social emotional actions. *Current Biology*, *21*(20), 1766–1770. http://doi.org/10.1016/j.cub.2011.08.050

von der Heydt, R., Adorjani, C., Hänny, P., & Baumgartner, G. (1978). Disparity sensitivity and receptive field incongruity of units in the cat striate cortex. *Experimental Brain Research*, *31*(4), 523–545. http://doi.org/10.1007/BF00239810

von Stein, A., Chiang, C., & Konig, P. (2000). Top-down processing mediated by interareal synchronization. *Proceedings of the National Academy of Sciences*, *97*(26), 14748–14753. http://doi.org/10.1073/pnas.97.26.14748

Wagner, T., Rushmore, J., Eden, U., & Valero-Cabre, A. (2009). Biophysical foundations underlying TMS: Setting the stage for an effective use of neurostimulation in the cognitive neurosciences. *Cortex*, *45*(9), 1025–1034. http://doi.org/10.1016/j.cortex.2008.10.002

Walsh, V., Pascual-Leone, A., & Kosslyn, S. (2003). *Transcranial magnetic stimulation: A neurochronometrics of mind*. MIT Press.

Wandell, B. A., Dumoulin, S. O., & Brewer, A. A. (2007). Visual Field Maps in Human Cortex. *Neuron*, *56*(2), 366–383. http://doi.org/10.1016/j.neuron.2007.10.012

Wassermann, E. M. (1998). Risk and safety of repetitive transcranial magnetic stimulation : report and suggested guidelines from the International Workshop on the Safety of Repetitive Transcranial Magnetic Stimulation , June 5 – 7 , 1996. *Electroencephalography and Clinical Neurophysiology*, *108*, 1–16.

Watanabe, M., Tanaka, H., Uka, T., & Fujita, I. (2002). Disparity-selective neurons in area V4 of macaque monkeys. *Journal of Neurophysiology*, *87*(4), 1960–1973. http://doi.org/10.1152/jn.00780.2000

Watt, S. J., & Bradshaw, M. F. (2002). Binocular information in the control of prehensile movements in multiple-object scenes. *Spatial Vision*, *15*(2), 141–155. http://doi.org/10.1163/15685680252875138

Weiss, C., Nettekoven, C., Rehme, A. K., Neuschmelting, V., Eisenbeis, A., Goldbrunner, R., & Grefkes, C. (2013). Mapping the hand, foot and face representations in the primary motor cortex — Retest reliability of neuronavigated TMS versus functional MRI. *NeuroImage*, *66*, 531–542. http://doi.org/10.1016/j.neuroimage.2012.10.046

Westheimer, G. (1979). Cooperative neural processes involved in stereoscopic acuity.

Experimental Brain Research, *36*(3), 585–597.

Wheatstone, C. (1838). Contributions to the Physiology of Vision. Part the First. On Some Remarkable, and Hitherto Unobserved, Phenomena of Binocular Vision. *Philosophical Transactions of the Royal Society of London*, *128*, 371–394. http://doi.org/10.1098/rstl.1838.0019

Whittaker, S. G., & Cummings, R. W. (1990). Foveating saccades. *Vision Research*, *30*(9), 1363–1366. http://doi.org/10.1016/0042-6989(90)90009-A

Windhoff, M., Opitz, A., & Thielscher, A. (2013). Electric field calculations in brain stimulation based on finite elements: An optimized processing pipeline for the generation and usage of accurate individual head models. *Human Brain Mapping*, *34*(4), 923–935. http://doi.org/10.1002/hbm.21479

Winter, W. R., Nunez, P. L., Ding, J., & Srinivasan, R. (2007). Comparison of the effect of volume conduction on EEG coherence with the effect of field spread on MEG coherence. In *Statistics in Medicine*. http://doi.org/10.1002/sim.2978

Zeki, S. M. (1978). The third visual complex of rhesus monkey prestriate cortex. *The Journal of Physiology*, *277*(1), 245–272. http://doi.org/10.1113/jphysiol.1978.sp012271

Zeki, S. M., Watson, J. D., Lueck, C. J., Friston, K. J., Kennard, C., & Frackowiak, R. S. (1991). A direct demonstration of functional specialization in human visual cortex. *Journal of Neuroscience*, *11*(3), 641–649. http://doi.org/5726

Ziemann, U., Lönnecker, S., Steinhoff, B. J., & Paulus, W. (1996). Effects of antiepileptic drugs on motor cortex excitability in humans: A transcranial magnetic stimulation study. *Annals of Neurology*, *40*(3), 367–378. http://doi.org/10.1002/ana.410400306